

Synthesis and development of enzymatically polymerized polyester based hydrogels for potential pharmaceutical applications

Dissertation

Zur Erlangung des
Doktorgrades der Naturwissenschaften (Dr. rer. nat.)

Vorgelegt der

Naturwissenschaftlichen Fakultät I
Biowissenschaften

der Martin-Luther-Universität Halle-Wittenberg

vorgelegt von

Herrn Haroon Rashid
geb. in Tank, Pakistan

Gutachter

1. Prof. Dr. Karsten Mäder
2. Prof. Dr. Jörg Kreßler
3. PD Dr. Christian Wölk

Datum der Verteidigung: 27.03.2024

Dedicated to
My Parents & Siblings

TABLE OF CONTENTS

1	INTRODUCTION	1
1.1	POLYMERS, BIODEGRADABLE POLYMERS, AND DRUG DELIVERY	1
1.2	POLYESTERS AND THEIR ENZYMATIC SYNTHESIS	3
1.2.1	<i>Functional polyester via enzymatic polymerization</i>	8
1.2.2	<i>Modification of functional polyester</i>	9
1.2.2.1	<i>Grafting of functional polyester</i>	10
1.2.2.2	<i>Crosslinking of functional polyester</i>	13
1.3	CROSSLINKED POLYMER NETWORK/HYDROGELS	14
1.3.1	<i>Types of hydrogels</i>	16
1.3.1.2	<i>Physical crosslinking methods to produce hydrogels</i>	17
1.3.1.1.1	<i>Ionic interactions</i>	17
1.3.1.1.2	<i>Hydrogen bonding</i>	18
1.3.1.1.3	<i>Hydrophobic interactions</i>	18
1.3.1.1.4	<i>Stereo-complexation</i>	19
1.3.1.1.5	<i>Crosslinking through protein interactions</i>	20
1.3.1.2	<i>Chemical crosslinking methods to produce hydrogels</i>	21
1.3.1.2.1	<i>Crosslinking through free radical polymerization</i>	21
1.3.1.2.2	<i>Crosslinking through enzymes</i>	22
1.3.1.2.3	<i>Crosslinking through radiation</i>	23
1.3.1.2.4	<i>Crosslinking mediated by functional group interactions</i>	24
1.4	AIMS AND OBJECTIVES	25
2	MATERIALS AND METHODS	28
2.1	MATERIALS	28

2.2	POLYMER SYNTHESSES	28
2.2.1	<i>Synthesis of poly(sorbitol adipate) (PSA)</i>	28
2.2.2	<i>Synthesis of mono- and bifunctional PEG</i>	29
2.2.3	<i>Synthesis of PSA-g-mPEG</i>	31
2.2.4	<i>Hydrogel syntheses of PSA and PSA-g-mPEG with disuccinyl PEG</i>	33
2.3	INSTRUMENTATION	33
2.3.1	<i>Nuclear magnetic resonance (NMR) spectroscopy</i>	33
2.3.1.1	<i>Solution NMR spectroscopy</i>	33
2.3.1.2	<i>Solid state NMR spectroscopy</i>	34
2.3.1.2.1	<i>¹³C Magic angle spinning (MAS) NMR spectroscopy</i>	34
2.3.1.2.2	<i>¹H Double quantum (DQ) NMR spectroscopy</i>	34
2.3.1.2.3	<i>¹H Pulsed field gradient (PFG) NMR spectroscopy</i>	34
2.3.2	<i>Gel permeation chromatography (GPC)</i>	35
2.3.3	<i>Differential scanning calorimetry (DSC)</i>	35
2.3.4	<i>Swelling studies</i>	35
2.3.5	<i>Polymer degradation/stability study</i>	36
2.3.6	<i>Sol-gel fraction of PSA-g-mPEG hydrogels</i>	36
2.3.7	<i>Structural parameters of the PSA-g-mPEG hydrogels</i>	37
2.3.8	<i>X-ray diffraction (XRD) of PSA-g-mPEG hydrogels</i>	38
2.3.9	<i>Loading study of the BSA-TMR and DY-781 into hydrogel matrices</i>	39
2.3.10	<i>Release study of the BSA-TMR and DY-781</i>	40
2.3.11	<i>Cytotoxicity study of PSA-g-mPEG hydrogels</i>	40
3	RESULTS AND DISCUSSION	42

3.1	POLYMER SYNTHESSES	42
3.2	STABILITY AND DEGRADATION STUDY	49
3.3	DIFFERENTIAL SCANNING CALORIMETRY	51
3.4	SOL-GEL FRACTION	54
3.5	SWELLING STUDIES	55
3.6	TEMPERATURE DEPENDENT SWELLING OF HYDROGELS	58
3.7	^1H DOUBLE-QUANTUM (DQ) NMR SPECTROSCOPY	59
3.8	^1H PULSED FIELD GRADIENT (PFG) NMR SPECTROSCOPY	66
3.9	PHYSICAL STRUCTURAL PARAMETERS OF HYDROGELS	70
3.10	X-RAY DIFFRACTION	75
3.11	LOADING AND RELEASE EXPERIMENT OF BSA-TMR AND DY-781	76
3.12	CYTOTOXICITY STUDY OF HYDROGELS	83
4	SUMMARY AND PERSPECTIVE	86
5	REFERENCES	91
	SUPPLEMENTARY DATA	114
	ACKNOWLEDGEMENT	116
	CURRICULUM VITAE	117
	PUBLICATIONS	118
	SELBSTSTÄNDIGKEITSERKLÄRUNG	119

ABBREVIATIONS AND SYMBOLS**ABBREVIATIONS**

Asp	Aspartic acid
^{13}C NMR	Carbon nuclear magnetic resonance spectroscopy
^1H NMR	Proton nuclear magnetic resonance spectroscopy
ATRP	Atomic transfer radical polymerization
BAM	Brewster angle microscopy
BSA-TMR	Bovine serum albumin-Tetramethylrhodamine
CALB	<i>Candida antarctica</i> Lipase B
DMAP	4-(dimethylamino)pyridine
DMF	<i>N,N</i> -dimethylformamide
DMSO	Dimethyl sulfoxide
DNA	Deoxyribonucleic acid
DQ	Double quantum
DSC	Differential scanning calorimetry
EDC	<i>N</i> -(3-di-methylaminopropyl)- <i>N'</i> -ethylcarbodiimide hydrochloride
FTIR	Fourier transform infrared spectroscopy
GPC	Gel permeation chromatography
His224	Histidine
MAS	Magic angle spinning
mPEG ₁₂ -Suc	α -methoxy, ω -succinyl poly(ethylene glycol)

MTX	Methotrexate
MWCO	Molecular weight cut off
NMR	Nuclear magnetic resonance spectroscopy
NPs	Nanoparticles
PBS	Poly(butylene succinate)
PBS	Phosphate buffer saline
PCL	Poly(ϵ -caprolactone)
PDLLAM	Poly(D,L-lactic acid) diacrylate macromer
PEG	Poly(ethylene glycol)
PEO	Poly(ethylene oxide)
PET	Poly(ethylene terephthalate)
PFG	Pulsed field gradient
PGA	Poly(glycerol adipate)
PGLA	Poly(lactic-co-glycolic acid)
pHEMA	Poly(2-hydroxyethyl methacrylate)
PLA	Poly(lactic acid)
PMMA	Poly(methyl methacrylate)
PSA	Poly(sorbitol adipate)
RH	Relative humidity
RNA	Ribonucleic acid
ROP	Ring-opening polymerization

RT	Room Temperature
Ser	Serine
Suc-PEG _n -Suc	α,ω -bis-succinyl poly(ethylene glycol)/disuccinyl PEG
THF	Tetrahydrofuran
UV	Ultraviolet
WAXS	Wide-angle X-ray scattering

SYMBOLS

T_m	Melting temperature
ΔG_{total}	Total Gibbs free energy
$\Delta G_{elastic}$	Change in the elastic free energy
ΔG_{mixing}	Change in the mixing free energy
M_c	Molar mass between neighboring crosslinks
M_n	Number average molar mass
v_1	Polymer's specific volume
V_1	Solvent's molar volume
$v_{2,s}$	Polymer volume fraction
pH	Potential of hydrogen
Ca ²⁺	Calcium ions
d	day
D ₂ O	Deuterium oxide

h	hour
LiBr	Lithium bromide
χ_1	Polymer solvent interaction parameter
ρ_s	Density of the solvent
ρ_p	Density of the polymer hydrogel in dried form
Q	Degree of swelling
ξ	Correlation length
\bar{r}_0^2	Square of end to end distance between two adjacent crosslinking points
C_n	Flory characteristics ratio
N	Number of links per chain
M_r	Molar mass of one repeating unit of the polymer chain
m_i	Swollen hydrogel
m_o	Dried hydrogel disc
W_0	Initial weight of hydrogel precursors before reaction
W_1	Final weight of dried clean hydrogels after washing

1 Introduction

1.1 Polymers, biodegradable polymers, and drug delivery

Polymers are large molecules synthesized by joining many smaller molecules, known as monomers. The word "polymer" comes from the Greek language which means "many members." Natural polymers have been present since the early days of the Earth and are essential for the existence of life, such as DNA, RNA, and proteins. Starch, cellulose, natural rubber, etc. are some of the natural polymers that are used to form different materials. On the other hand, synthetic polymers are comparatively new materials and are formed by chemical reactions giving limitless possibilities to make different polymers [1]. Polymers can be broadly classified into two types, one is addition polymers while second is condensation polymers. In addition polymers, identical repeating units called monomers (usually having carbon-carbon double bond) are added up to form a polymer via chemical reaction. Examples of addition polymers are polyethylene, polystyrene, polyacrylates, etc. While condensation polymers on the other hand are formed when multifunctional molecules combine with removal of a small molecule as a byproduct like water [2]. Examples of condensation polymers are polyester, polyurethane, polyamide etc. [2,3].

Polymeric drug delivery research has undergone continuous advancement in last few decades [4–7]. Exploring novel drug delivery systems and innovative mechanisms of action stand at the forefront of these research goals. These objectives confine to diverse scientific disciplines, driving significant strides in enhancing the therapeutic index and improving the bioavailability of drugs through versatile delivery mechanisms [8]. Polymers play a vital role by integrating conventional methods of drug delivery with engineered technologies, enabling the precise targeting of drug release points and/or rates within the body [9]. Establishment of novel or modified polymer chemistries that offers distinct degradation properties is essential for tailoring the technology of drug delivery. Biodegradable polymers in the current times have been extensively studied for the development of various drug delivery carriers in order to enable them for attainment of sustained drug release [10].

Biodegradable polymers refer to polymers that break down within a specific timeframe after insertion into the body, serving a temporary supportive purpose. They disintegrate into less complex elements, eliminating concerns related to the lasting existence of foreign substances. Through enzymatic or non-enzymatic processes, they undergo breakdown into byproducts

that are both biocompatible and harmless [10,11]. Biodegradable polymers can be classified as either natural or synthetic in origin. The utilization of biodegradable natural polymers in the realm of medicine has historical roots. Opting for synthetic polymers instead of naturally occurring materials brings forth various advantages. Foremost, synthetic polymers can be synthesized using reproducible methods to consistently yield polymers with identical compositions. This production method ensures an uninterrupted supply and allows for tailoring a wide array of physical, chemical, and mechanical properties to suit diverse applications [12].

Polymers belonging to the polyester family, notably poly(lactic acid) (PLA) and poly(glycolic acid), along with their copolymers like poly(lactic-co-glycolic acid) (PGLA), are extensively utilized synthetic biodegradable polymers. When these polyesters were first developed approximately 50-60 years ago, they were especially synthesized to be biodegradable across a spectrum of biomedical and drug delivery applications [13,14]. Using biodegradable polymers presents various advantages over its alternatives. Key benefits include the capacity to adjust mechanical characteristics, control degradation rates, and mold them into various shapes. The primary advantage of biodegradable polymers is their inherent degradability, which reduces the need for subsequent surgical removal, leading to saved time and reduced expenses [15]. However, the formation of degradation byproducts can also present challenges. These include complex patterns of release and degradation, auto-catalyzed polymer degradation, and the establishment of microenvironments with an acidic nature. Scientific investigations conducted under *in vivo* and *in vitro* environments have indicated the occurrence of remarkably low pH values, often falling below 2 [16–18]. As Taylor *et al.* pointed out, the breakdown products of poly(lactic acid) and poly(glycolic acid) exhibited significant toxicity upon accumulation due to their acidic nature. This results in a localized increase in acid concentration, potentially triggering undesirable local inflammatory reactions [19]. This concern becomes more pronounced with larger implants, particularly in orthopedic applications. Moreover, the synthesis and processing of these polymers can be intricate and costly, especially when modifications are required [12]. Another drawback associated with these aliphatic polyesters pertains to their absence of available free functional groups suitable for linkage with diverse polymers or pharmaceutical agents [20–22]. This deficiency restricts their potential for tailored enhancement of material properties or the attainment of specific desired characteristics [23].

1.2 Polyesters and their enzymatic synthesis

Polyesters are the polymers that are made up of monomer units joined through ester bonds. There can be naturally occurring polyesters as well as commercially manufactured polyesters [24]. Cutin (from plant cuticles) [25], polyester bees [26], and shellac are some of the examples of naturally occurring polyesters while synthetic polyesters include poly(lactic acid), poly(ethylene terephthalate) (PET), poly(butylene succinate) (PBS) etc. [24].

Polyesters can be classified as aliphatic, semi-aromatic, or aromatic based upon their chemical composition in the main chain as shown in Figure 1.

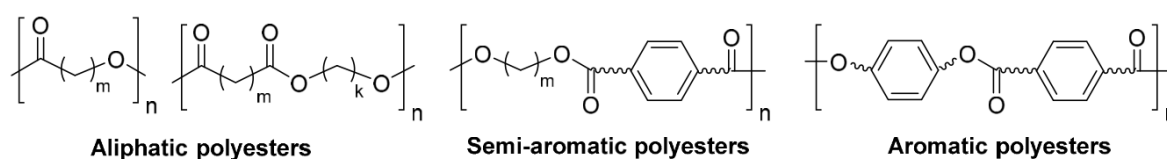


Figure 1. Chemical structure of polyesters.

Out of these types, aliphatic polyesters are extensively employed polyesters having widespread use in medical and pharmaceutical applications. Poly(lactic acid), poly(lactic-co-glycolic acid) (PLGA), poly(glycolic acid), and poly(ϵ -caprolactone) (PCL) are some of the conventional aliphatic polyesters that have been extensively used for the controlled delivery of drugs, peptides, and proteins, as well as in a variety of biomedical applications [27–29].

Polyesters can be synthesized by two primary methods: one is step-growth polycondensation while second is ring-opening polymerization (ROP). Each of these methods has pros and cons [30,31]. Polycondensation can use monomers derived from renewable resources that are inexpensive but require adverse conditions to remove by-products which can lead to undesired side reactions. ROP, on the other hand, produces no by-products and is carried out under relatively mild conditions, but requires catalysts that are often heavy metal salts, making the resulting products less suitable for pharmaceutical applications due to difficulty in completely removing the catalysts from the final product.

Enzymatic polymerization presents an alternative approach for the synthesis of both functional polyesters and conventional biodegradable polymers, offering distinct advantages [24,32]. This technique has gained prominence as a versatile and environmentally friendly method for polymer synthesis, utilizing enzymes as biocatalysts to drive chemical reactions in

a precise and efficient way [33–36]. Unlike conventional polycondensation techniques that employ catalysts primarily composed of metal salts (such as aluminum, germanium, tin, nickel, antimony, etc.), which may carry possible toxicity risks, enzymatic polymerization provides a solution to this concern [36]. Another advantage of employing enzymes as catalysts lies in the regioselectivity that is rendered to the polymers due to the synthesis process being carried out under mild reaction conditions. This leads to the development of predominantly linear polymers with minimum branching even in the presence of the monomers consisting of multiple hydroxyl groups, such as glycerol or various sugars [37,38].

Enzymatic reactions are governed by two fundamental characteristics. The initial theory, known as the 'key and lock' hypothesis, was introduced by E. Fischer in 1894. This theory explains the precise interaction between an enzyme and its substrate. In accordance with this concept, enzymes serve as catalysts by identifying and binding with a particular substrate, much like a key might easily fit into a lock. This recognition process causes the enzyme and substrate to form a complex in which the substrate, which resembles a key, precisely conforms to the enzyme in a geometrically favorable manner, facilitating the reaction to occur [39].

The second principle was elucidated by L. Pauling, which explains why enzymatic reactions take place under mild reaction conditions. Reason explained by L. Pauling says that activation energy which is needed to start a chemical reaction is significantly reduced compared to non-enzymatic reaction. Activation energy gets lowered due to formation of enzyme-substrate complex that actually stabilizes the transition state. As a result, enzymatic reactions exhibit remarkable rate accelerations, ranging from 10^6 to 10^{12} -fold, and in certain cases, even up to 10^{20} -fold [40,41].

Among the six enzyme classes designated by the Enzyme Commission, three of them, due to their high catalytic activity, have been utilized extensively for enzymatic polymerization. Hydrolases, transferases, and oxidoreductases are commonly used as catalysts in enzymatic polymerizations [42,43]. Out of these three enzymes, hydrolases are of particular interest as they have the capability to facilitate catalysis of the reaction in aqueous media. This happens when they facilitate hydrolytic break down of esters comprising fatty acids in aqueous media. More interestingly they can also catalyze esterifications and transesterifications in organic solvents [44]. Lipase, a form of hydrolases, particularly lipase B stands as the predominant biocatalyst utilized in the synthesis of polyesters. It is derived from *Candida antarctica*

(CALB) and it catalyzes the reaction through esterification and transesterification. CALB has been extensively studied for its potential in polyester production due to its stability, commercial availability, and ease of production [45,46].

Immobilization of enzymes is crucial to maintain their biological activity in organic media, which is essential for successful polyester polymerization and functionalization. The most commonly used method for immobilizing CALB is physical adsorption onto hydrophobic supports, such as the commercially available Novozym 435, which physically adsorbs the lipase on a macroporous acrylic resin. However, this approach presents certain limitations such as enzyme leakage, interaction of the polymer support, and solubility problems with polar solvents. To overcome these issues, other strategies, such as the physical trapping of CALB within poly(glycidol)-based microgels and the covalent immobilization of the enzyme on methacrylic resin, have been developed. As a result of this covalent immobilization of the enzyme onto resin, new commercial versions have been produced, e.g. Fermase CALB 10000. This approach renders integrity, reusability and easy removal of the enzyme [47,48].

Figure 2 provides an illustration of the catalysis process of polycondensation which is being catalyzed by CALB enzyme. Within the enzyme's active center, three residues of the amino acid configure the catalysis triad. These residues include serine (Ser105), histidine (His224), and aspartic acid (Asp187), that undergo electronic stabilization [49–52]. This active site also possesses two distinct pockets. A large hydrophobic one is referred to as the “oxyanion hole” which plays an important role in stability of the substrate's carbonyl group during intermediate synthesis. Next one is the lid which is another important feature of the enzyme. This lid plays its role by shielding the enzyme's active site when no lipid-water interface is present while it opens when interface is present allowing substrate access to the site [53].

The mechanism of CALB-catalyzed polycondensation starts with the acylation step when histidine pulls proton from serine. Nucleophilic Ser105 then interacts with substrate's carbonyl group. This interaction between nucleophilic serine and substrate forms the first tetrahedral intermediate. This intermediate is being stabilized by hydrogen bonds which can be found in the oxyanion hole. In the formation of this intermediate product, carbonyl group gets negative charge on its oxygen. Simultaneously, acyl-enzyme complex is formed when the carboxylic acid from Asp187 facilitates the His224 residue in pulling the proton R'O-H (the acylating phase). This liberation due to the acylating phase happens at same time when the byproduct is taken away from His224 during this procedure. This process is then followed by

deacylation step in which nucleophile attacks acyl-enzyme complex in a way that diol's alcohol reacts with the carbon of the carbonyl group. Hydrolysis occurs when the nucleophile is water, whereas alcoholysis takes place when the nucleophile is an alcohol. This leads to formation of second intermediate product. After deacylation, regeneration of enzyme occurs causing catalysis leading to esterification [54].

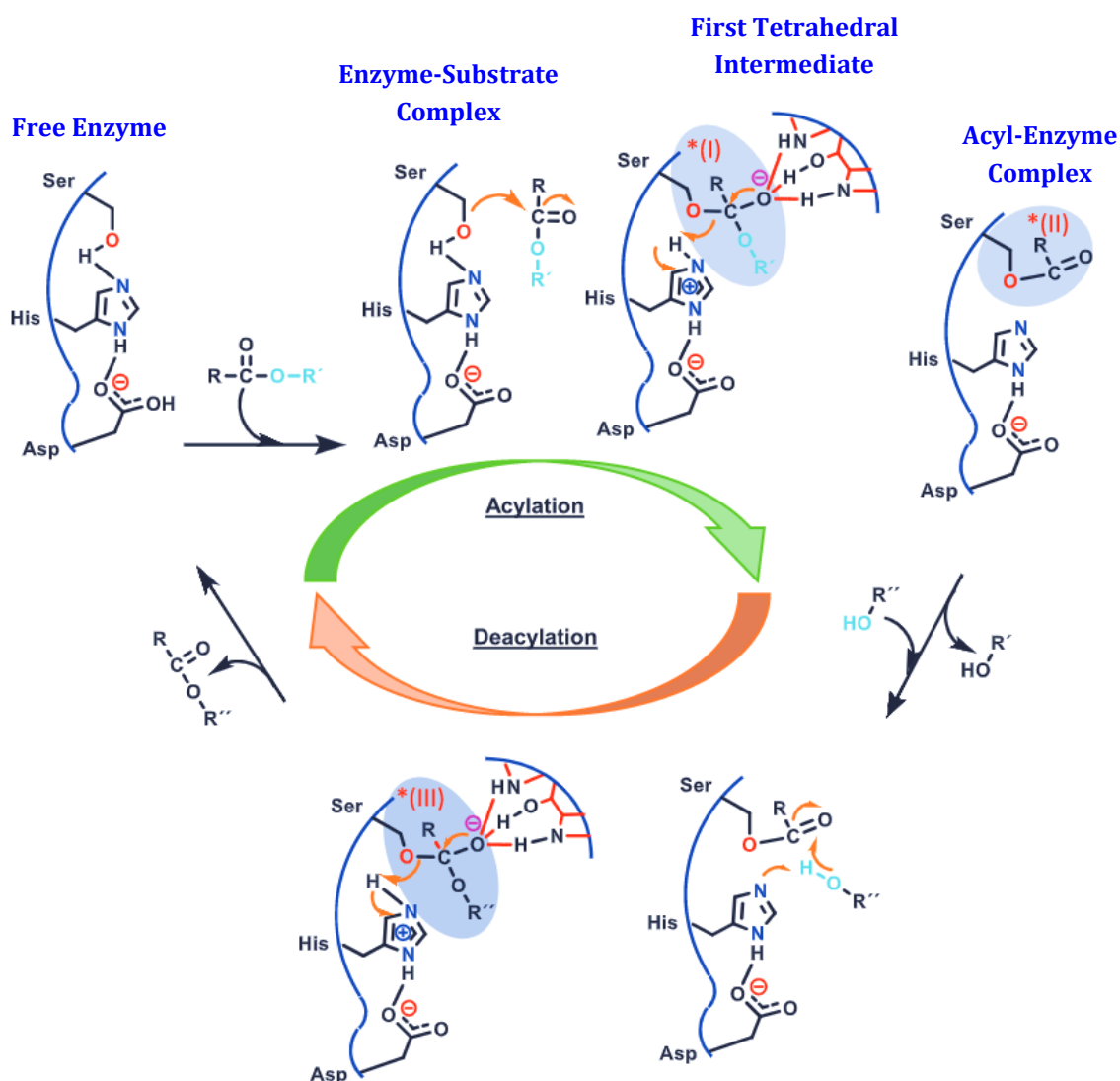


Figure 2. CAL-B (lipase) catalytic mechanism through acylation and deacylation adapted from [54].

Immobilizing enzymes allows for advancements not only in research on polycondensation reactions but also in industrial settings [55–57]. These reactions have been widely used in the synthesis of aliphatic polyesters which are based on polyols and diacids, however because the reactions are reversible, the syntheses frequently give low molar mass products [58]. The removal of byproducts such as water is an important factor in shifting the equilibrium towards polymerization [59]. Researchers have considered various strategies, such as the usage of activated esters, to overcome this limitation. Haloalkyl, alkyl, and vinyl esters are the commonly utilized activated esters, typically formed through the esterification of the carboxylic acid group. Utilizing vacuum conditions along with alkyl diesters in place of dicarboxylic acids increases the yield and molar mass of the polyesters while producing a much more volatile byproduct (alcohol). Scientists have carried out various two-stage and three-stage strategies by applying high vacuum to achieve high molar mass polymers via enzymatic polymerization. While azeotropic distillation has shown effectiveness in this regard, the approach that is frequently employed to eliminate byproducts from enzyme-mediated polymerization of polyesters remains the use of diesters in conjunction with vacuum treatment in a two-stage polycondensation process [60].

Another method involves employing halo esters like bis(2,2,2-trifluoroethyl) glutarate along with diols and shifting the equilibrium towards the synthesis of polyesters. Halogenated alcohols are produced in this process as byproducts. Researchers suggest that reactive end-groups' alcoholysis can be prevented by reducing the leaving group' nucleophilicity. However, it has been established that halogenated alcohols produced as byproducts can hydrolyse the activated ester end-groups. This happens because halogenated alcohols speed up the release of enzyme-bound water. Thus, it was concluded that this activation technique was not so efficient as anticipated in producing high molar mass polymers [61].

Vinyl esters, a kind of dicarboxylic acid alkylene esters, have also gained popularity recently for acylations catalyzed by lipase [62,63]. They have proven effective to produce products with larger molar masses without the usage of vacuum or high reaction temperatures. As a polycondensation leaving group, vinyl esters cause the formation of unstable enols (vinyl alcohols) as a byproduct. These quickly tautomerize to an aldehyde, causing an irreversible reaction that favors the formation of products. Formation of acetaldehyde can reduce enzyme activity upon reaction with vinyl esters, which can have an impact on the reuse of the biocatalyst. However, it has been observed that CALB is very stable when exposed to acetaldehyde in gaseous form at RT as compared to other enzymes. Divinyl esters in

comparison to dicarboxylic acids and diethyl esters have proved to be most efficient and reactive in synthesis of polyesters. They can form polyesters with molar masses ranging from 7K to 3K g/mol under given synthetic conditions and monomers used [59].

Vinyl esters offer several advantages over alkyl or haloalkyl esters in enzymatic polycondensations. One of the main advantages is that the esterification process is much faster, resulting in products with higher molar mass [64]. Additionally, the cleanup of byproducts does not require the use of vacuum or high temperatures, maintaining the regioselectivity of the lipases. This makes it easier to make linear polyesters featuring hydroxyl functionalities attached as pendant entities and allowing polyols to be used as possible monomers. The mild reaction conditions also allow for more effective control of hydrazide-containing monomer reactions, produce aromatic polyesters efficiently, and prepare reactive polyesters that retain the nonsaturated components from sustainable phyto-oils for subsequent crosslinking processes [54].

1.2.1. Functional polyester via enzymatic polymerization

Enzymatic polymerization gives a versatile option to synthesize functional polyesters, which are characterized by pendant functionalities including azide, halides, mercapto, hydroxyl, solketal group etc. In the conventional method of synthesizing functional polyesters, cyclic monomers are pre-modified initially, and then ring-opening polymerization takes place. This technique utilizes hazardous metal-based catalysts that are challenging to remove from the finished product in a number of protection-deprotection steps. Enzymatic polymerization is a suitable alternative to polycondensation processes, which produce hyperbranched or cross-linked polymers from monomers with more than two functional groups. The regio-, enantio-, and stereo-selective characteristics of enzymes enable the synthesis of functional polyesters from monomers with numerous functional groups. This also includes monomers derived from renewable sources, which are challenging to polymerize with traditional chemical catalysts.

Enzymatic polyesterification utilizes a large number of triglyceride-derived monomers to form polyesters. In multiple processes involving the presence of lipases, glycerol, has been used extensively in the synthesis of functional polyesters. Under given mild reaction conditions of enzymatic polymerization, the primary functional groups of glycerols (the hydroxyl groups) serve as the primary sites of reaction while 5-10% reacts at secondary groups achieving linear polymer with minimal branching such as poly(glycerol adipate) and

poly(glycerol sebacate) etc. There are numerous other multi-hydroxy alcohols which are produced by reduced sugars. Hydroxyl alcohols like xylitol, glucitol, sorbitol, mannitol etc. can also be subjected to enzymatic polymerization in the same manner as glycerol but their polymerization faces challenges due to their solubility in solvents with high polarity level like DMSO, DMF etc. Since it is known that they can change the enzyme's confirmation, these solvents have an unwanted effect on enzyme activity. Additionally, high boiling point of these monomers can lead to highly branched polymers in case of bulk polymerization. However, numerous studies suggest that the synthesis of sugar alcohols-based polyesters was successfully accomplished by employing a substantial proportion of CALB, typically ranging from 60% to 80% by weight relative to the total monomer mass. These reactions were conducted at a temperature of 60 °C within acetonitrile environment.

Factors like concentration of enzyme, presence of water, temperature, type of solvent, and pressure can all have a substantial impact on enzymatic polymerization processes. Due to the possible implications on enzyme selectivity and monomer configuration, the choice of organic solvent is particularly important. Low polarity solvents, like toluene, diethyl ether, and n-hexane, are generally preferred in enzymatic processes as compared to solvents with more polarity because the latter might end up in removing essential bound water from the enzyme's active site, breaking down the ester link and producing low molar mass products. Reactivity of the polymerization may also be affected by the radius of gyration and the way how polymer conforms in a solvent. Stoichiometric ratios of the precursors also play a vital role in obtaining high molar mass polymer via enzymatic polymerization. If the equimolarity of the precursors is disturbed, it may lead to formation of lower molar mass polymers. Similarly, high molar mass polyesters can be synthesized by increasing enzyme ratio to the concentration of substrate.

1.2.2. Modification of functional polyester

Polymer modification has gained a lot of attention in recent decades due to its versatility and by addressing various challenges required to produce better polymeric material, which, other way around, is an arduous task to perform through newly synthesized polymers. Polymer modifications have resulted in enhancement of material properties by transforming surface and bulk properties of the conventional polymers. Grafting, blending, crosslinking and composites are the primary techniques used to modify polymers for their enhanced physical and chemical properties [65]. I will be focusing here on grafting and crosslinking of

functional polyesters synthesized through enzymatic polymerization as they have been utilized in the current study.

1.2.2.1. Grafting of functional polyester

In general, different techniques can be employed to synthesize grafted copolymers; these include grafting-onto, grafting-onto with non-covalent bonding motifs, grafting-from and grafting-through strategies [66]. Enzymatically synthesized functional polyesters carry pendant functional groups which can be utilized for grafting purposes as per desirable properties [54]. Utilizing hydroxyl functionalities of poly(glycerol adipate), researchers have directly esterified them with fatty acids to produce amphiphilic comb-like polyesters. These polymers were further employed to develop nanoparticulate drug delivery systems [67]. Some other researchers grafted PGA with different amino acids and fatty acids to form varying sized nanoparticles [68–71]. Based upon the calculation of surface free energy via contact angle measurements, they were then able to predict best copolymer having characteristics in order to be used further for loading of drugs [72]. Researchers have also used other techniques beside esterification to synthesize graft copolymers. e.g. Naoulou *et al.* used different chemical strategies of atomic transfer radical polymerization (ATRP) and click chemistry to synthesize PGA based comb-polymers consisting of poly(ethylene oxide) and poly(ϵ -caprolactone) as crystallizable side chains. They provided a thorough explanation of the grafted copolymers' crystallization behavior before and after grafting onto PGA through light scattering techniques [73]. They further employed Langmuir isotherms and Brewster angle microscopy (BAM) to explain temperature-based phase transitions of the PCL-*b*-PEO crystals occurring at the air/water interface [74]. Pendant functionalities of enzymatically polymerized polyesters were successfully transformed into macro-initiators by Jbeily *et al.* in order to be utilized for ATRP. Poly(glycerol monomethacrylic acid) was then copolymerized via ATRP to PGA to make it a water soluble copolymer. Dynamic light scattering was utilized to assess its self-assembling behavior in an aqueous solution [75]. In another study, Kallinteri *et al.* focused not only on the improvement of the reaction conditions but they also showed a keen insight to emphasize on functionalizing the side groups, which improved the properties of the final material. They created a hydrophobic environment through the acylation process using caprylic acid (C8) and stearic acid (C18) at different quantities ranging from 20% to 100%, which facilitated the formation of nanoparticles and allowed for effective drug encapsulation. While the acylation process had a noticeable impact on particle size and encapsulation

effectiveness, it had slight effect on the cytocompatibility of HepG2 and HL-60 cell lines as they exhibited low level of toxicity [67].

Numerous studies have been conducted on the acylation of PGA with fatty acids, including evaluations of their physical characteristics, self-assembly into nanoparticles, and its potential for delivering lipophilic and hydrophilic pharmacological agents [70,72,76,77]. To fully understand their influence on the ultimate amphiphilic balance of the polymer, different fatty acids like butyric acid, behenic acid, stearic acid etc. and various degrees of substitution have been carefully examined. The nanoparticles are significantly shaped by these variables, which also have an impact on drug interactions, nanoparticle metabolism, and cellular absorption [77–79]. Notably, Weiss *et al.* revealed that a lower degree of substitution with various fatty acids suggests an interaction between the fatty acid chains within the particle core. This leads to enhancement of particle packing and overall reduction in nanoparticle size compared to unmodified PGA. These particles exhibited non-spherical morphologies with an interior lamellar structure. In contrast, higher degrees of substitution led to the formation of larger ellipsoidal or spherical particles, likely attributable to either expanded space occupied by the acyl groups or increased aggregation numbers. Interestingly, the chain length of the fatty acids did not exhibit a pronounced effect on particle size [77].

Tchory and his co-researchers formulated a unique procedure to track the penetration of nanoparticles (NPs) in animal models in order to demonstrate the adaptability of enzymatically synthesized functional polyester (PGA). What's noteworthy is that the researchers discovered that NPs with a size of about 100 nm, produced from PGA-Oleate end functionalized with PEG, demonstrated comparable penetration capabilities to considerably smaller (50 nm) commercially available polystyrene NPs. This method thus provided promising insights into *in vivo* distribution and drug encapsulation of modified PGA based nanoparticles [80].

Thompson *et al.* worked on another novelty of the enzymatically synthesized functional polyesters. Utilizing various molar proportions of polymer to drug, they conjugated ibuprofen to the polyesters using the free hydroxyl functionalities. Characterization of the conjugates revealed that the ibuprofen's addition to the polyester backbone changed the melting temperature (T_m), distinct crystalline domains, and the degree of polymer crystallinity. The relationship between the achieved drug loading in the polymer-drug conjugate with 100% conjugation and those in the 25% and 50% conjugates did not exhibit a direct proportionality.

The results of gel permeation chromatograph showed a nonlinear relationship between the polymer's molar mass and the degree of conjugation. The polymer-drug conjugates demonstrated reduced burst release and overall sustained drug release in comparison to unconjugated drug-polymer dispersions. It's possible that unconjugated ibuprofen was present in the conjugates which might have led to observed burst release. The analyses based on UV and chromatographic investigations revealed that the ester linkages connecting the polymer with ibuprofen, as well as those existing within specific polymer domains, exhibited an exceptionally high degree of stability. To potentially achieve a more faster ibuprofen release rate and a zero-order drug release profile, it was postulated that a transition to a more readily cleavable bonding configuration might be required [81,82].

Wersig *et al.* also investigated another anti-inflammatory drug (indomethacin) as a drug conjugate to poly(glycerol adipate). Using the drug-free polymer backbone as a comparison, they thoroughly analysed the properties of drug-polymer conjugate involving indomethacin-poly(glycerol adipate). Through a simple, quick, and economic esterification reaction aided by *N*-(3-di-methylaminopropyl)-*N'*-ethylcarbodiimide hydrochloride (EDC·HCl), indomethacin was successfully attached to the polymer. This reaction allowed for drug loading control and the modulation of characteristics that matched their particular needs in drug delivery. The indomethacin-poly(glycerol adipate) conjugates were analyzed via thorough characterization employing cutting-edge methods like NMR, GPC, FTIR, and UV-Visible spectroscopy. They further investigated the dynamic physical characteristics of the conjugates through differential scanning calorimetry, contact angle methods, and rheology with oscillation. Over the course of a month, *in vitro* drug release experiments were performed, and the results showed remarkably low release rates in a phosphate buffer saline (PBS) setting. It was found that indomethacin release was increased in the presence of lipase and somewhat acidic circumstances. This demonstrated, how poly(glycerol adipate)-indomethacin conjugates could serve as promising prodrugs for indomethacin's localized and sustained release. Additionally, these polymers could also provide adaptability for the development of various dosage forms. They also then used these formulations for development of nano- and microparticles, with a focus on investigating their release characteristics [18,83,84].

In another study, Suksiriworapong *et al.* performed first known conjugation of poly(glycerol adipate) with an anticancer agent. Their study demonstrated the possibility of linking Methotrexate (MTX) with poly(glycerol adipate). The MTX molar content in the MTX-PGA

conjugates was attained till 27.5 mol%. With regard to particle characteristics, physical stability under physiological settings, sustained stability of the polymer-drug linker over a period of one month, and enzymatic hydrolysis, these conjugates showed promising features. The MTX-PGA conjugate underwent self-assembly to form these nanoparticles. The size of the resulting nanoparticles was determined by the amount of MTX conjugated and the medium's pH. When subjected to hydrolysis at pH 7.4, these nanoparticles demonstrated strong chemical stability over the course of 30 d. They did, however, show enzymatic hydrolysis susceptibility, which led to the selective release of free MTX. Interestingly, when evaluated on 791T cells, the 30% MTX-PGA nanoparticles revealed just a slight decrease in efficacy compared to free MTX [85]. When compared to earlier studies employing MTX conjugated to human serum albumin, where the effectiveness was merely 1/300th of that observed with free MTX [86], this is a major improvement. The results of enzymatic degradation, along with details on cytotoxicity and what is known about PGA degradation in cellular lysosomes, evidently suggest that the polymer conjugation process employed with PGA does not need a complex linking process. This offered a novel potential for polymer-drug conjugates, allowing streamlined synthesis combined with improved therapeutic outcomes. However, constant efforts should be taken to increase the potency and specificity of these conjugates [85].

1.2.2.2. Crosslinking of functional polyesters

Crosslinking is a process that results in the formation of network architectures in polymers through multidirectional chain extension. Crosslinking can be achieved by condensation of monomers with functionality larger than two, by irradiation, vulcanization of sulfur, or other chemical processes via covalent bonds between monomers. Crosslinking boosts a polymer's resistance to heat, light, and physical forces by limiting chain movement and enhancing elasticity while also supplying dimensional stability, mechanical strength, and resistance to chemicals and solvents [87].

The degree of crosslinking, homogeneity or heterogeneity of the formed network, and crystallization are the main factors that determine how crosslinking influences the physical properties of polymers [88–91]. Reduced crystallinity in crystalline polymers can lead to increased softness, elasticity, and a lower melting temperature because chain alignment is hampered. In addition to changing the local molecular packing, crosslinking also decreases free volume and raises the glass transition temperature. Crosslinking also enhances creep

behavior by limiting viscous flow. Crosslinking is therefore very crucial to boost various properties of the polymers [87].

1.3. Crosslinked polymer network

Crosslinked polymers are utilized in wide-ranging applications across a diverse spectrum of technical and biological domains. These three-dimensional cross-linked structures known as polymer networks or gels are used in a variety of industries, from the rubber industry to the food industry to the bio-medical industry and the pharmaceutical sector [92–97]. Over the past few decades, a lot of experimental and theoretical research has been carried out over the crosslinked polymers, but there are still some issues that need to be resolved. A polymer gel represents a complex three-dimensional macromolecular structure originated from joining of polymer chains through crosslinking process. Crosslinking may happen through chemical or physical bonding [98]. The term "hydrogels" is frequently used to describe these crosslinked hydrophilic polymer chains when exposed to water [95]. Because of their extraordinary water-absorption capabilities, hydrogels have become an appealing target for researchers looking into the fundamentals of swollen polymeric networks. Hydrogels, with their unique attributes, have been extensively utilized across diverse technical fields. In addition to being essential components for contact lenses and protein separation, they serve as matrices for encasing cells and as controlled release mechanisms for medications and proteins [99].

Among the many properties that hydrogels possess, two of the most significant ones are maintaining elasticity and their ability to avoid dissolution into solvents. Contrary to uncrosslinked polymer chains hydrogels swell rather dissolved when exposed to solvents because they can hold much more solvent molecules inside their compact structure [100–102]. At low or moderate concentrations, where considerable chain entanglement is absent, hydrophilic polymers show Newtonian behavior in aqueous solutions. But when crosslinks between various polymer chains are added, the resulting gels exhibit viscoelastic characteristics, occasionally even exhibiting pure elasticity [99]. The entropy of a system increases when a dry polymer gel interfaces with appropriate solvent molecules. This happens as a result of the solvent molecules and network chains being mixed and dispersed. However, the stretching of the network chains triggered due to swollen or expanded network combats this tendency [103].

The Flory-Rehner theory [103] offers insights into the structure of hydrogels through an integration of thermodynamic and elasticity principle. In accordance with this theory,

hydrogel after immersing into solvent attains equilibrium with respect to its surroundings and is opposed by two forces. One is thermodynamic mixing force that is produced due to interaction of polymer chains with the solvent molecules while second is retractive force that originates due to elasticity of the polymer chains of the hydrogel. It thus may be described in relation to Gibbs free energy as follows [104–109],

$$\Delta G_{total} = \Delta G_{elastic} + \Delta G_{mixing} \quad (\text{eq. 1})$$

where ΔG_{total} is total Gibbs free energy, $\Delta G_{elastic}$ is the change in the elastic free energy while ΔG_{mixing} is the change in the mixing free energy.

Under constant temperature and pressure conditions, equation 2 can be derived from equation 1 with regard to number of solvent molecules as follows,

$$\mu_1 - \mu_{1,0} = \Delta\mu_{elastic} + \Delta\mu_{mixing} \quad (\text{eq. 2})$$

Equation 2 basically describes the chemical potential of the polymer gel where it relates to solvent in polymer gel as μ_1 while chemical potential of pure solvent molecules is represented by $\mu_{1,0}$. The chemical potential becomes identical in a state of equilibrium when solvent molecules are present inside and outside of the gel and thus can be expressed as, $\mu_1 = \mu_{1,0}$.

As a result, it is crucial to maintain equilibrium between elastic forces and the chemical potential differences brought on by mixing. By taking into account the heat and entropy involved in the mixing process, it becomes feasible to quantify the shift in chemical potential resulting from mixing. Rubber elasticity theory can also be used to determine how the chemical potential changes as a result of the elastic retractive forces imposed by polymer chains [110–113]. By combining the above two factors, an equation can be obtained for ascertaining the molar mass between neighboring crosslinks (\bar{M}_c). This equation is expressed as follows,

$$\frac{1}{\bar{M}_c} = \frac{2}{\bar{M}_n} - \frac{\bar{v}_1 [\ln(1-\nu_2) + \nu_{2,s} + \chi_1 \nu_{2,s}^2]}{[(\nu_{2,s})^{\frac{1}{3}} - (\frac{\nu_{2,s}}{2})]} \quad (\text{eq. 3})$$

where M_n is used to refer to a polymer's molar mass that was formed under similar circumstances, but without the use of a crosslinker. The polymer's specific volume is

simultaneously represented by \bar{v} , while the solvent's molar volume is denoted by V_1 . Additionally, the hydrogels' polymer volume fraction is shown by $v_{2,s}$ [111].

Thus, it can be deduced that the complex interaction between the miscibility of the polymer with the solvent vs potential elastic energy held within the polymer networks under stretched conditions, fundamentally controls the process by which hydrogels swell. To create hydrogels with optimal mechanical as well as swelling characteristics, it is crucial to employ fabrication techniques that consider the presence of functional groups like hydroxyl, carboxyl, amide etc. and create flexible three dimensional structures. These techniques should aim to achieve three objectives: (1) optimal water absorption and retention properties characterized by change in volume and density of the hydrogel, (2) hydrogel's facile regeneration, and (3) improved structural integrity. Structural properties due to hydrogel's water retention are significantly impacted by the effects of polymeric material, crosslinking density, surfactant content, and ionic strength. Specifically, factors like charge density, ionic strength of the solution, intrinsic elastic properties of the gels, existence of hydrophilic functionalities, and degree of crosslinking are crucial variables that have a profound impact on swelling ratio [114]. Generally speaking, hydrogels are known for their good biocompatible character due to their hydrophilic surfaces, which lead them to lower interfacial free energy when they come into contact with bodily fluids. This property of hydrogels minimizes protein and cell adhesion. The crosslinking of the polymer chains inside hydrogels contributes to their soft and elastic nature, which reduces irritation to the tissue around it [115].

1.3.1. Types of hydrogels

Hydrogels can be categorized into different classes based on their preparation procedures, ionic charges, structural properties [116] and crosslinking [99]. In terms of preparation methods, they can be categorized as (i) homopolymeric hydrogels, consisting of cross-linked networks made from a single hydrophilic monomer unit, (ii) copolymeric hydrogels, resulting from the cross-linking of two comonomer units with at least one exhibiting hydrophilicity to render swelling, (iii) multipolymer hydrogels, generated by the simultaneous reaction of three or more comonomers, [117] and (iv) interpenetrating polymeric hydrogels, which first cause a network to swell in monomer and then form a secondary intermeshing network structure by using these monomers [118]. Similarly, they can be categorized as cationic, anionic and neutral based upon the ionic charges. Structure wise, they can be classified as amorphous and semi-crystalline in nature [116]. While based upon the nature of bonds and crosslinking,

hydrogels can be classified as physical crosslinked hydrogels and chemical crosslinked hydrogels. Physical crosslinked hydrogels rely on weaker, reversible crosslinks. These are physical interactions that allow them to resist against dissolution of the crosslinked structure while chemically crosslinked hydrogels are held together by covalent bonds which provides integrity to their crosslinked structure [99].

Here, I will discuss physical and chemical crosslinking methods to produce hydrogels in detail.

1.3.1.1. Physical crosslinking methods to produce hydrogels

Hydrogels have the ability to undergo crosslinking and form reversible or physical polymer networks. These networks result from the interplay of molecular entanglements and a range of physicochemical interactions. Hydrogen bonding, hydrophobic associations, electrostatic interactions, and other non-covalent interactions etc. are just a few examples of the processes covered by these interactions. Although each interaction may be weak on its own, their presence together causes the hydrogels to behave in complicated and varied ways. One of the key advantages of these hydrogels is their responsiveness to external stimuli, including pH levels, solvent composition, ion concentration, and temperature. They differ from covalently bonded materials because of their adaptability. Next section will be focused into some of the primary hydrogels formed through physical interactions [119].

1.3.1.1.1. Ionic interactions

Crosslinking can be accomplished through ionic interactions that occur between polymers and monomers consisting of functional groups responsible for the ionization or protonation of these groups. Gelation can be initiated by adjusting the pH to induce these ionization and protonation interactions. These interactions can also occur due to electrostatic interaction between oppositely charged molecules. The physical gel known as an ionotropic hydrogel is formed when a polyelectrolyte reacts with a multivalent ion of the opposite charge [120]. Depending on variables including the concentration level, ion concentration, and hydrogen ion concentration of the solution, two polyelectrolytes with opposing charges can precipitate or gel, leading to the formation of a complex or polyionic product [121].

Alginate represents a well-established illustration of a polymer amenable to crosslinking through ionic interactions. It constitutes of a polysaccharide which can be crosslinked by calcium ions through residues of mannuronic and glucuronic acid [122]. It is noteworthy that

this crosslinking procedure can be conducted at ambient temperature and bodily pH. As a result, alginate hydrogels find extensive application as matrices for encapsulating viable cells [123] and facilitating protein release [124]. An interesting feature of this type of gelation is their ability to destabilize through a chelating agent by removing the calcium ions. Alginate microparticles made by spraying a sodium alginate solution into an aqueous calcium chloride solution can be coated with positively charged polymers like chitosan [125,126] and polylysine to control the release of proteins [126].

1.3.1.1.2. Hydrogen bonding

Hydrogen bonding can also be used as a noncovalent method to crosslink hydrogels. This type of crosslinking typically occurs when polymer chains possess compatible geometries. Physically cross-linked hydrogels with excellent injectability and resemblance to extracellular matrix can be produced from mixtures of natural polymers [127]. But without additional cross-linking mechanisms, hydrogels formed solely through hydrogen bonding have little real-world applicability. These hydrogels need additional cross-linking mechanisms to maintain their survival *in vivo* since the force used during injection can break hydrogen bonds [128].

Complexes of poly(acrylic acid) and poly(methacrylic acid) can be formed by combining them with poly(ethylene glycol) through hydrogen bonds, where their carboxylic group interacts with the oxygen of poly(ethylene glycol). Hydrophobic interactions also aid in the complexation of poly(methacrylic acid) [129]. In addition to poly(methacrylic acid) and poly(ethylene glycol), poly(methacrylic acid-*g*-ethylene glycol) has also been reported to exhibit hydrogen bonding [130,131]. Since the protonation of carboxylic acid groups is required for the formation of hydrogen bonds, it suggests that pH plays a substantial role in how these gels behave after swelling. Furthermore, the low pH-prepared poly(ethylene glycol) and poly(methacrylic acid) complex can be dissolved using ethanol. Upon injection, the system becomes gel due to ethanol diffusion from the liquid phase. Over time, the gel gradually dissolves due to dissociation [132].

1.3.1.1.3. Hydrophobic interactions

Polymers can also crosslink through hydrophobic interaction when they utilize their hydrophobic domains upon contact with the water. This phenomenon results in the "sol-gel" transition, a reversible heat gelation process. Using techniques like post-graft polymerization

or block copolymerization, a hydrophilic polymer and a hydrophobic polymer is initially coupled together to produce an amphiphilic polymer by crosslinking via hydrophobic interactions [120,133,134]. At lower temperatures, these amphiphiles are initially water-soluble, but gelation takes place with increase of temperature as a result of the accumulation of hydrophobic domains [135]. Examples of amphiphiles with both hydrophilic and hydrophobic groups include hydrogels made of poly(lactic acid)-poly(ethylene glycol) (PLA-PEG). These hydrogels can be employed *in situ* for various biomedical applications [9,136,137].

Various polysaccharides have the capacity for modification by incorporating hydrophobic chains that self-assemble, leading to the formation of nanohydrogels. For instance, pullulan can be modified with cholesterol to produce nanoparticles, as shown by Akioishi *et al.* [138–140]. These 20–30 nm nano-hydrogels may successfully encapsulate a variety of compounds, including proteins [140] and drugs [141]. Furthermore, pullulan can be modified to covalently bond it to galactoside lactoside to form nanoparticles that specifically target the RCA lectin receptor [119].

Another example is the formation of unilamellar polymer vesicles through use of another polysaccharide, chitosan that do so after its modification with Palmitoyl chains [142]. These vesicles with bio- and hemocompatible characteristics can then be utilized for encapsulation of various water-soluble drugs [143].

1.3.1.1.4. Stereo-complexation

Another unique phenomenon of physical crosslinking is stereo-complexation in which composite with different physical properties from the original polymers is formed, which involves the selective association of polymers with different stereochemistry [144]. Poly(lactic acid) based hydrogels are one such example where the polymers can be crosslinked with the help of stereo-complexation technique. In contrast to PLA alone, the stereo-complex formed by the robust bonding between D- and L-lactides exhibits remarkable attributes, including exceptional mechanical characteristics, an elevated melting point upto 230 °C, and increased stability. In order to synthesize the PLA-PEG hydrogels that are widely used in a variety of biomedical applications, PLA undergoes considerable stereo-complexation. Stereo-complexed hydrogels with a range of properties can be produced by modifying the molar masses and changing the mixing ratios of D and L-lactides [145,146].

PEG grafted to L- and D- lactides of PLA have been used for formation of various stereo-complex crosslinked hydrogels. Mao and colleagues have studied these PLA-PEG based hydrogels crosslinked through stereo-complexation employing both diblock and triblock polymers. The crosslinking within these hydrogels was achieved through formation of stereo-complexes between D- and L- lactides of PLA which was facilitated by linking bridges of triblock and diblock polymers [147].

1.3.1.1.5. Crosslinking through protein interactions

Using genetically modified proteins or antigen-antibody interactions, cross-linking can be achieved through protein interactions. Genetic coding can be customized to produce peptide sequences possessing particular physical traits, and the progress in genetic engineering has even opened the door to the development of synthetic amino acids [148]. Tirrell and Cappello were the early pioneers who utilized proteins for crosslinking [149,150]. Cappello and colleagues pioneered the development of a protein-polymer hybrid having higher molar mass, designed to mimic the amino acid sequence found in silk and elastin. In this composition, sheets or strands made of the insoluble silk-like segments are connected by hydrogen bonds. These protein mixtures that resemble silk elastin in particular, known as ProLastins, undergo gelation in physiological solutions.

By adjusting the temperature, the solution's properties, and the incorporation of additives, one can facilitate or obstruct hydrogen bond-induced polymer chain crystallization, thereby controlling the sol-gel transition [151]. Recombinant proteins exhibiting reversible gel-forming properties in reaction to variations in temperature or pH were developed by Tirrell *et al.* using recombinant DNA techniques. Proteins consist of two flexible center segments surrounded by terminal leucine zipper domains that are produced by a water-soluble polyelectrolyte. In aqueous solutions with a pH close to neutral and at room temperature, coiled aggregates form within the terminal domains and form crosslinked network. In this network, polyelectrolyte encaptures the solvent, preventing the polymer chain from precipitating. The terminal aggregates are split apart by an increase in pH or temperature, which dissolves the hydrogel. These hydrogels may be used for controlled cells and drugs release as suggested by the applied gentle pH and temperature conditions [152]. Another way of forming hydrogels is by crosslinking it through antigen-antibody interactions. In this procedure, researchers mainly focuses on attaching or binding polymer system to the antigen-antibody where hydrogel system responds to the antigens mainly by affecting its properties

[153–155]. Researchers have also used heat induced [156], change of pH [157] and ethanol addition techniques to form hydrogels with albumin [158].

1.3.1.2. Chemical crosslinking methods to produce hydrogels

When hydrogels are crosslinked through covalently linking, they are known as chemical hydrogels. They can also be referred as permanent gels. Chemical hydrogels have non-uniform characteristics, much like physical hydrogels do. They typically consist of regions with both lower and higher cross-linking densities leading to higher and lower degree of swelling (known as clusters). Chemical hydrogels can further be classified into following groups [120].

1.3.1.2.1. Crosslinking through radical polymerization

One of the procedures to obtain chemical hydrogels is to crosslink lower molar mass monomers through radiations. Poly(2-hydroxyethyl methacrylate) (pHEMA) based hydrophilic gel was one of the first polymeric crosslinked networks that was synthesized through radical polymerization. These HEMA based hydrogels were first pioneered by Wichterle and Lim that were utilized for biological use. The formation of this hydrogel system occurs via the polymerization of HEMA, coupled with a compatible crosslinker such as ethylene glycol dimethacrylate. This network of hydrophilic polymer chains had been the subject of significant scientific explorations in biological field due to its biocompatible nature [159]. Employing similar techniques, a diverse range of alternative hydrogel systems have been synthesized [160]. The properties of these hydrogels, including their swelling behavior, can be tailored by adjusting crosslinker's amount [99].

In addition to monomer blends consisting of vinyl functionality, water-soluble polymers that can also be radical polymerized to form chemically crosslinked hydrogels. This method has made use of a large variety of hydrophilic polymers from natural, semi-synthetic, and synthetic origins. Of particular interest, dextran, which is a fundamental natural polymer, plays a crucial role in preparing hydrogels designed to degrade over time. The bacterial polysaccharide dextran, which is mainly made up of α -1,6-linked D-glucopyranose units, has been utilized as plasma expanders. More specifically, dextran fractions with smaller molar masses, typically in the 40–100 kDa range, have worked well for this application [161]. This application has led to extensive documentation of dextran's pharmacological effects and

potential side effects. Consequently, dextran has been explored for its suitability in drug delivery, protein delivery, and as in imaging procedures [162].

Sawhaney *et al.*, devised a technique to create macromers featuring a core poly(ethylene glycol) block. This macromer was elongated with the help of α -hydroxy acid oligomers while through acrylic acid, it was terminated. Hydrogel was prepared through radical polymerization of these acrylic acid groups which was achieved by inducing radicals through subjecting an aqueous macromer solution to UV light, along with the introduction of a photoinitiator (2,2-dimethoxy-2-phenylacetophenone). These resulting hydrogels exhibited biodegradability, yielding products of degradation such as PEG, lactic acid, and oligo(acrylic acid). The rate of degradation spanned from 1 d to 4 months and was modifiable based on the chosen macromer, particularly the selection of the degradable linkage [163].

Zhang *et al.* presented an alternative method for developing hydrogels based on dextran. They introduced modifications in dextran by introducing a polymerizable group, like acryloyl chloride [164]. These modified derivatives of dextran were dissolved in *N,N*-dimethylformamide (DMF) alongside a macromer called poly(D,L-lactic acid) diacrylate (PDLLAM). Through the utilization of UV-induced polymerization, hydrogels were formed. The extent of swelling exhibited by these hydrogels was dependent upon various factors, including the hydrogel's dextran to PDLLA ratio, dextran substitution, and UV exposure time. These hydrogels underwent examination as carriers for albumin with controlled release properties. The composition of the gel specifically controlled albumin release, which was influenced by a mix of matrix-diffusion and degradation processes [165].

1.3.1.2.2. Crosslinking through enzymes

The enzymatic approach offers a significant benefit due to its ability to induce hydrogel crosslinking under gentle conditions, eliminating the requirement for utilizing low molar mass compounds such as monomers, initiators, and cross-linkers, as well as avoiding exposure to radiation or precursor modification to enhance crosslinking [99]. Enzymes are known for their high substrate specificity, minimizing the occurrence of unwanted byproducts during the crosslinking process. With this distinct feature, crosslinking kinetics can be precisely controlled and predicted, which in turn controls the rate of crosslinking and thus, this technique is well-suited for *in situ* gelation systems [166,167].

Transglutaminases function as enzymes that are dependent on calcium ions (Ca^{2+}). With this concept, Westhaus *et al.* developed a novel system designed to initiate gel formation under specific conditions. This system retained its liquid consistency when liposomes loaded with calcium were combined to transglutaminases and fibrinogen at ambient temperature. However, upon reaching a temperature of 37 °C, rapid gelation occurred. The heat application induced the breakdown of the liposomes, consequently releasing calcium ions into the surrounding fluid. This simultaneous release of Ca^{2+} ions activated the transglutaminase enzyme. The system's dual characteristic of having stability at room temperature and transformation into a solid state at 37 °C propose the potential use of this gel system as a matrix for delivering biological active substances [168].

1.3.1.2.3. Crosslinking through radiation

Within the array of techniques available for polymer grafting, gamma radiation is another method that can be used for grafting polymers [169] with an advantage of having no requirement of initiators and troublesome additives that could pose challenges for their removal from the product [170]. Without initiator and crosslinker, this method displays compatibility with a wide spectrum of vinyl monomers. It's worth highlighting that both polymerization and cross-linking processes can be triggered under ambient conditions and the radiation acts as a catalyst, initiating a co-polymerization mechanism that link the polymer matrix (the substrate material) with the monomer slated for grafting. This prompts the polymer matrix to generate reactive sites, primed to interact with the designated grafting molecule, thereby starting free radical polymerization [171].

Various hydrogels synthesized via irradiation have undergone investigation for their potential in controlled drug release. Bustamante-Torres and colleagues successfully prepared hydrogels by graft copolymerizing agar and AAc using gamma radiation. These monomers were easier to crosslink with the help of a Cobalt-60, which resulted in pH-responsive hydrogels suitable for charge-based and controlled drug release applications. Loading these hydrogels with ciprofloxacin and silver nanoparticles, they subjected them to evaluation against *Staphylococcus aureus* and *Escherichia coli*, revealing exceptional antimicrobial properties [172].

1.3.1.2.4. Crosslinking mediated by functional group interactions

These interactions involve reactions that take place covalently between the functional groups (primarily hydroxyl (-OH), carboxyl (-COOH), and amino (-NH₂) groups) within the polymers [173,174]. Covalent bonds are established between different chains of polymers through the interaction of functional groups that possess complementary reactivity [99]. Polymers having hydroxyl and amino functional groups can be crosslinked using molecules containing aldehyde groups. One often used technique is the formation of a Schiff's base, which is the result of an amino group and an aldehyde interaction. Notably, glutaraldehyde is an aldehyde cross-linking agent having reaction affinity with amino groups even in mild reaction environments and has been extensively studied in this field. This method is useful for cross-linking polysaccharides and proteins [119]. The drawback of utilizing glutaraldehyde, however, is that it is poisonous even at low concentrations, which may cause it to be released in the body during matrix decomposition leading to inhibition of the growth of the cell. Due to these toxic concerns, alternative small molecules with dual functionalities are being suggested as potential crosslinking molecules [175].

Crosslinking can also be performed through addition reactions as well as condensation reactions. Hydroxyl or amino functionalities undergo condensation reactions with carboxyl groups (or their analogs). These reactions can be commonly employed in polymer synthesis to produce polyesters and polyamides. One of the widely agents for inducing cross-linking in hydrophilic polymers is *N*-(3-dimethylaminopropyl)-*N'*-ethylcarbodiimide which induces so via amide linkages. For maximum control over cross-linking density and minimize potential side reactions, this agent is often paired with *N*-hydroxysuccinimide. Employing such compounds has enabled the cross-linking of biocompatible polymers like gelatin [176].

In a study on PEG-hydrogels that were crosslinked using the hydrolyzable polyrotaxane method was conducted by Yui and colleagues. The gel was made by threading α -cyclodextrins onto a PEG chain and capping it with biodegradable ester end groups. Then, carbonyl diimidazole was used to activate the hydroxyl groups of the cyclodextrins, and PEG-bisamines were used to crosslink the molecules. The hydrolysis of the ester groups led to the degradation of the gels. By varying the gel composition, the degradation time was varied that ranged from 500 to 2200 h. These particular gels were specially prepared as scaffolds for soft tissue regeneration [177].

1.4. Aims and objectives

Over the recent years, a variety of polymers have undergone investigation to serve a wide spectrum of pharmaceutical and biomedical needs [178–182]. Among these man-made polymers, aliphatic polyesters have experienced significant advancements, largely attributed to their promising ability to biodegrade and their compatibility with living organisms. These attributes have rendered them highly potential candidates for applications in the field of biomedicine [183–185]. Polymers belonging to the polyester family, notably poly(lactic acid) (PLA) and poly(glycolic acid), along with their copolymers like poly(lactic-co-glycolic acid) (PGLA), are extensively utilized synthetic biodegradable polymers. When these polyesters were first developed approximately 50-60 years back, they were especially synthesized to be biodegradable across a spectrum of biomedical and drug delivery applications. These polyesters were specifically designed to function as materials capable of biodegradation, serving a variety of purposes within the field of biomedicine and drug delivery [186–188]. Unfortunately, most of them tend to exhibit a robust hydrophobic nature and also lack additional functional groups extending from the main chain [189,190], which could otherwise facilitate grafting with polymers and bioactive like drugs, proteins, antibodies, and more [191–194]. As a result, the limitation of these functional groups attached to the polymer's backbone limits polymer's ability to adjust and achieve the desired characteristics of the material [23,195]. Unlike conventional polycondensation techniques that employ catalysts primarily composed of metal salts (such aluminum, germanium, tin, nickel, antimony, etc.), which may carry possible toxicity risks, enzymatic polymerization also provides a solution to this concern [196,197]. Researchers have also highlighted several drawbacks associated with poly(glycolic acid), PLA and PLGA. These include complex profiles for release and degradation, auto-degradation catalyzed by the polymers themselves, and the emergence of microenvironments characterized by their acidic properties. Scientific investigations conducted under *in vivo* and *in vitro* environments, have indicated the occurrence of remarkably low pH values, often falling below 2 [16–18,36,70,114,198,199].

Enzymatic polymerization offers an alternative method to the above mentioned polymers and their limitations, utilizing eco-friendly principles to synthesize functional polyesters. This process involves employing enzymes as biocatalysts, enabling the synthesis of aliphatic polyesters without resorting to metal-based catalysts that carry inherent toxicity risks in conventional polymerization techniques [24,32–34,36]. Research teams of Prof. Kressler and Prof. Maeder alongside a handful of other research groups, have been working to explore

enzymatically polymerized aliphatic polyester known as poly(glycerol adipate). Scope of the work is aimed to formulate various drug delivery systems, encompassing nanoparticles [70,77,83], micelles [200], microparticles [201], and as polymer-drug conjugates [18]. Furthermore, poly(glycerol adipate) which has previously been synthesized enzymatically, features a single pendant hydroxyl group in its constituent monomeric units. It has been utilized in drug delivery applications but it constitutes of an amphiphilic character while lacking water solubility [202].

The first part of my research work is aimed and focused around using enzymatic synthesis to produce aliphatic polyester. For this purpose, my aim was to synthesize poly(sorbitol adipate) through the transesterification of D-sorbitol with divinyl adipate. The sorbitol component of the linear polyester repeating unit features four pendant secondary OH-groups, rendering hydrophilicity to the polyester structure [38]. Utilizing the multiple hydroxyl functionalities in poly(sorbitol adipate) (PSA), my next aim was to graft PSA with poly(ethylene glycol) (PEG) side chains via the Steglich esterification mechanism. This grafting strategy serves the purpose of enhancing the hydrophilicity of PSA and subsequently the swellability of the resulting hydrogels. I then aimed at synthesizing bifunctional crosslinking agents based on PEG with varying molar masses. These crosslinkers will be crucial in the formation of PSA-based hydrogels and PSA-g-PEG based hydrogels, each contributing towards changing swelling profiles. Hydrogels were then subjected to crosslinking via Steglich esterification using above mentioned crosslinking agents. The utilization of enzymatically synthesized aliphatic polyesters to formulate crosslinked polymer hydrogels is something, which will be pioneered in. Comparison of swelling profiles involved not only the swelling behaviors across hydrogels with different crosslinker molar masses, but also reviewing the swelling profiles of PSA-based and PSA-g-PEG based hydrogels. To validate the successful synthesis of the aforementioned polymers and crosslinkers, they were then analyzed through ^1H NMR and ^{13}C NMR spectroscopy. In order to determine molar masses of the polymers, they were investigated through gel permeation chromatography (GPC), while their thermal properties were investigated using differential scanning calorimetry (DSC). For thorough assessment of the hydrogel's structural dynamics, aim was extended to measure them using various solid-state NMR techniques. The homogeneity or heterogeneity of the hydrogels was probed using ^{13}C Magic Angle Spinning (MAS) NMR Spectroscopy and ^1H Double Quantum (DQ) NMR spectroscopy. The diffusion coefficients of the hydrogels were determined through ^1H Pulsed field gradient (PFG) NMR spectroscopy.

Second phase of my research work focuses on the potential pharmaceutical applications of the synthesized hydrogels, employing various *in vitro* based techniques. Hydrogels based on PSA grafted to PEG were selected for this purpose because of its better swelling profile as compared to PSA based hydrogels. Firstly, polymers were subjected to evaluation for its degradation at different temperature and humidity conditions. Dynamic and equilibrium swelling behavior of hydrogels were performed to ascertain their water taking capacity and how it behaves with the passage of time. Swelling as a property holds foremost significance when hydrogels are employed as molecular release carrier [203–205]. Considering the equilibrium swelling profile, Flory theory (modified form) was used to understand the crosslinked structure of the hydrogels and how it responds to modifying the chain lengths of the crosslinkers [206,207]. For this purpose, different physico-chemical parameters like theoretical calculations of the polymer volume fraction, molar mass between two crosslinks, and mesh size of the hydrogels were derived. Crystallinity of the hydrogels was evaluated through X-ray diffraction examination. One of the most important aims was to evaluate the *in vitro* release characteristics of the hydrogels. For this purpose, hydrogels were thoroughly analyzed through fluorescence spectroscopy for its capability to release protein (BSA-TMR) as high molar mass molecule and dye (DY-781) as lower molar mass molecule, with an emphasis on the *in vitro* post-release dynamics of these molecules. Finally, hydrogels were evaluated for its cytocompatible characteristics.

2. Materials and methods

2.1. Materials

Novozyme 435, Lipase derived from *Candida antarctica* type B (CAL-B) and immobilized on acrylic resin, was purchased from Sigma Aldrich, St. Louis, MO, USA. It was vacuum dried over phosphorous pentoxide for 24 h prior to use. Sorbitol (98%) and divinyl adipate (96%) were purchased from Sigma Aldrich (Steinheim, Germany) and TCI GmbH (Eschborn, Germany), respectively. Phosphorous pentoxide ($\geq 99\%$), 4-(dimethylamino)pyridine (DMAP), anhydrous *N,N*-dimethylformamide (DMF, 99.8%), anhydrous tetrahydrofuran (THF, 99.9%), 1-ethyl-3-(3-dimethylaminopropyl)carbodiimide hydrochloride (EDC·HCl), dialysis membranes with 1,000 g/mol molar mass cut off (MWCO) and 10,000 g/mol MWCO (Spectra/Por®, made from regenerated cellulose) were purchased from Carl Roth, Karlsruhe, Germany. Deuterated chloroform (CDCl_3) and deuterated dimethyl sulfoxide (DMSO-d_6) were purchased from Armar (Europa) GmbH (Leipzig, Germany). α,ω -bis-hydroxy poly(ethylene glycol)_n (OH-PEG_n-OH, with n = 9 (400 g/mol), 23 (1000 g/mol), and 45 (2000 g/mol)) and α -methoxy, ω -hydroxy poly(ethylene glycol)₁₂ (mPEG₁₂-OH, molar mass: 550 g/mol) were purchased from Alfa Aesar (Kandel, Germany). DY-781 Amine (molar mass: 781 g/mol) and DY-784 NHS-ester (molar mass: 1188 g/mol) were purchased from Dyomics GmbH (Jena, Germany) while BSA-TMR (bovine serum albumin conjugated to tetramethylrhodamine) was purchased from Thermo Fisher Scientific Inc. (Waltham, MA, USA).

2.2. Polymer syntheses

2.2.1. Synthesis of poly(sorbitol adipate) (PSA)

PSA was synthesized by enzymatic polymerization as described as mentioned by Rashid *et al.* [38]. An equimolar amount of sorbitol (10.0 g, 54.9 mmol) and divinyl adipate (DVA) (10.88 g, 54.9 mmol) was added to a 250 ml three neck round bottom flask. The flask was connected with a reflux condenser having a calcium chloride drying tube and to a mechanical stirrer. It was then charged with 50 ml acetonitrile and stirred for 30 min at 50 °C until the temperature was equilibrated. Novozyme 435 (2.1 g, 10% w/w of total mass of PSA and DVA) was then added to start the polymerization. The reaction mixture was stirred for 92 h which was then stopped and diluted with DMF followed by the removal of enzyme beads by filtration with Whatman® filter paper. The concentrated filtrate was processed through

dialysis against deionized water for 7 d using a dialysis membrane with 1,000 MWCO (molecular weight cut off). Finally, the polymer solution was freeze dried to obtain the final pure product of PSA (Figure 3). The purity of the product was confirmed from ^1H NMR spectroscopy (Figure 8(a), Chapter 3). ^1H NMR (400 MHz, DMSO- d_6) δ (ppm): 4.95–4.58 (m, 2H), 4.57–4.33 (m, 2H), 4.28–3.86 (m, 2H), 3.82–3.72 (m, 2H), 3.61–3.34 (m, 2H), 2.38–2.18 (m, 4H), 1.61–1.41 (m, 4H).

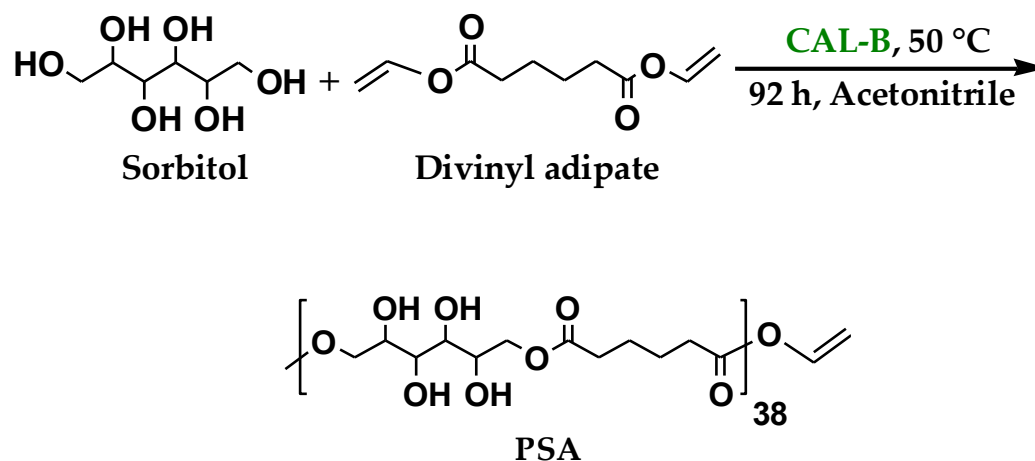


Figure 3. Synthesis scheme of poly(sorbitol adipate)

2.2.2. Synthesis of mono- and bifunctional PEG

In a typical procedure to synthesize bifunctional PEG based crosslinkers, α,ω -bis-succinyl poly(ethylene glycol) ((Suc-PEG $_n$ -Suc (disuccinyl PEG)) with $n = 9, 23, 45$ (where 9 = PEG-400, 23 = PEG-1000 and 45 = PEG-2000) (Figure 5) and α -methoxy, ω -succinyl poly(ethylene glycol) (monosuccinyl mPEG-550) (Figure 4), PEG was acylated by reaction with succinic anhydride through a procedure described elsewhere [208,209]. For the synthesis of monosuccinyl mPEG-550, mPEG of molar mass 550 g/mol was used while for the synthesis of Suc-PEG $_n$ -Suc (disuccinyl PEG), OH-PEG $_n$ -OH having molar mass of 400 g/mol, 1,000 g/mol, and 2,000 g/mol were used, respectively. Suc-PEG $_n$ -Suc ^1H NMR [(400 MHz, CDCl_3) δ (ppm), Figures 12, Chapter 3]: 4.28-4.20 (m, 4H), 3.73-3.57 [(m, 34H (Suc-PEG $_9$ -Suc); 92H (Suc-PEG $_{23}$ -Suc); 180H (Suc-PEG $_{45}$ -Suc)], 2.68-2.58 (m, 8H). monosuccinyl mPEG-550 ^1H -NMR [(400 MHz, CDCl_3) δ (ppm), Figure 9]: 4.25-4.21 (m, 2H), 3.68-3.51 (m, 50H), 3.35 (s, 3H), 2.67-2.56 (m, 4H).

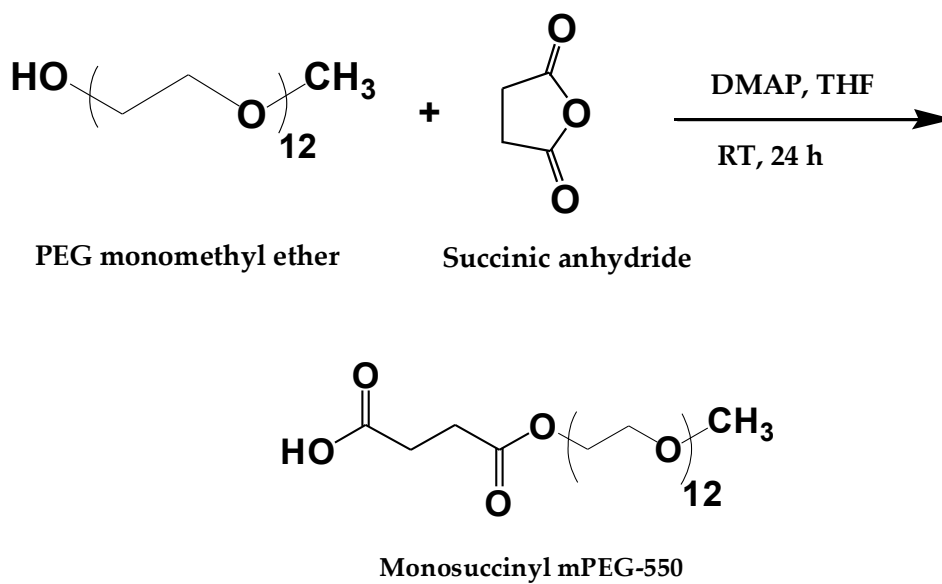


Figure 4. Synthesis scheme of monofunctional PEG (Monosuccinyl mPEG-550)

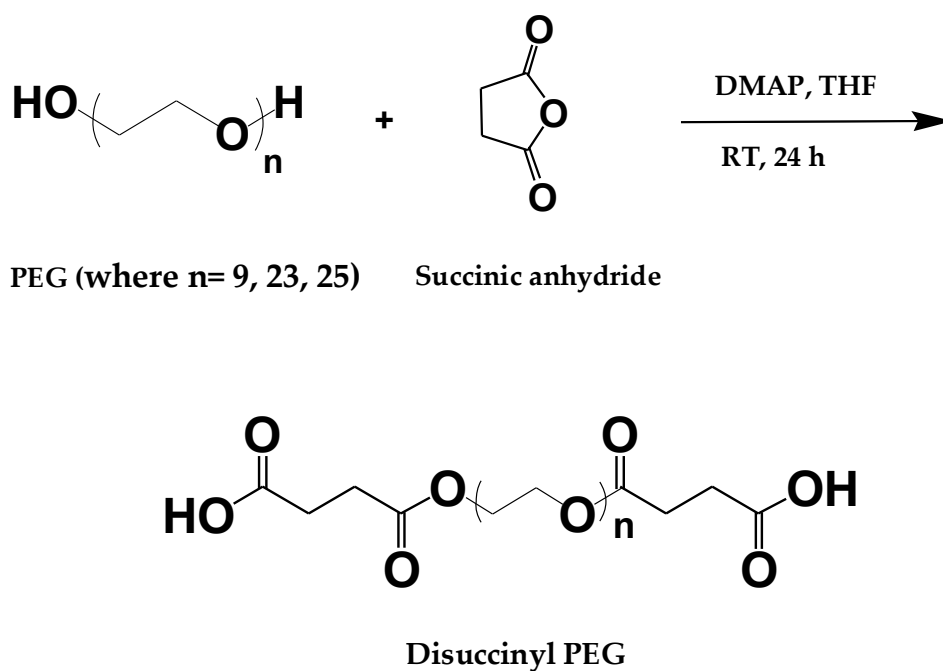


Figure 5. Synthesis scheme of bifunctional PEG (Disuccinyl PEG/Suc-PEG_n-Suc)

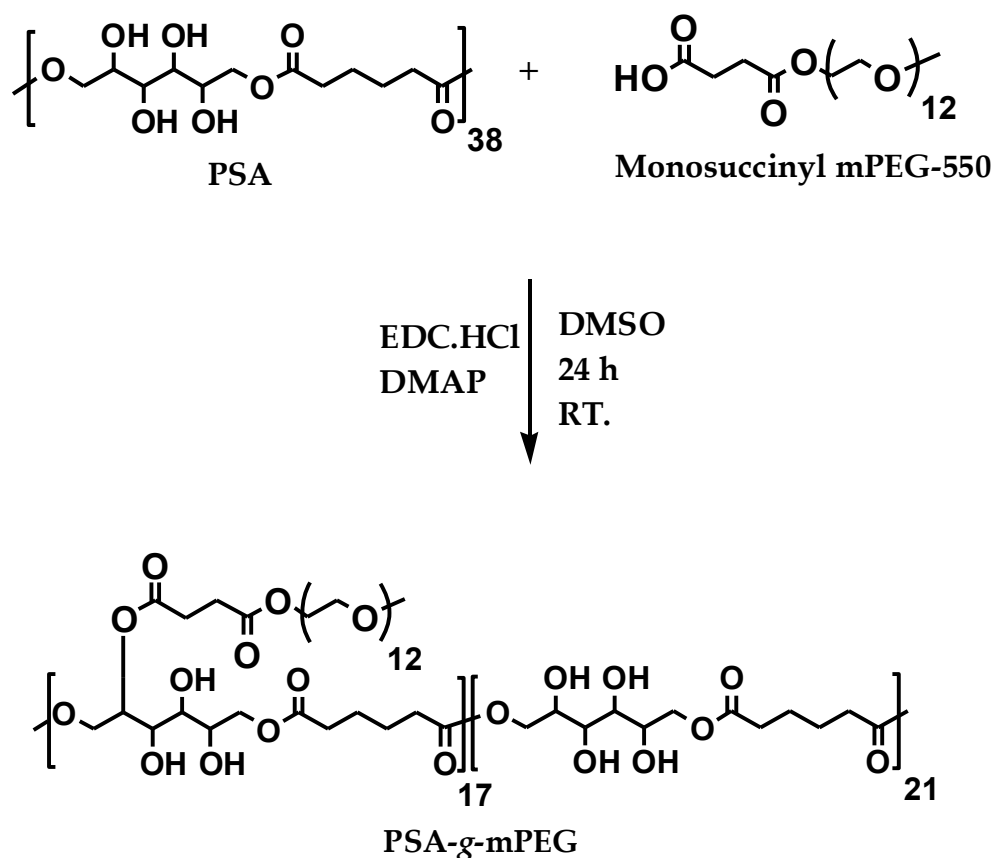


Figure 6. Synthesis scheme of PSA-g-mPEG

2.2.3. Synthesis of PSA-g-mPEG

PEG was introduced as a side chain to PSA through Steglich esterification [210] by reacting pendant hydroxyl groups of PSA and carboxyl groups from monosuccinyl mPEG-550 to get PSA-g-mPEG (Figure 6). The overall procedure is as follows. PSA (2.0 g, 27.3 mmol) and monosuccinyl mPEG-550 (2.67 g, 4.11 mmol) were charged into a two neck round bottom flask together with anhydrous DMSO. DMAP (0.15 g, 1.2 mmol) and EDC·HCl (2.35 g, 12.3 mmol) were added as catalysts to the reaction mixture. It was stirred for 24 h at room temperature. The crude product was then purified by dialyzing it in deionized water through a dialysis membrane for 5 d using a membrane with MWCO 10,000 g/mol. The diluted product solution was then freeze dried to obtain the final product. It is important to mention here that polymer batch used for the stability study was different from the batch used for the synthesis of hydrogels. Number average molar mass (M_n) of PSA was 11,000 g/mol. M_n of PSA-g-mPEG utilized for the stability study was 16,000 g/mol while M_n of PSA-g-

mPEG utilized for the preparation of hydrogels was 22,000 g/mol. ^1H NMR [(400 MHz, DMSO- d_6) δ (ppm) (Figure 8(b), Chapter 3)]: 4.95–4.58 (m, 2H), 4.57–4.33 (m, 2H), 4.16–4.08 (m, 2H), 4.28–3.86 (m, 3H), 3.82–3.72 (m, 2H), 3.56–3.45 (m, 50H), 3.23 (s, 3H), 2.61–2.52 (m, 4H), 3.61–3.34 (m, 2H), 2.38–2.18 (m, 4H), 1.61–1.41 (m, 4H).

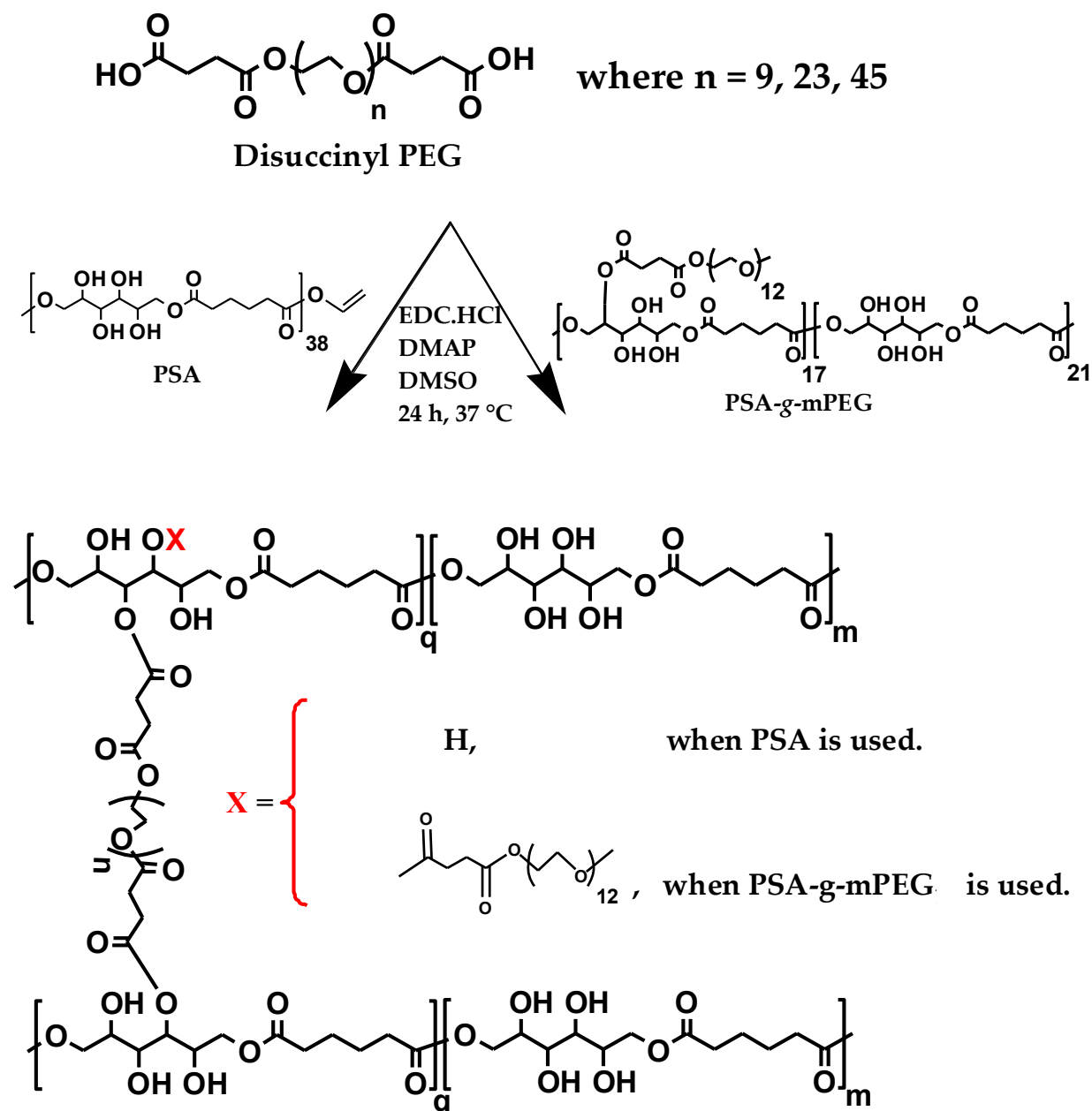


Figure 7. Synthesis scheme of PSA and PSA-g-mPEG based hydrogels through disuccinyl PEG (Suc-PEG $_n$ -Suc) Crosslinker

2.2.4. Hydrogel Syntheses of PSA and PSA-g-mPEG with disuccinyl PEG

Hydrogels were synthesized by esterifying free hydroxyl groups from PSA or PSA-g-mPEG with carboxyl groups of disuccinyl PEG (Suc-PEG_n-Suc where n = 9, 23, 45) using Steglich esterification as shown in Figure 7. In a typical experiment, PSA (0.500 g, 6.85 mmol) was first dissolved in DMSO followed by the addition of DMAP (0.17 g, 1.36 mmol) and EDC·HCl (2.61 g, 13.69 mmol) in a vial. At the end, Suc-PEG₉-Suc (1.23 g, 2.05 mmol) was added to the above reaction mixture and kept overnight at 37 °C to obtain PSA gels.

A similar procedure was adopted to synthesize hydrogels from PSA-g-mPEG. For both PSA and PSA-g-mPEG based hydrogels (Figure 7), three different Suc-PEG_n-Suc (disuccinyl PEG) crosslinkers with varying chain lengths were used (with n = 9, 23, 45). The same concentration, i.e. 30 mol% of cross-linker with respect to free hydroxyl groups available at the polymer backbone, was used for the syntheses of both types of hydrogels. The gels were then cut into discs and washed with deionized water as washing medium with repeated replacements for 3 times per day. The washing process was continued for 7 d in order to remove all impurities present in the hydrogels. Purified swollen hydrogel discs were then dried in a vacuum oven at 37 °C to obtain the dry and clean product. It is important to mention here that hydrogel batch used for temperature based swelling study, dynamic swelling study, determination of physico-chemical parameters, and loading/release studies was crosslinked at a rate of 35 mol% with respect to free hydroxyl groups available at the polymer backbone.

2.3. Instrumentation

2.3.1. Nuclear magnetic resonance (NMR) spectroscopy

2.3.1.1. Solution NMR spectroscopy

Solution NMR spectroscopy (¹H NMR and ¹³C NMR) was performed using an Agilent VNMRS spectrometer 400 MHz at 27 °C. Tetramethylsilane (TMS) was used as internal calibration standard. Deuterated solvents DMSO-d₆ and CDCl₃ were used for measuring spectra of polymers. Measurements were evaluated through MestReNova software (version 11.0.4) developed by Mestrelab Research, Spain, while the peaks were assigned using ChemDraw Ultra software (version 7.0) developed by CambridgeSoft Corporation, USA.

2.3.1.2. Solid state NMR spectroscopy

2.3.1.1.1. ^{13}C Magic angle spinning (MAS) NMR spectroscopy

^{13}C MAS cross-polarization (CP) and single-pulse (SP) experiments were performed on a Bruker Avance 400 spectrometer, operating at a ^{13}C Larmor frequency of 100 MHz. A 4 mm triple-resonance probe head was used and a MAS spinning frequency of 10 kHz was applied in all experiments. The sample temperature was controlled by a standard Bruker BVT-controller and calibrated with methanol. For all experiments, the temperature was set to 30 °C. The ^{13}C $\pi/2$ pulse length varied between 2.5 and 3.0 μs . The recycle delay was chosen such to meet the condition of $5 \cdot T_1$ of protons to allow complete restoration of the initial signal. The corresponding relaxation times were estimated by means of the saturation-recovery pulse sequence. Dry samples were filled into a Kel-F insert for a standard 4 mm rotor. The spectrum was referenced according to the COO resonance of alanine. The line assignment was carried out using ChemDraw Ultra software (version 7.0) developed by CambridgeSoft Corporation, USA.

2.3.1.1.2. ^1H Double quantum (DQ) NMR spectroscopy

^1H DQ NMR experiments were performed on a Bruker Avance III 200 MHz spectrometer using a static 5 mm Bruker probe. The temperature was controlled with a BVT-3000 heating-device with an accuracy of ± 1 °C. For all experiments, the temperature was set to 30 °C. ^1H $\pi/2$ pulse of 3 μs length and recycle delay of 2s were applied. For the DQ measurements, samples were swollen in D_2O to equilibrium and then filled into 5 mm glass tubes. A small amount of D_2O was added to prevent the samples from drying out during the long measurement. Afterwards the tube was sealed.

2.3.1.1.3. ^1H Pulsed field gradient (PFG) NMR spectroscopy

^1H PFG NMR spectroscopy was carried out for diffusion coefficient measurements. The spectra were recorded with a Bruker Avance II 400 MHz instrument at 30 °C. A stimulated echo with bipolar gradient (STEBP) was used as sequence with gradient time δ of 1-2 ms and a varying diffusion time Δ of 20–80 ms, depending on the sample. ^1H $\pi/2$ pulse length between 3.0 and 3.5 μs and recycle delays of at least $5 \cdot T_1$ were applied. Samples swollen in D_2O to equilibrium were filled into 5 mm glass tubes. The amount of HDO molecules in deuterated water is sufficient to obtain a good signal, which is comparable in intensity to the

signal from the hydrogel. No additional D₂O was added. This ensures that there is no signal contribution from free water outside the hydrogel. Since the diffusion measurements usually take few hours and were performed at room temperature, the drying of the samples could be neglected.

2.3.2. Gel permeation chromatography (GPC)

GPC measurements were performed using a Viscotek GPCmax VE 2002 having columns of HHRH Guard-17360 and GMHHR-N-18055 with refractive index detector (VE 3580 RI detector, Viscotek) at room temperature. DMF with addition of 0.01 M LiBr was used as an eluent with a sample concentration of 5 mg/mL. Poly(methyl methacrylate) (PMMA) was used as calibration standard and flow rate was 1 mL/min. The number average molar mass (M_n), the weight average molar mass (M_w), and the dispersity (D , M_w/M_n) were determined.

2.3.3. Differential scanning calorimetry (DSC)

The thermal analysis of all precursor polymers and dried gels was carried out using a DSC, Mettler Toledo DSC823e module, Mettler-Toledo GmbH, Greifensee, Switzerland under nitrogen flow. Pre-weighed 6-10 mg samples were placed in aluminum crucibles and were scanned against temperature ranging from -60 °C to 80 °C. A heating rate of 1 °C/min was employed and the nitrogen flow rate was 10 mL/min. All the samples underwent a specific heating and cooling cycle. This cycle consisted of 4 scans. In first cycle, the samples were initially heated to a temperature of $T = 125$ °C and maintained at this temperature for 5 min to reset their thermal history. In second cycle, they were then cooled down to $T = -60$ °C at a rate of 1 °C/min. Melting endotherm was then recorded by reheating samples to 80 °C at a rate of 1 °C/min. Finally, temperature was decreased to room temperature. Overall, the second heating scan data was used for records of melting endotherms was observed and stated as DSC data.

2.3.4. Swelling studies

Dried hydrogel discs were investigated for solvent uptake studies in D₂O. In a typical experiment, pre-weighed dry gel samples were immersed into water and allowed to swell for 24 h at room temperature until they reached their equilibrium state. Swollen discs of both PSA and PSA-g-mPEG based hydrogel were then taken out and rolled over blotting paper in order to remove water from the surface and then weighed. The degree of swelling was finally

calculated by taking into account the weights of dry and swollen samples. After the initial results, PSA-g-PEG based hydrogels were selected for molecular release study. Therefore, their dynamic and equilibrium swelling degree was calculated by taking into account the initial dry weight and swollen weights of hydrogels at different time intervals [206]. Rest of the procedure remained the same as stated above. Moreover, equilibrium swelling degrees for all samples were also calculated at RT, 37 °C, 50 °C, and 75 °C to evaluate and investigate the effect of increasing temperature on hydrogel samples as general physicochemical characteristics of this polymeric system. Measurement was done in triplicate. The degree of swelling was calculated using equation 4, where m_t refers to the mass of the swollen hydrogel while m_o refers to the mass of the dried hydrogel disc.

$$Q = \frac{m_t - m_o}{m_o} \quad (\text{eq. 4})$$

2.3.5. Polymer degradation/stability study

Polymers (PSA and PSA-g-mPEG) were exposed to 2 different types of temperatures. One part was placed at 4 °C in a fridge while the second part was placed at 40 °C and relative humidity (RH) of 75% to check its degradation and stability. For this purpose, 5 mg of polymer was taken at each time point and samples were kept in the fridge and Heraeus B 6760 climate chamber (Thermo Fisher Scientific Inc., Waltham, MA, USA). At various time points (d), samples were taken and measured through gel permeation chromatography (GPC). For GPC measurement, samples were analyzed at room temperature by using Viscotek GPCmax VE 2002. 5 mg/mL of sample was taken and dissolved in DMF (along with 0.01 M LiBr). For construction of calibration curve in order to obtain relative molar mass, poly(methyl methacrylate) was used while a 1 mL/min flow rate of eluent was adopted for the measurement. Samples were finally analyzed by determination of the number average molar mass (M_n).

2.3.6. Sol-gel fraction of PSA-g-mPEG hydrogels

Sol-gel fraction investigation of PSA-g-mPEG hydrogels was performed to know about the crosslinked and uncrosslinked portions of polymers on which these hydrogels are based. For that, hydrogel samples after synthesis containing uncrosslinked polymers, catalysts and solvent were immersed in double distilled water. Water was replaced 3 times per day for an interval of one week to remove the uncrosslinked portions of the hydrogels. It is pertinent to

mention here that all the reactants involved in the preparation of the hydrogels were soluble in water. Finally, hydrogels were dried and weighed. Sol-gel fraction of hydrogels was calculated with the help of the equations 5 and 6 [211,212] where W_0 refers to the initial weight of hydrogel precursors before reaction while W_1 refers to the final weight of dried clean hydrogels after washing.

$$\text{Gel fraction (wt. \%): } \frac{W_0 - W_1}{W_0} \times 100 \quad (\text{eq. 5})$$

$$\text{Sol fraction (wt. \%): } 100 - \text{Gel fraction} \quad (\text{eq. 6})$$

2.3.7. Structural parameters of the PSA-g-mPEG hydrogels

Swelling measurements were then utilized to calculate various physical parameters related to the polymeric structure of the PSA-g-mPEG hydrogel system. One of these important physical parameters is \bar{M}_c , molar mass between two crosslinks which allow for determining the degree of crosslinking between the polymeric chains. \bar{M}_c can be calculated through modified Flory-Rehner's theory by using equation 7 [206,207].

$$\frac{1}{\bar{M}_c} = \frac{2}{\bar{M}_n} - \frac{\frac{v_1}{V_1} [\ln(1-v_2) + v_{2,s} + \chi_1 v_{2,s}^2]}{[(v_{2,s})^{\frac{1}{3}} - (\frac{2}{\phi})v_{2,s}]} \quad (\text{eq. 7})$$

Here, \bar{M}_n represents polymer's number average molar mass prior to the crosslinking, i.e. of PSA-g-mPEG (17,500 g/mol), v_1 is the specific volume of the polymer, V_1 is the molar volume of the solvent, ϕ is the functionality of the crosslinker, i.e. 2, χ_1 is the polymer-solvent interaction parameter also called as Flory-Huggins parameter or chi parameter while $v_{2,s}$ is the polymer volume fraction in the swollen state. To solve this equation, polymer solvent interaction parameter (χ_1) was taken of PEG which is 0.426. This assumption was based on the fact that the molar mass of the PEG in the hydrogel system was larger as compared to the PSA and the swelling properties of the hydrogel system were driven by PEG. Similar type of assumption has been reported elsewhere also [213]. The specific volume of the polymer, v_1 , was determined by calculating the density of the polymer hydrogels. Molar volume of the solvent (V_1) is 18.1 mL/mol. Polymer volume fraction tells about the efficiency of the hydrogel systems to absorb water. It is calculated by taking the volume ratio of the dry hydrogels to the swollen hydrogels that can be related to the degree of swelling as well as to

the densities of the hydrogels and solvent. It can be calculated [206] by using the following equation 8.

$$v_{2,s} = \frac{\rho_s}{Q\rho_p + \rho_s} \quad (\text{eq. 8})$$

Here, ρ_s is the density of the solvent while ρ_p is the density of the dry hydrogel while Q is the degree of swelling.

Once \bar{M}_c is calculated, it is easy to determine the mesh size or correlation length of the respective hydrogels. The correlation length (ξ) is a common structural parameter used to describe the size of the pores of the hydrogels. It represents the linear distance between two neighboring crosslinks and can be calculated [111,214] through the value of

$$\xi = v_{2,s}^{-1/3} (\bar{r}_0^2)^{1/2} \quad (\text{eq. 9})$$

where $v_{2,s}$ is the polymer volume fraction of the hydrogels while \bar{r}_0^2 is the square of end to end distance between two adjacent crosslinking points and can be determined as

$$(\bar{r}_0^2)^{1/2} = l(C_n N)^{1/2} \quad (\text{eq. 10})$$

Here, l is the bond length which was assumed to be the average bond length of one PSA repeating unit, i.e. 1.51 Å. C_n is the Flory characteristics ratio that tells about the flexibility or rigidity of the polymer chain [215]. Since, Flory characteristics ratio of PSA hasn't been determined till yet, C_n of a polyamide, Nylon 6,6 (6.5) [216] is assumed whose one repeating unit has almost same length as of PSA. While N , the number of links per chain, can be determined as equation 11, where \bar{M}_c refers to the average molar mass between the two crosslinks while M_r is the molar mass of one repeating unit of the polymer chain. Molar mass of one repeating unit of PSA-g-mPEG is assumed here as 640 g/mol.

$$N = \frac{2\bar{M}_c}{M_r} \quad (\text{eq. 11})$$

2.3.8. X-ray diffraction (XRD) of PSA-g-mPEG hydrogels

Wide-angle X-ray scattering (WAXS) measurements of PSA-g-mPEG were performed with an Incoatec I μ S (Geesthacht, Germany) equipped with a microfocus source and a

monochromator for Cu K α radiation ($\lambda = 0.154$ nm). 2D scattering patterns are recorded using a Vantec 500 2D detector (Bruker, AXS, Karlsruhe, Germany).

The samples were kept in glass capillaries of 1 mm diameter (manufactured by Hilgenberg, GmbH, Malsfeld, Germany) while gel samples were measured in transmission mode having 01 mm thickness. The exposure time was 3 min. The distance between the sample and detector was 9.85 cm for wide-angle scattering experiments.

2.3.9. Loading study of the BSA-TMR and DY-781 into PSA-g-mPEG hydrogel matrices

In order to assess release pattern of lower and higher molar mass molecules from PSA-g-mPEG hydrogel matrices, DY-781 as lower molar mass molecule (molar mass: 781 g/mol) and model protein bovine serum albumin conjugated with tetramethylrhodamine (BSA-TMR) (molar mass: 66,000 g/mol) as high molar mass molecule, were loaded into hydrogels as follows. In detail, BSA-TMR solution was prepared by dissolving 100 μ g of BSA-TMR in 1 mL phosphate buffer saline having pH 7.4 at a concentration of 0.1 mg/mL (PBS) while DY-781 was prepared by dissolving 10 μ g of DY-781 in 1 mL phosphate buffer saline (PBS) having pH 7.4 at a concentration of 0.01 mg/mL. Different dried hydrogel samples having diameter of 3mm (PSA-g-mPEG crosslinked with disuccinyl PEG-400, PSA-g-mPEG crosslinked with disuccinyl PEG-1000, and PSA-g-mPEG crosslinked with disuccinyl PEG-2000) were then placed in these solutions for 48 h. Hydrogels were allowed to swell so that BSA-TMR and DY-781 may diffuse inside hydrogel samples. After 48 h, hydrogels were then subjected to freeze drying in order to get dried hydrogel samples. Loading efficiency was calculated keeping in view the concentration of the initially prepared solutions and loaded concentration inside hydrogels measured through fluorescence spectroscopy. Additionally, DY-784 was also loaded through the same method as described before for an illustration of dye loaded hydrogels. MaestroTM imaging system (Cambridge Research & Instrumentation Inc., Hopkinton, MA, USA) was used to capture fluorescence images by using near-infrared filter set. A filter set designed for near-infrared (NIR) wavelengths, including a 710 nm to 760 nm excitation filter and an 800 nm long-pass emission filter, was employed to capture the DY-784 signal. Image cubes were systematically acquired in 10 nm increments spanning the range of 780 to 950 nm. The analysis of these images was conducted using MaestroTM software (Version 2.10.0). The exposure time was automatically optimized, and the software correlated the total fluorescence signal to the corresponding value.

2.3.10. Release study of the BSA-TMR and DY-781

BSA-TMR and DY-781 loaded hydrogel samples were then subjected to a release study in order to evaluate their release from these hydrogel matrices. For this purpose, dried hydrogel samples were taken and placed in glass vials having conserved PBS pH 7.4 as the release medium. Glass vials were placed in a shaking water bath at 60 rpm and 37 °C temperature. The water bath was protected from the sunlight. 500 µL of aliquots were taken at different time intervals and were replaced with the same volume of fresh PBS in order to maintain the sink conditions of the release media. BSA-TMR and DY-781 aliquots were then analyzed through fluorescence spectroscopy by using FluoroMax-4 spectrofluorometer (HORIBA Jobin Yvon GmbH, Bensheim, Germany). The detection of the DY-781 signal involved a single-point acquisition with an excitation wavelength of 784 nm and an emission wavelength of 796 nm while for BSA-TMR excitation wavelength was 535 nm and emission length was 576 nm. Measurements were conducted in a 10 mm quartz cuvette, and the data obtained were analyzed using FluorEssence™ software (HORIBA Jobin Yvon GmbH, Version 3.8.0.60). The final calculation of the release data was done by constructing a calibration curve of BSA-TMR and DY-781. The experiment was performed in triplicate.

2.3.11. Cytotoxicity study of PSA-g-mPEG hydrogels

In vitro cell toxicity studies were performed for all three PSA-g-mPEG hydrogel samples that were utilized for release study. They were PSA-g-mPEG crosslinked with disuccinyl PEG-400, PSA-g-mPEG crosslinked with disuccinyl PEG-1000 and PSA-g-mPEG crosslinked with disuccinyl PEG-2000. Hydrogels were exposed to 37 °C for a longer period of time till they degraded to solution form. Two different cell lines were used. The first was the 3T3 cell line which is a murine embryonic fibroblast cell line originally isolated from kidney tissue, while the second cell line used was NHDF which is a normal human dermal fibroblast cell line originally isolated from a human foreskin sample.

Seeding of the cells took place in 96 well plates (TPP® tissue culture test plate flat bottom, TPP Techno Plastic Products AG, Trasadingen, Switzerland). These cells were grown in an incubator (Heraeus HeraCell CO₂ incubator, Thermo Fisher Scientific Inc., Waltham, MA, USA) in 100 µL culture media at 37 °C and 5% CO₂ for overnight. In case of the NHDF cell line, the culture medium used for the cultivating of the cells consisted of Dulbecco's Modified Eagle Medium (DMEM; Sigma-Aldrich GmbH, Taufkirchen, Germany), 10% (v/v) fetal bovine serum (FBS, Sigma-Aldrich GmbH, Taufkirchen, Germany) and 1%

penicillin/streptomycin solution (Sigma-Aldrich GmbH, Taufkirchen, Germany). 4 mM sodium pyruvate was added in addition for the culture medium in case of 3T3 cell line. Column 1 of the well plate was left blank without any seeding of cells to get the background signal. Column 2 was considered as a negative control as cells were left untreated to get 100% vitality while column 3 was made positive control by treating cells with 0.05% (v/v) Triton® X-100 solution to get 0% vitality (or 100% cell death). In the remaining columns of the well plates, hydrogel solutions were added to the cells and incubated for 4 h, 24 h, and 96 h.

Resazurin assay was used to determine the viability in % by metabolic activity of the cells. 20 µL of Resazurin solution (440 µM) was added to the well plate followed by its incubation for 2 h. Well plate was then placed in a multi-mode cell imaging reader (Cytation™ 5 cell imaging reader, BioTek Instruments Inc., Winooski, VT, USA). Using a filter set with an excitation wavelength of 531 nm and an emission wavelength of 593 nm, fluorescence intensities were recorded. The final cell viability percentage was then determined by taking into account the negative control after subtracting the blank (background signal).

3. Results and Discussion

3.1. Polymer syntheses

Poly(sorbitol adipate) (PSA) was synthesized through lipase CAL-B catalyzed polycondensation reaction using the sugar alcohol sorbitol and divinyl adipate. The selection of divinyl esters was preferred over dicarboxylic acids or dialkyl esters because the latter ones result in reaction by-products like water, methanol etc. which require vacuum and high temperatures in order to be removed from the reaction mixture [217]. Another reason to select divinyl adipate is connected with the fact that relatively high molar mass polyesters are obtained. Here, the byproduct vinyl alcohol, which is not stable and tautomerizes spontaneously to acetaldehyde, leaves the reaction as a gas. This process drives the reaction irreversibly towards the forward direction [218–220]. The sugar alcohol sorbitol is selected since the two primary OH-groups are converted during the polycondensation process but four secondary OH-groups per repeat unit of the polyester remain free which guarantee the water solubility of PSA [202].

Linearity of polymer is attained due to the highly reactive nature of the enzymes that react specifically and selectively with the primary functional groups rather than secondary functional groups [221]. This regioselective nature of enzymes enables the formed polymer to be utilized later on for crucial modifications. In this case, it leaves secondary hydroxyl groups to be used for further modifications.

Regioselectivity of these enzymatically catalyzed reactions is attained by conducting polymer synthesis at lower temperatures rather than at higher temperatures. Synthesizing a polymer at a lower temperature leads to a linear polymer while polymer synthesis at higher temperature results in a branched polymer as well as a polymer with high molar mass [202,222].

The PSA structure was confirmed from ^1H NMR, ^{13}C NMR, and ^{13}C MAS NMR spectra given in Figure 8 (a), Figure 10(a), and Figure S1 (Supplementary Data), respectively.

The objective was to synthesize biocompatible PSA hydrogels which can be used as hydrogel for potential applications in pharmacy and medicine. For this purpose, PSA was firstly modified by grafting with PEG chains. This further improves the hydrophilicity of the polymer [223]. PEG has been known as a versatile biocompatible polymer with a well-

recognized safety profile. For these reasons, it has been in use for decades for different purposes in the pharmaceutical industry [224]. One of the many important purposes for its use inside the pharmaceutical industry is to graft it to biodegradable polymers and enhance half-life of various drugs [223,224]. In addition to its benefits, PEG has been documented to trigger antibody formation within human body which may diminish the therapeutic effectiveness of the drugs [225,226].

To achieve the grafting reaction, mPEG-550 was firstly reacted with succinic anhydride in the presence of 4-(dimethylamino)pyridine (DMAP) to obtain the monofunctional α -methoxy, ω -succinyl poly(ethylene glycol) (monosuccinyl mPEG-550) (Figure 4, synthesis scheme, Chapter 2). The reaction was verified by ^1H NMR spectroscopy (Figure 9) through integrals of methyl peak (b) and methylene peak (d).

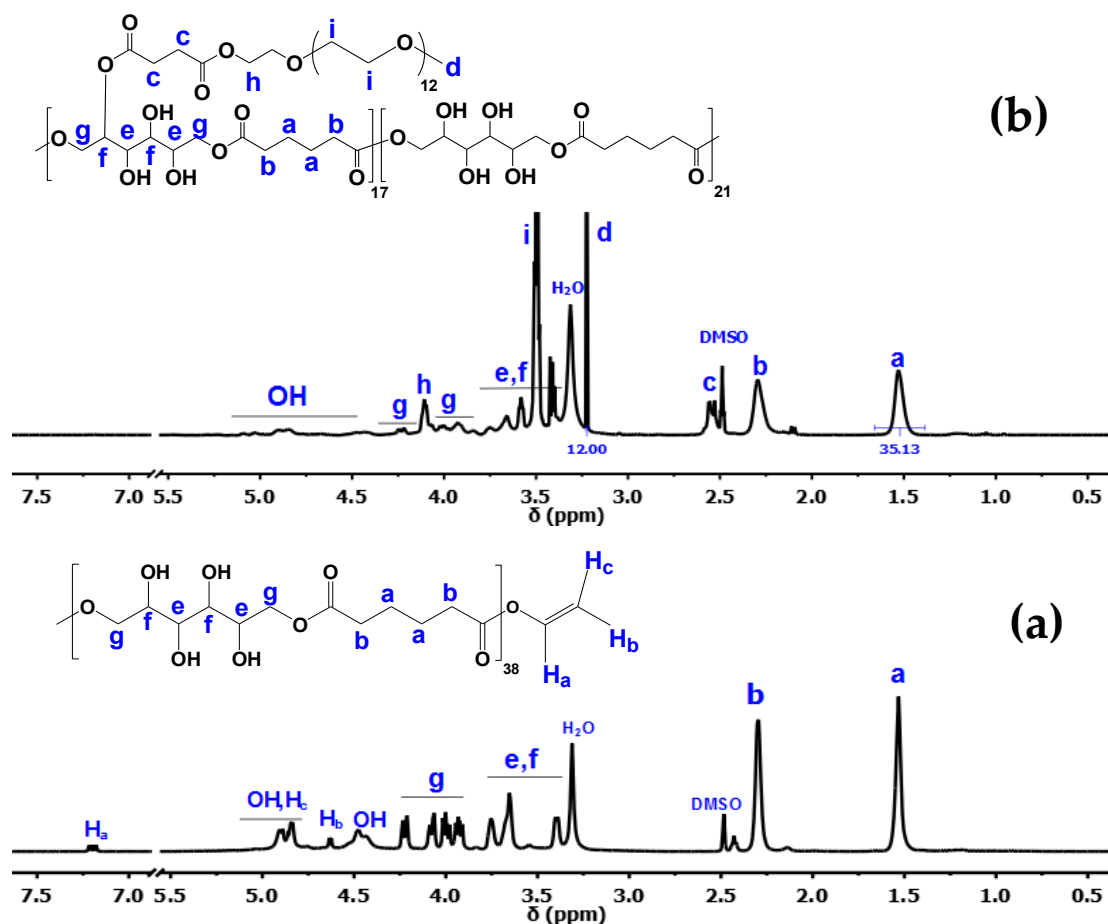


Figure 8. ^1H NMR spectra of (a) PSA and (b) PSA-g-mPEG measured at 27 °C using DMSO-d_6 as solvent.

To synthesize PSA-g-mPEG, Steglich esterification was adopted for the grafting procedure via the reaction between free hydroxyl groups from PSA and carboxyl groups from monosuccinyl mPEG-550. The synthesis of PSA-g-mPEG can be confirmed from ^1H NMR (Figure 8 (b)) and ^{13}C NMR spectra (Figure 10(b)). The appearance of the methyl peak at 3.23 ppm and methylene peak at 3.50 ppm of PEG in the ^1H NMR spectrum while in the ^{13}C NMR spectrum, the carbon signal of the methyl group at 58.10 ppm and the carbon signal of the methylene group at 69.85 ppm of PEG, verifies the grafting of mPEG-550 chain to PSA. Equation 12 is employed for the calculation of the degree of grafting in mol%.

$$\text{Degree of grafting} = \frac{1/3 f d}{1/4 f a} \times 100 \quad (\text{eq. 12})$$

Where d represents the protons of the methyl group of PEG and a represents the protons of the methylene groups of PSA.

The degree of grafting is calculated as ~ 45 mol% per polymer chain, i.e. nearly one out of eight OH-groups is esterified with monosuccinyl mPEG-550. The degree of grafting can also be confirmed by taking the same ^1H NMR integrals of the mentioned peaks with CDCl_3 as solvent given in Figure S2 (Supplementary Data).

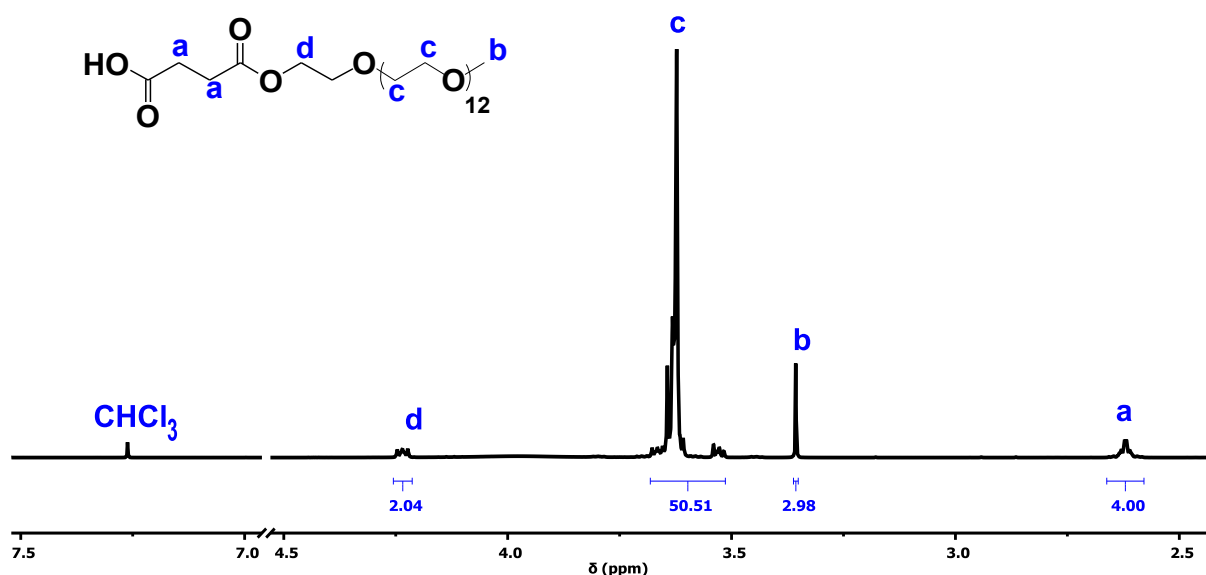


Figure 9. ^1H NMR spectrum of monosuccinyl mPEG-550 measured at 27 °C using CDCl_3 as solvent.

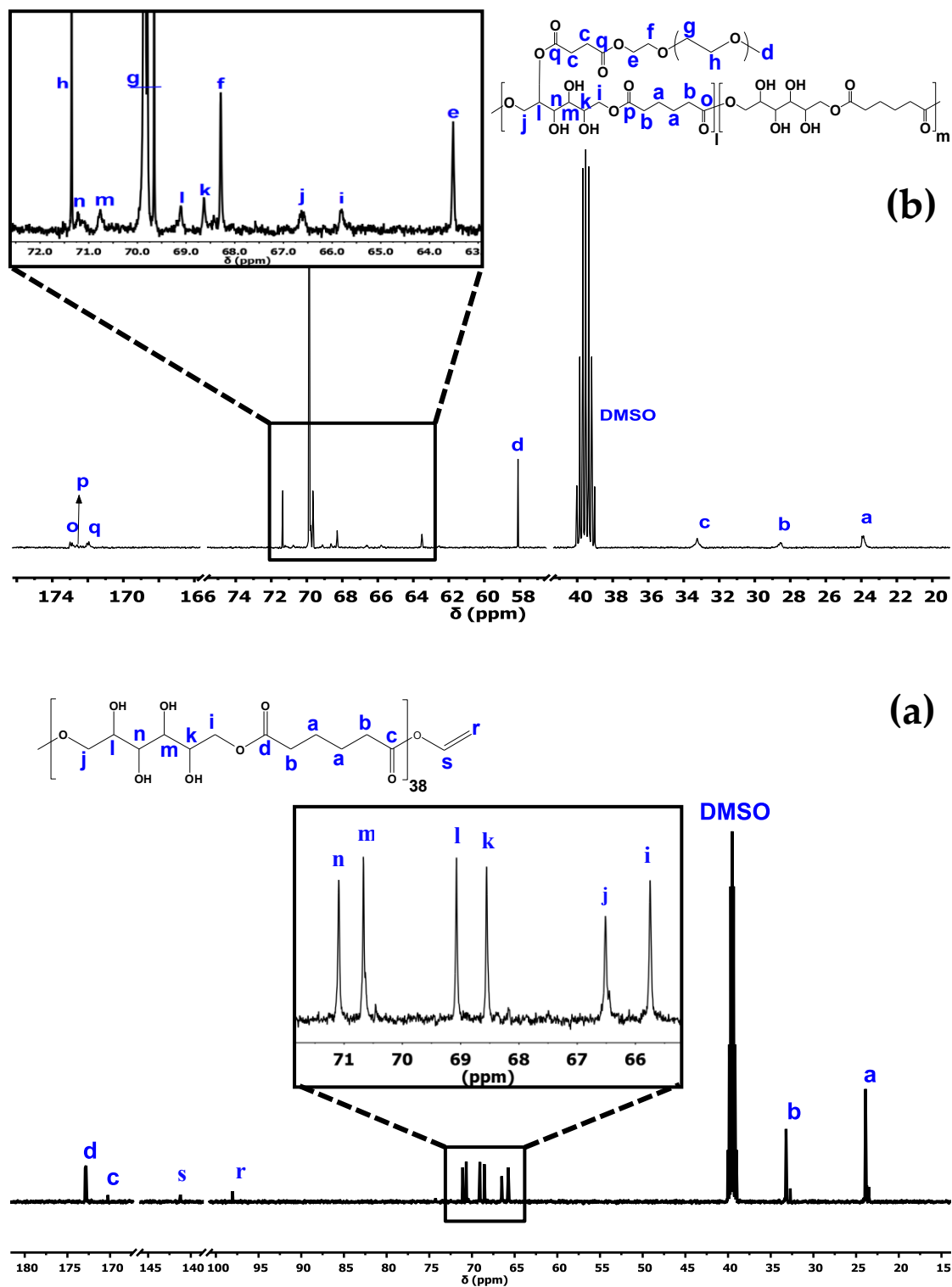


Figure 10. ^{13}C NMR spectra of (a) PSA and (b) PSA-g-mPEG measured at 27 °C using DMSO- d_6 as solvent.

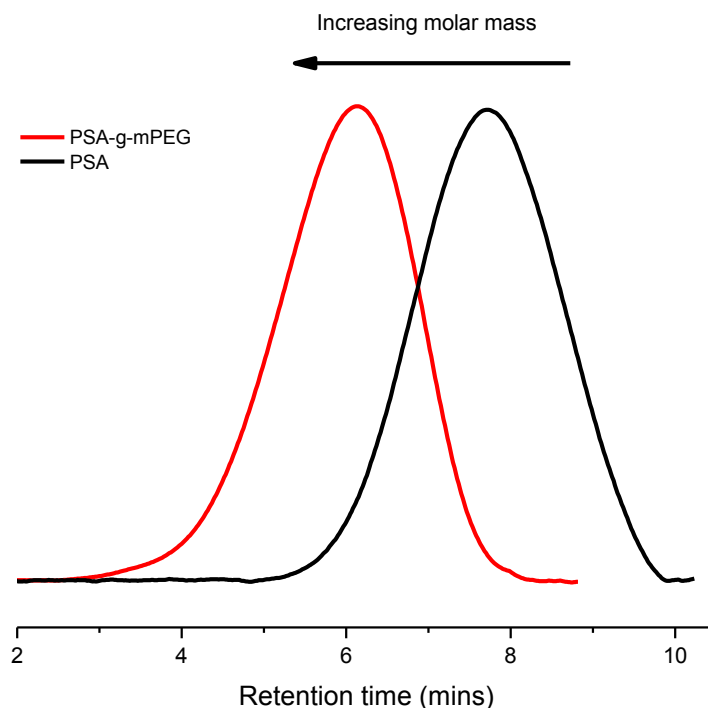


Figure 11. GPC traces of PSA before and after modification with monosuccinyl mPEG-550.

The grafting was also verified by GPC traces through a shift towards shorter retention time (Figure 11). Suc-PEG_n-Suc (disuccinyl PEG) was synthesized through carboxylation of OH-PEG-OH on both sides with succinic anhydride (Figure 5, synthesis scheme, Chapter 2). By the same procedure, as followed for the synthesis of monosuccinyl mPEG-550, esterification took place between OH-PEG-OH and succinic anhydride to get disuccinyl PEG (Figure 6, synthesis scheme, Chapter 2). Succinylation on both sides of PEG was verified by ¹H NMR spectroscopy (Figure 12) by taking integrals of methylene peak (b).

Using Suc-PEG_n-Suc (disuccinyl PEG) with varying chain length of PEG ((where n = 9 (PEG-400), 23 (PEG1000), 45 (PEG-2000)), polymer (PSA and PSA-g-mPEG) hydrogels were then prepared through Steglich esterification. Esterification took place between hydroxyl groups from PSA or PSA-g-mPEG and the carboxylate groups of the succinyl part of disuccinyl PEG in order to study the effect of different chain lengths of the cross-linkers on the overall behavior of hydrogels. An ideal hydrogel structure is given in Figure 14 while it can be verified by ¹³C CP MAS NMR spectra (Figure 13).

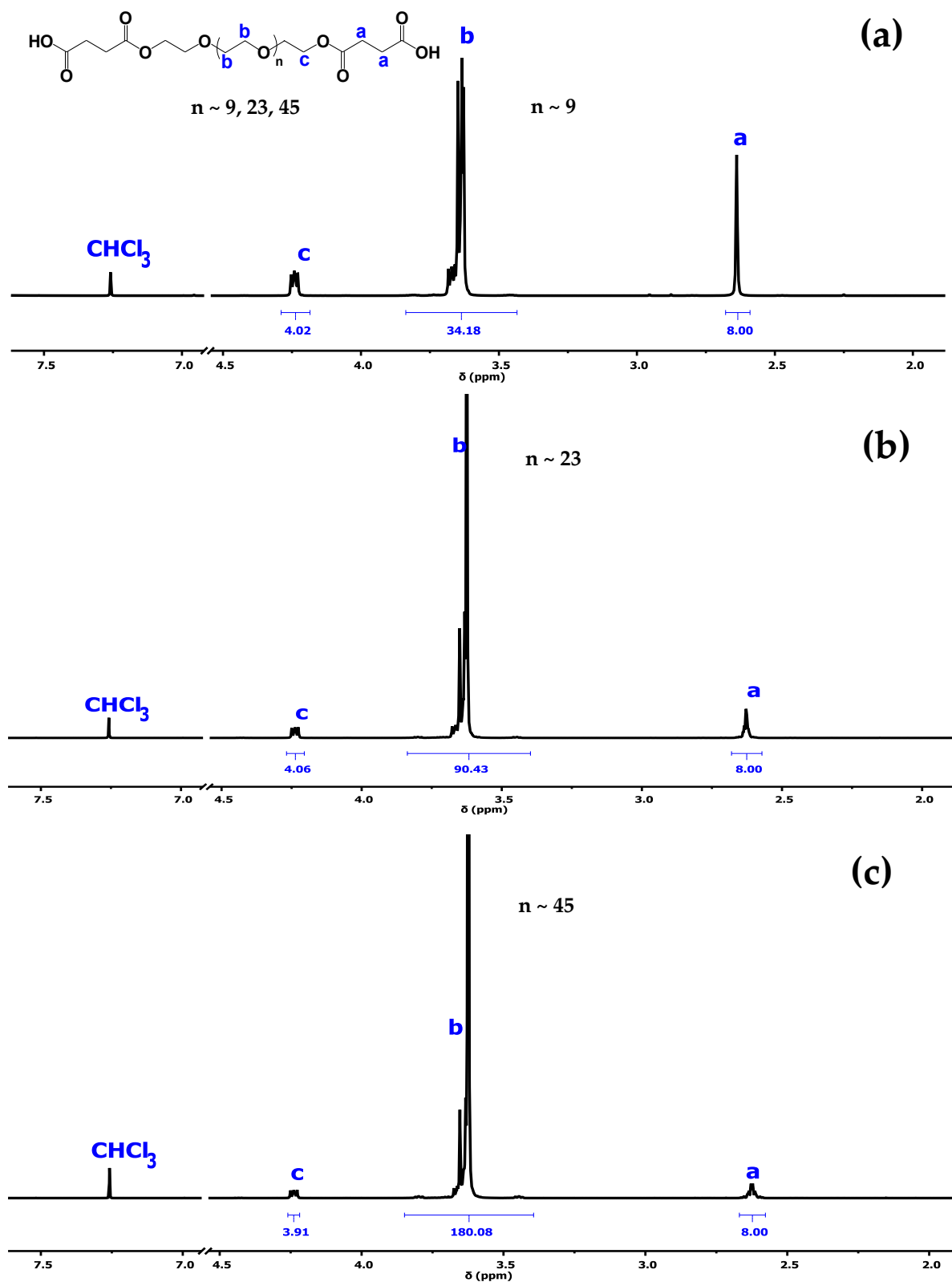


Figure 12. ^1H NMR spectrum of (a) disuccinyl PEG-400, (b) disuccinyl PEG-1000, and (c) disuccinyl PEG-2000 measured at 27 °C using CDCl_3 as solvent.

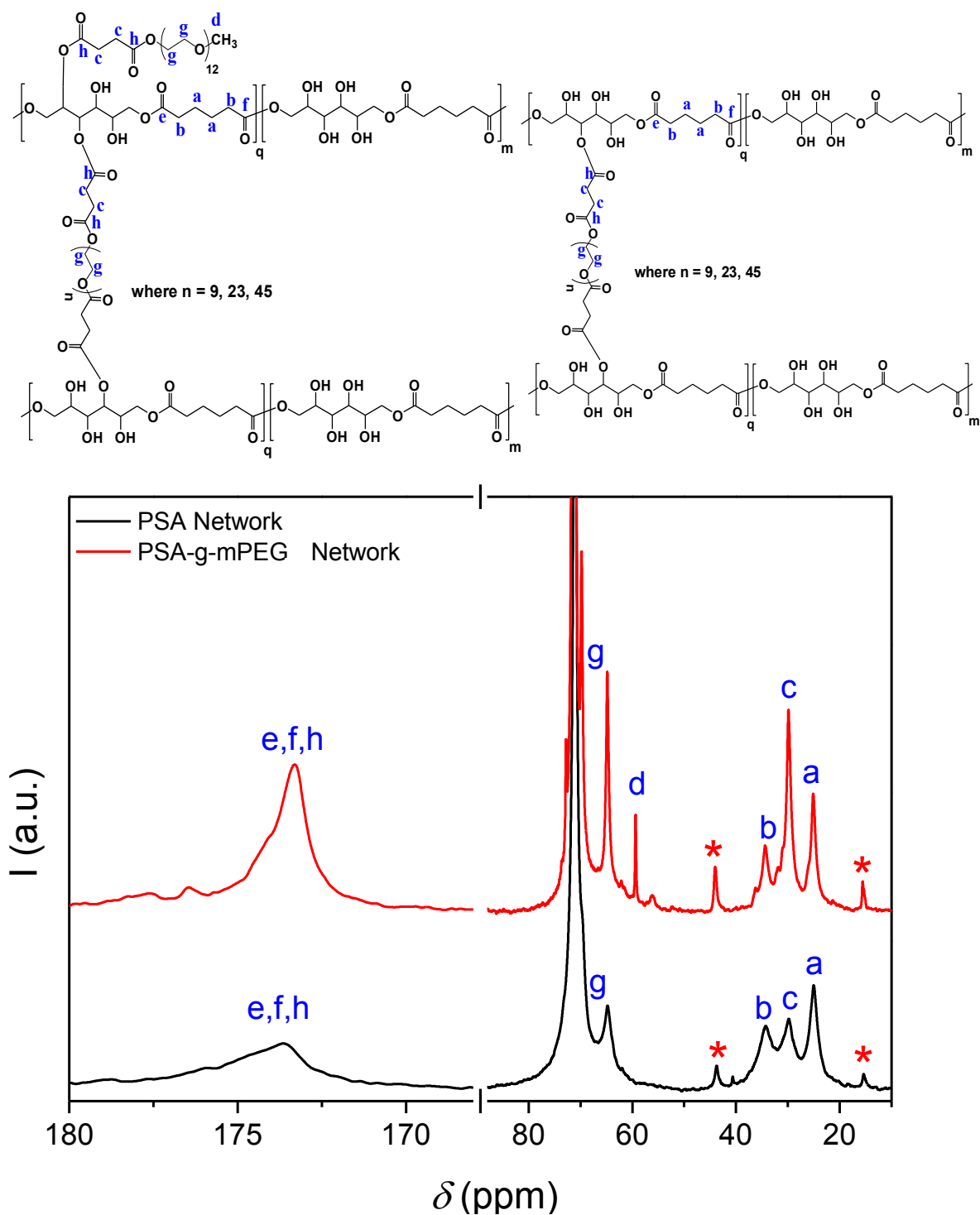


Figure 13. ^{13}C MAS SP spectra of PSA and PSA-g-mPEG hydrogels with a disuccinyl PEG-400 cross-linker.

Both spectra (Figure 13) from hydrogels crosslinked with disuccinyl PEG-400 verifies the crosslinking of the polymers and show incorporation of identical cross-linker's succinyl peaks at 30 ppm while carbon peaks from ethylene glycol part are appearing around 70 ppm. Difference between both types of hydrogels is that PSA-g-mPEG hydrogel shows a carbon

peak of methyl at 58 ppm from mPEG-550 which is absent in the PSA hydrogel. Furthermore, from PSA-g-mPEG hydrogel spectra, carbon peaks at around 30 ppm (c) and 173 ppm (h) show greater intensity due to the grafted chains of monosuccinyl mPEG-550. There are two unknown extra carbon peaks appearing around 15 ppm and 45 ppm, marked by an asterisk. One possible reason can be peak splitting of PEG based cross-linker after formation of the hydrogel.

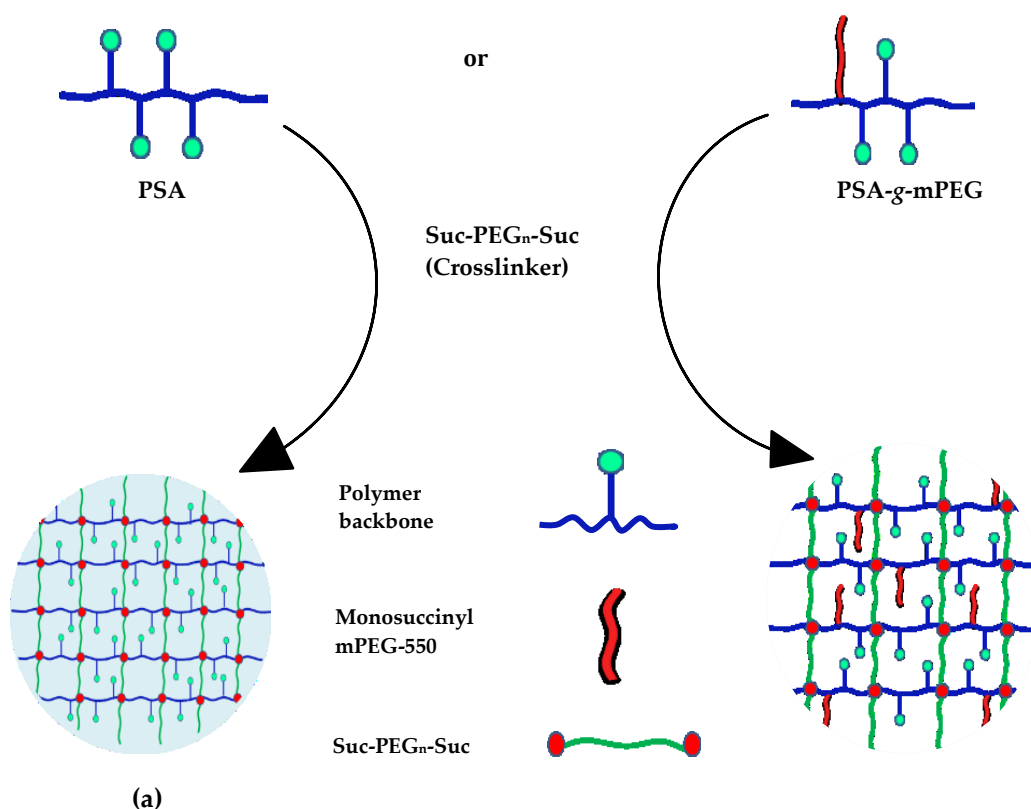


Figure 14. Presumed network formation using Suc-PEG_n-Suc (disuccinyl PEG) with (a) PSA or (b) PSA-g-mPEG when the network cross-links occur ideally.

3.2. Stability and degradation study of PSA and PSA-g-mPEG

Enzymatically synthesized aliphatic polyesters have been reported as biodegradable which breaks down to their initial monomeric products after degradation [227,228]. Studies suggest that post-polymerization modification can lead to a decrease in polymer degradation which may be a result of an increase in the steric hindrance of the polymer [229]. The same kind of study has also been conducted here in which polymers were exposed to two different types of temperatures to check their stability and degradation before (PSA) and after modification (PSA-g-mPEG).

The stability study suggests through GPC measurements that no change was observed in the number average molar mass (M_n) before and after modifications when polymers were kept at 4 °C. In contrast to 4 °C, a decrease in molar mass was observed when these polymers were kept at 40 °C and 75% RH. As it can be seen in Figure 15 (a) that the PSA initial molar mass was 11,000 g/mol on d 0 but with the passage of time, it is gradually decreasing. It is reduced to 8,400 g/mol on d 28 while on d 84, it is degraded to 4,800 g/mol. Similar trend was observed with the PSA-g-mPEG (Figure 15 b). On d 0, the molar mass of PSA-g-mPEG was 16,000 g/mol which reduced slightly to 15,000 g/mol on d 30 while it decreased to 11,800 g/mol on d 84.

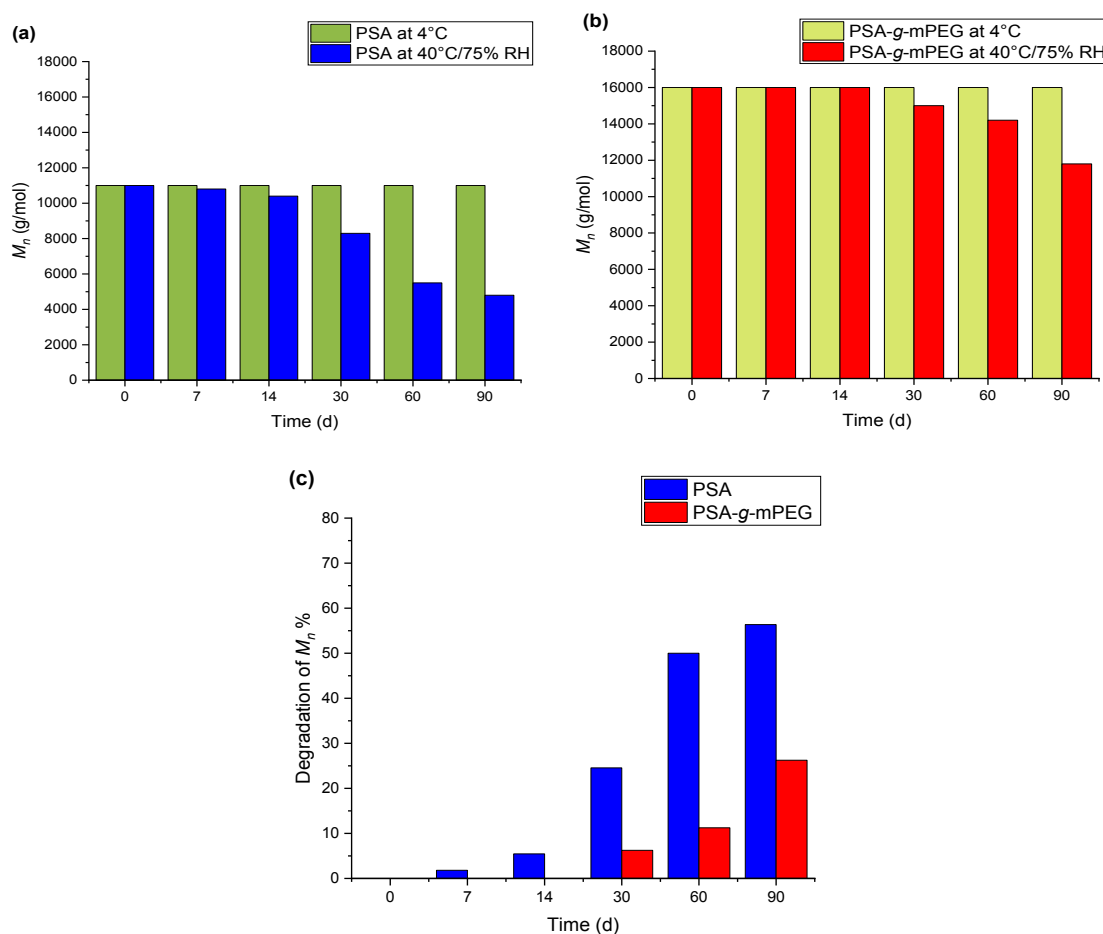


Figure 15. (a) Number average molar mass (M_n) of PSA at 4 °C and 40 °C/75% RH with respect to time (84 d), (b) M_n of PSA-g-mPEG at 40 °C/75% RH with respect to time (84 d), and (c) % degradation of M_n for PSA and PSA-g-mPEG at 40 °C/75% RH with respect to time (84 d).

In both polymers (PSA and PSA-g-mPEG), degradation of the polymer is observed at high temperature (40 °C) as compared to lower temperature (4 °C) which happens to be the result

of the hydrolysis [230–232]. Hydrolysis can be the result of high temperature and humid conditions which was provided to the polymers. Degradation of the poly(glycerol adipate) (PGA), which is also a sugar alcohol based polyester, has also been reported when it was exposed to similar environmental conditions [232]. It is also pertinent to mention here that PSA degrades more as compared to PSA-g-mPEG. If the degradation of PSA and PSA-g-mPEG at d 84 (Figure 15 c) is compared, PSA degrades to 43% of its initial molar mass while PSA-g-mPEG degrades to 73% of its initial molar mass. This also justifies the fact that modification of the polymer increases the steric hindrance of the cleavable ester bonds present in the polymer which delays the degradation of the PSA-g-mPEG as compared to PSA [230–232]. A similar trend was also reported by Swainson *et al.* when they exposed poly(glycerol adipate) (PGA) and poly(glycerol adipate) modified with PEG (PGA-PEG) to enzymatic degradation. They found that PGA-PEG was more stable to degradation effect as compared to PGA only, hence PEG providing the increase in the steric hindrance of the polymer [227]. Another potential scenario involves PEG acting as a polymer that can adhere to water due to its hygroscopic properties [233], thereby potentially reducing the amount of water accessible for hydrolysis and delaying the degradation process.

3.3. Differential scanning calorimetry

Figure 16 and Table 1 summarize all DSC data taken in the range between $-60\text{ }^{\circ}\text{C}$ and $80\text{ }^{\circ}\text{C}$. Figure 16 (a) indicates the amorphous nature of PSA and PSA-g-mPEG since only a glass transition temperature T_g is observed in the respective heating trace. In contrast, monosuccinyl mPEG-550 shows a clear melting endotherm. Thus, the amorphous nature of PSA-g-mPEG indicates that the PSA backbone prevents the crystallization of the grafted PEG chains. PSA shows a T_g at $-1\text{ }^{\circ}\text{C}$ which is reduced to $-34\text{ }^{\circ}\text{C}$ after grafting with monosuccinyl mPEG-550 and resulting in PSA-g-mPEG. The bifunctional cross-linker disuccinyl PEG-400 also does not show any melting peak but shows a T_g at $-45\text{ }^{\circ}\text{C}$ (see Figure 16 (b)). When PSA is cross-linked with disuccinyl PEG-400, the T_g is lowered to $-11\text{ }^{\circ}\text{C}$. When PSA-g-mPEG is cross-linked with disuccinyl PEG-400, the T_g appears at $-29\text{ }^{\circ}\text{C}$. Both hydrogel structures cross-linked with disuccinyl PEG-400 do not show any melting peak demonstrating that the gels formed with disuccinyl PEG-400 are completely amorphous. In contrast, hydrogels formed with disuccinyl PEG-1000 and disuccinyl PEG-2000, respectively, cross-linkers are semi-crystalline indicated by their melting endotherms in the DSC traces, no matter if they are synthesized from PSA or PSA-g-mPEG (Figure 16 (c) and (d)). Here, the crystallinity is

obviously imparted by the cross-linkers disuccinyl PEG-1000 and disuccinyl PEG-1000 since they are also semi-crystalline.

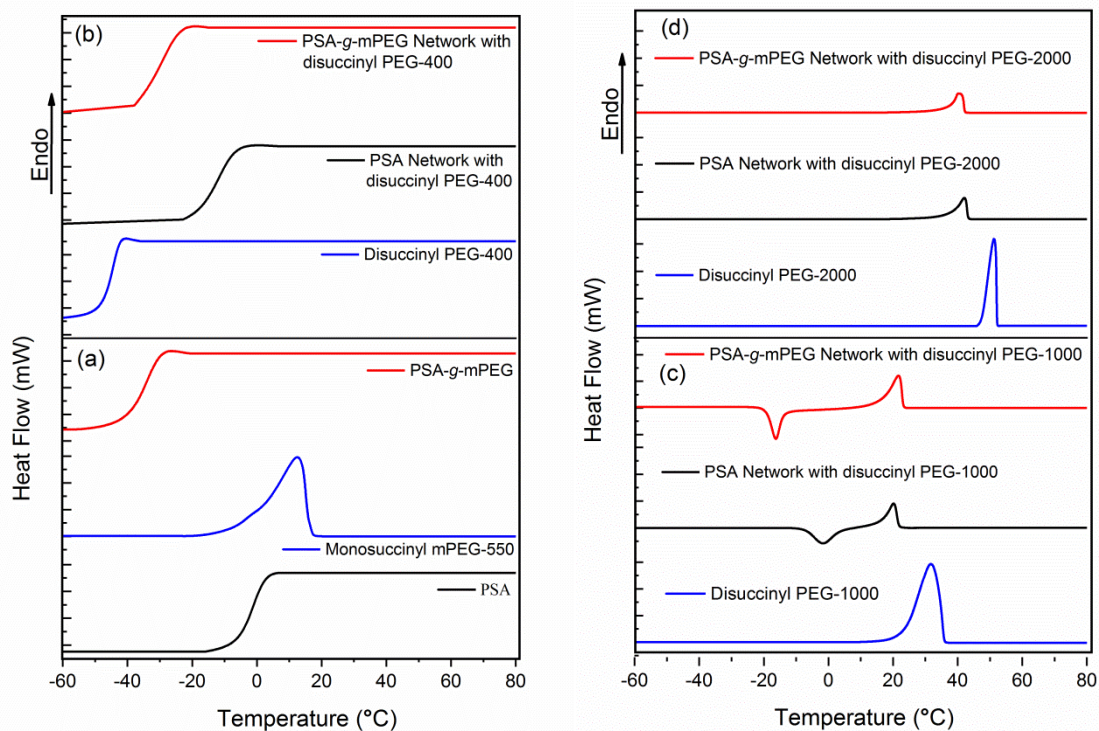


Figure 16. DSC heating traces with at heating rate of 1 °C/min. (a) Polymers; PSA, monosuccinyl mPEG-550, and PSA-g-mPEG, (b) disuccinyl PEG-400 crosslinker, PSA hydrogels crosslinked with disuccinyl PEG-400, and PSA-g-mPEG based hydrogels crosslinked with disuccinyl PEG-400, (c) disuccinyl PEG-1000, PSA hydrogels cross-linked with disuccinyl PEG-1000, and PSA-g-mPEG based hydrogels cross-linked with disuccinyl PEG-1000, (d) disuccinyl PEG-2000, PSA hydrogels cross-linked with disuccinyl PEG-2000, and PSA-g-mPEG based hydrogels cross-linked with disuccinyl PEG-2000.

Table 1. Average number molar mass M_n , dispersity (\mathcal{D}), glass transition temperature T_g , melting temperature T_m , and melting enthalpy ΔH_m of polymer precursors and hydrogels.

Polymers and hydrogels	M_n (g/mol)	\mathcal{D}	T_g (°C)	T_m (°C)	ΔH_m (J/g)
PSA	11,000 ¹	1.8 ³	-1	---	---
Monosuccinyl mPEG-550	650 ²	---	---	12	45
PSA-g-mPEG	22,000 ²	1.5 ³	-34	---	---
Disuccinyl PEG-400	600 ²	---	-45	---	---
PSA cross-linked with disuccinyl PEG-400	---	---	-11	---	---
PSA-g-mPEG cross-linked with disuccinyl PEG-400	---	---	-29	---	---
Disuccinyl PEG-1000	1,200 ²	---	---	31	86
PSA cross-linked with disuccinyl PEG-1000	---	---	---	20	23
PSA-g-mPEG cross-linked with disuccinyl PEG-1000	---	---	---	22	40
Disuccinyl PEG-2000	2,200 ²	---	---	51	123
PSA cross-linked with disuccinyl PEG-2000	---	---	---	42	32
PSA-g-mPEG cross-linked with disuccinyl PEG-2000	---	---	---	41	34

¹Molar mass of PSA is obtained by GPC measurements.

²Molar mass of graft copolymer (PSA-g-mPEG) is calculated on the basis of the degree of grafting obtained from ¹H NMR spectroscopy and taking into account molar mass of polymer (PSA) backbone obtained from GPC.

³ \mathcal{D} is calculated from GPC measurements.

These traces also indicate a decrease in the melting temperature and melting enthalpies when the cross-linker molecules are located between PSA-based polymer backbones compared to the native cross-linker. For the PSA hydrogels formed with disuccinyl PEG-1000, the phenomenon of cold-crystallization can also be observed [234]. Obviously, all hydrogels formed by disuccinyl PEG-400 are amorphous, but when disuccinyl PEG-1000 is

employed for gel formation, it needs some thermal activation that the PEG-1000 chains can form crystals. In the case of disuccinyl PEG-2000, the PEG-2000 chains are long enough in order to be packed into polymer crystals immediately after the synthesis of the gels. Furthermore, disuccinyl PEG-2000 based gels show higher melting temperatures as compared to disuccinyl PEG-1000 based gels [235,236].

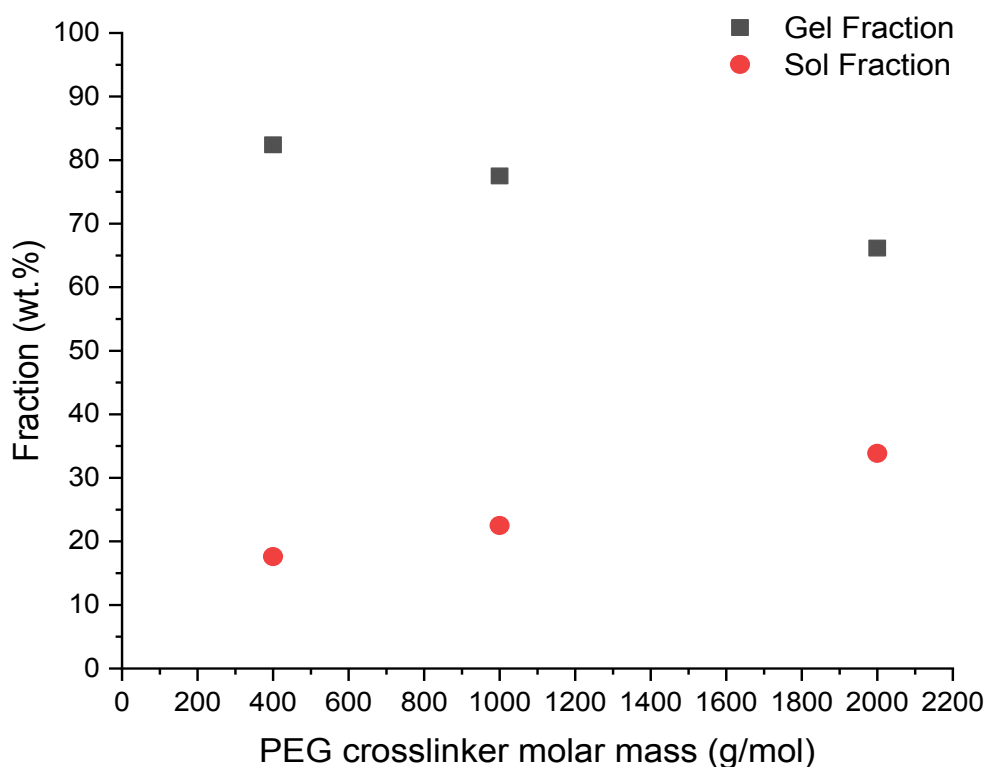


Figure 17. Sol-Gel fraction (wt.%) of hydrogels crosslinked with varying molar mass of PEG crosslinker.

3.4. Sol-gel fraction of PSA-g-mPEG hydrogels

PSA-g-mPEG hydrogels were analyzed to identify crosslinked as well as uncrosslinked polymers/reactants during the reaction. This property can also tell about the efficiency of the Steglich esterification reaction when it is used to form a crosslinked polymeric gel. So, to assess the amount of reactants consumed during the hydrogel formation, the sol-gel fraction of all the hydrogels was calculated in wt.%. It can be revealed from Figure 17 that the gel percent for the hydrogels crosslinked with PEG-400 was attained as 82%; hydrogels crosslinked with PEG-1000 attained as 77% while the hydrogels crosslinked with PEG-2000 attained as 66%. Sol% of all the mentioned hydrogels was attained as vice versa. According

to Chen *et al.*, an increase in number of crosslinking precursors can lead to an increase in grafting sites of the polymer network and crosslink density which will eventually end up in a high gel fraction [237]. In case of the PSA-g-mPEG hydrogels, gel percent is related to the chain length of the PEG. As the chain length of PEG based crosslinker is increased from PEG-400 to PEG-2000, the gel percent is decreased. Current results can also be explained in a way that Steglich esterification proves to be more efficient when lower chain length of PEG as crosslinker is used as compared to the higher chain length of PEG. It is assumed that the probability of effective collision in a chemical reaction is decreased with the increase in chain length of PEG due to the reason that the high molar mass of PEG has a low degree of freedom to be mobile enough and react with the other chemical species at reactive sites [238].

3.5. Swelling studies

Swelling is an important phenomenon of hydrogels which renders them soft and elastic nature similar to natural tissues [99]. After getting into contact with the thermodynamically compatible solvent, the transition occurs from a glassy or partially rubbery state to a relaxed rubbery state. Hence, swelling can be described as a property of the polymer hydrogel that evolves due to the elasticity of the polymer chains resulting from the interaction with a thermodynamically compatible solvent [239]. Due to this unique property, hydrogels have been studied in different biomedical applications [240].

In the first part, swelling studies of the both PSA and PSA-g-mPEG based hydrogels are performed in D₂O up to maximum water uptake (see Figure 18). This point can be considered as the equilibrium degree of swelling [195,241]. The studies revealed that the degree of swelling of all hydrogels increases with the chain length of PEG based cross-linkers. There exists a nearly linear relation between the equilibrium degree of swelling and the degree of polymerization n of the PEG-based bifunctional cross-linkers. Both PSA and PSA-g-mPEG hydrogels showed the highest degree of swelling when Suc-PEG₄₅-Suc (disuccinyl PEG-2000) was used as cross-linker while it showed the lowest degree of swelling when Suc-PEG₉-Suc (disuccinyl PEG-400) was used. In comparison to PSA hydrogels, the PSA-g-mPEG hydrogels show higher degrees of swelling since the grafted PEG chains render the networks more hydrophilic.

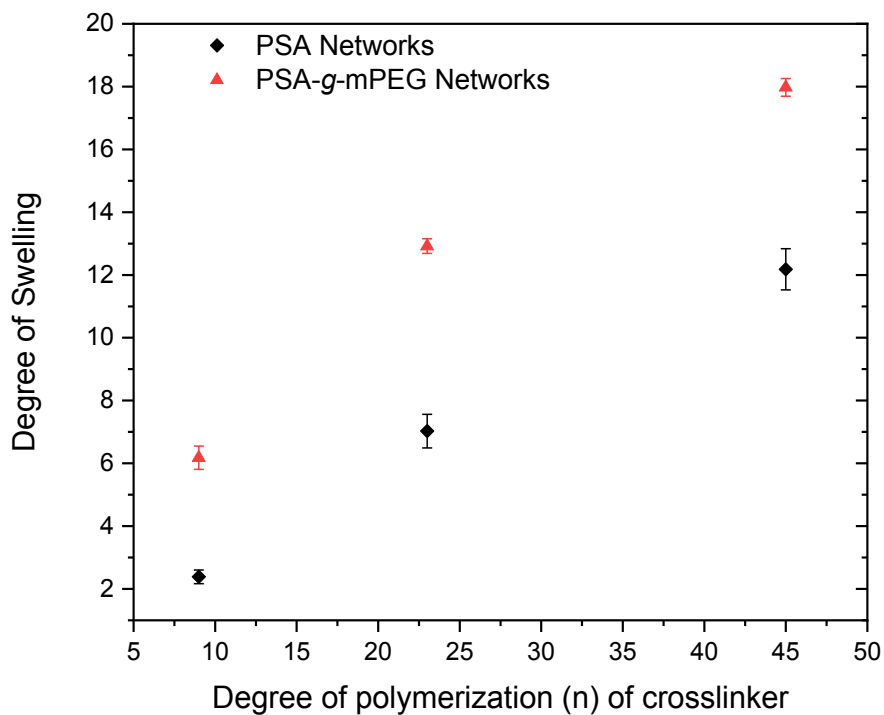


Figure 18. Degree of swelling of PSA and PSA-g-mPEG based hydrogels as a function of degree of polymerization (n) in D_2O at room temperature.

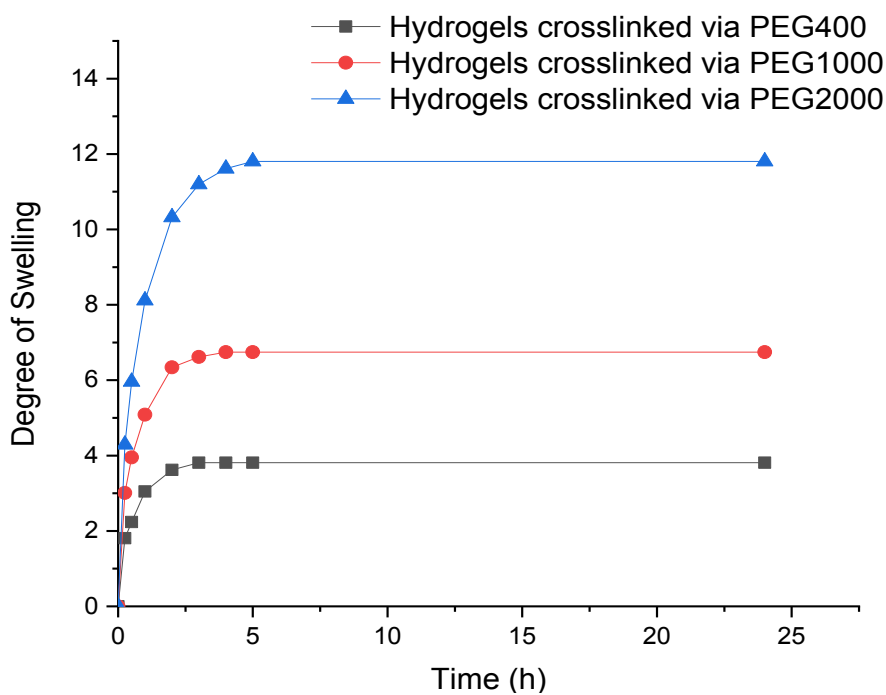


Figure 19. PSA-g-mPEG based hydrogel samples showing dynamic swelling behavior in H_2O at room temperature.

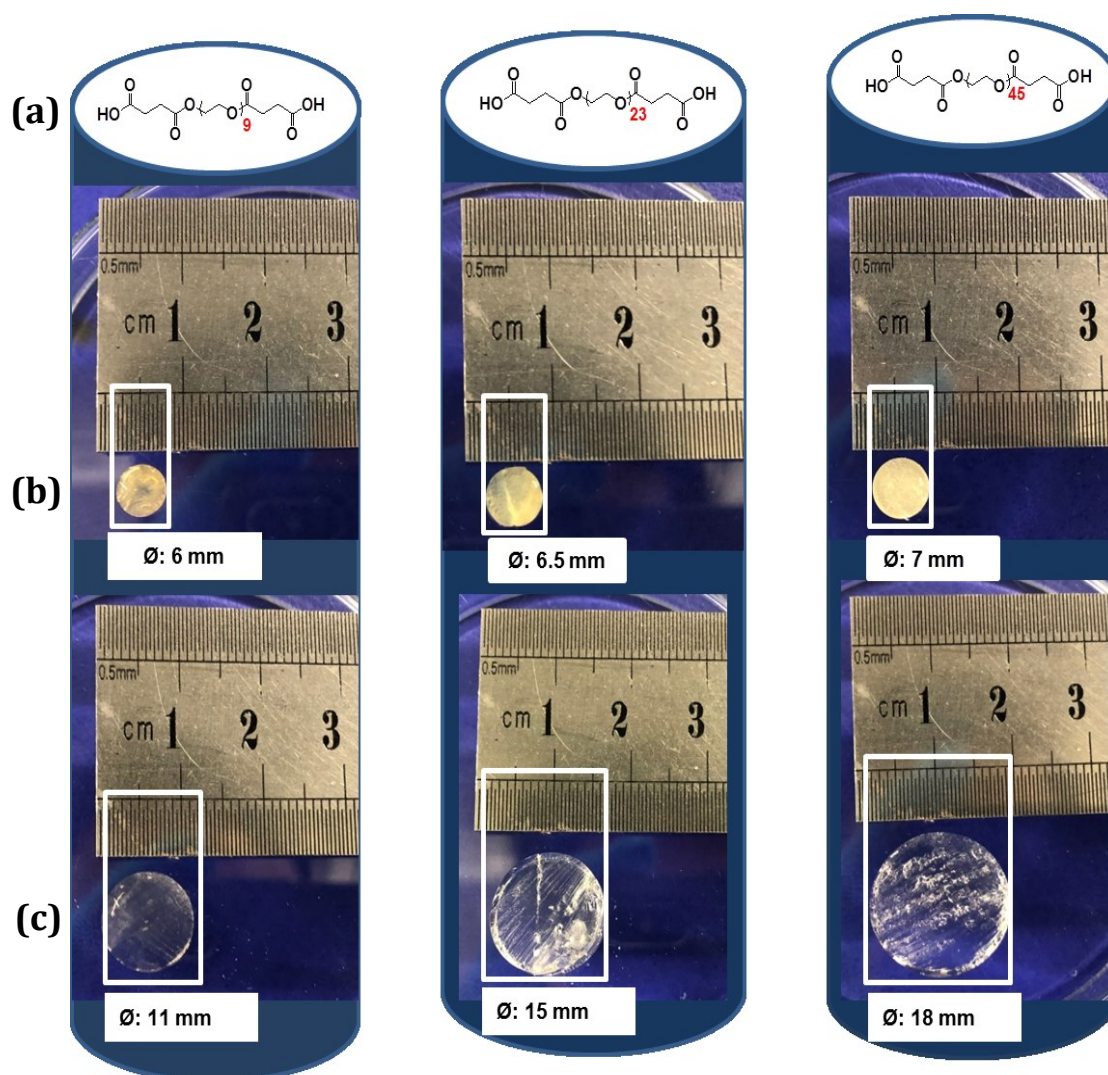


Figure 20. An example of change in the hydrogel diameter of disks of PSA-g-mPEG hydrogels cross-linked by (a) increasing molar mass of PEG based cross-linkers, when they are in (b) dry form and (c) swollen form after D₂O uptake.

PEG dependent swelling degrees were also reported by various authors illustrating that an increase in molar mass of the PEG leads to an increase in molar mass of the macromer. They further outline that an increase in the swelling of the system can not only be attributed to the enhancement in overall hydrophilicity of the hydrogel system but also due to a decrease in crosslinking density [206,213,242]. Figure 20 shows photographic images as examples for the different water uptake at room temperature. The images verify the two most important aspects of the swelling experiments: i) The degree of swelling is larger for PSA-g-mPEG samples compared to PSA based samples using identical cross-linkers and ii) The degree of swelling

increases with the degree of polymerization n of the cross-linker molecules when identical precursor polymers are employed, i.e. PSA and PSA-g-mPEG, respectively.

In the second part, based upon the better swelling data and potential application in pharmaceuticals, PSA-g-mPEG based hydrogels were then further investigated for dynamic swelling (Figure 19) in distilled H₂O to reveal its swelling data in relation to time. It was found that equilibrium swelling for PSA-g-mPEG based hydrogel samples crosslinked with all types of crosslinking agents was achieved within 4 h of the study. This swelling data vs time was then taken into account while explaining the post release dynamics of model protein and model dye from these hydrogel matrices as potential application in pharmaceutical field. It is worth mentioning here that one can see difference between equilibrium swelling of PSA-g-PEG in Figure 18 and Figure 19. It is due to the fact that polymer used belonged to two different batches (Figure 18 M_n : 22,000 g/mol, Figure 19 M_n : 16,000 g/mol) while the hydrogel crosslinking ratio based upon mol% was 30% in case of Figure 18 while it was 35% in case of Figure 19. These are the reasons that one can see less equilibrium swelling in Figure 19 as compared to Figure 18.

3.6. Temperature dependent swelling behavior of PSA-g-mPEG hydrogels

Swelling of hydrogels was also investigated at different temperatures (22 °C, 37 °C, 50 °C and 75 °C) to know the effect of an increase in temperature over its swelling capability. It was revealed that the swelling degree decreases with the increase in temperature [243–245]. Figure 21 shows that the degree of swelling for all types of hydrogels crosslinked with different molar masses of PEG based crosslinkers, decreases as the temperature was increased from 22 °C to 75 °C. The swelling degree of hydrogels crosslinked with PEG-400 shrank from 3.84 at 22 °C to 1.32 at 75 °C, hydrogels crosslinked with PEG-1000 shrank from 6.73 at 22 °C to 4.60 at 75 °C while hydrogels crosslinked with PEG-2000 shrank from 11.81 at 22 °C to 9.08 at 75 °C.

Such type of behavior has been explained as a PEG based property due to its lower critical solution temperature (LCST) which is known to be ~ 95 °C [243,245,246]. Literature data further reveals that hydrogen bonding plays an important role in performing that behavior by forming hydrates when water comes into contact with PEG based hydrogels. It is thus obvious that temperature would have a significant impact on the hydrogen bond formation between the PEG's oxygen atom and water's hydrogen atom. Hence, such bonding is susceptible to

breaking as the temperature rises, while interactions between hydrophobic molecules are strengthened [247–249].

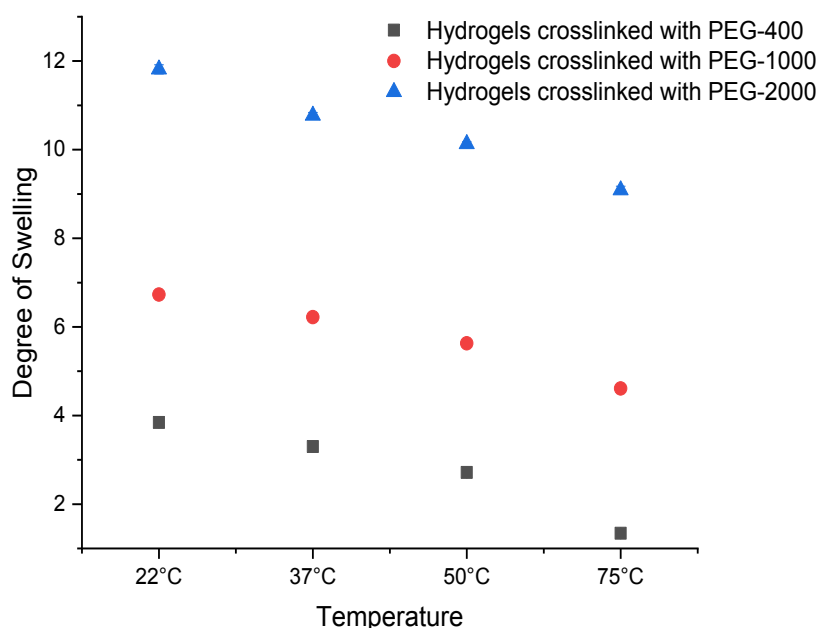


Figure 21. Swelling degree of PSA-g-mPEG hydrogels as a function of temperature when it is increased from 22 °C to 75 °C.

3.7. ^1H Double-Quantum (DQ) NMR spectroscopy

For the characterization of the hydrogel samples, the ^1H DQ measurements were performed. This method allows the analysis of the dynamics and the determination of the hydrogel structure. It also permits to distinguish the network-forming loops of different lengths, as well as various defects [250]. The exact details of a DQ experiment and the pulse sequence according to Baum and Pines [251] used in this work can be taken from Saalwächter article [252].

For the determination of the dipolar coupling constant, the mobile and uncoupled components, so-called *tail* fraction, are first subtracted from the signal. Two *tail* components are expected in a swollen real polymer hydrogel. First one is the solvent *tail*, which is caused by residual protons in the solvent since the samples contain an excess of D_2O , an increased amount of this component is expected. Second is the network *tail*, which is caused by the network defects such as loops and dangling chain ends (unreacted chains).

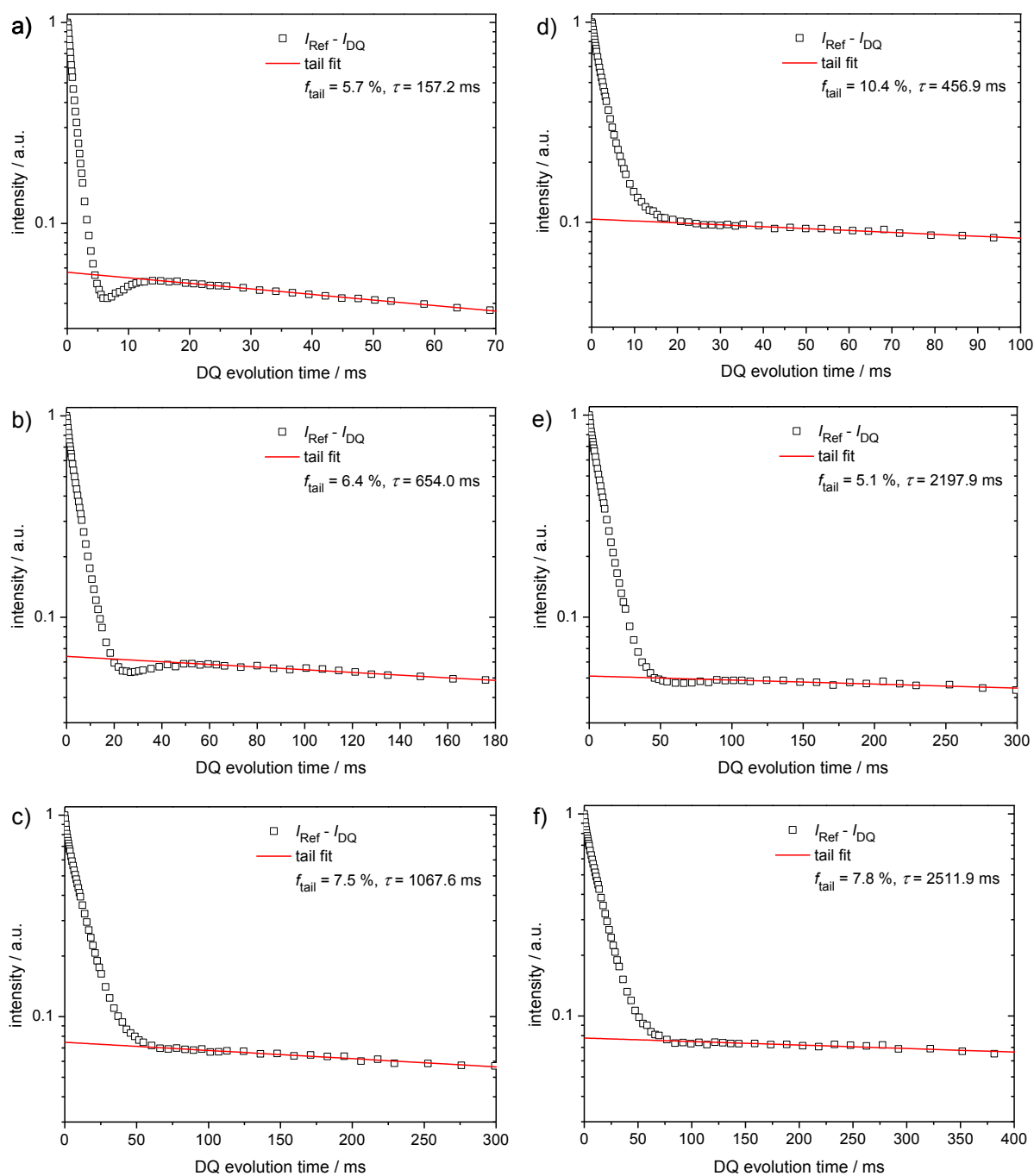


Figure 22. Determination of the tail fraction through ^1H DQ NMR for (a-c) PSA hydrogels cross-linked with the disuccinyl PEG (Suc-PEG_n-Suc where $n = 9, 23, 45$) and (d-f) PSA-g-mPEG hydrogels cross-linked with the Suc-PEG_n-Suc (where $n = 9, 23, 45$).

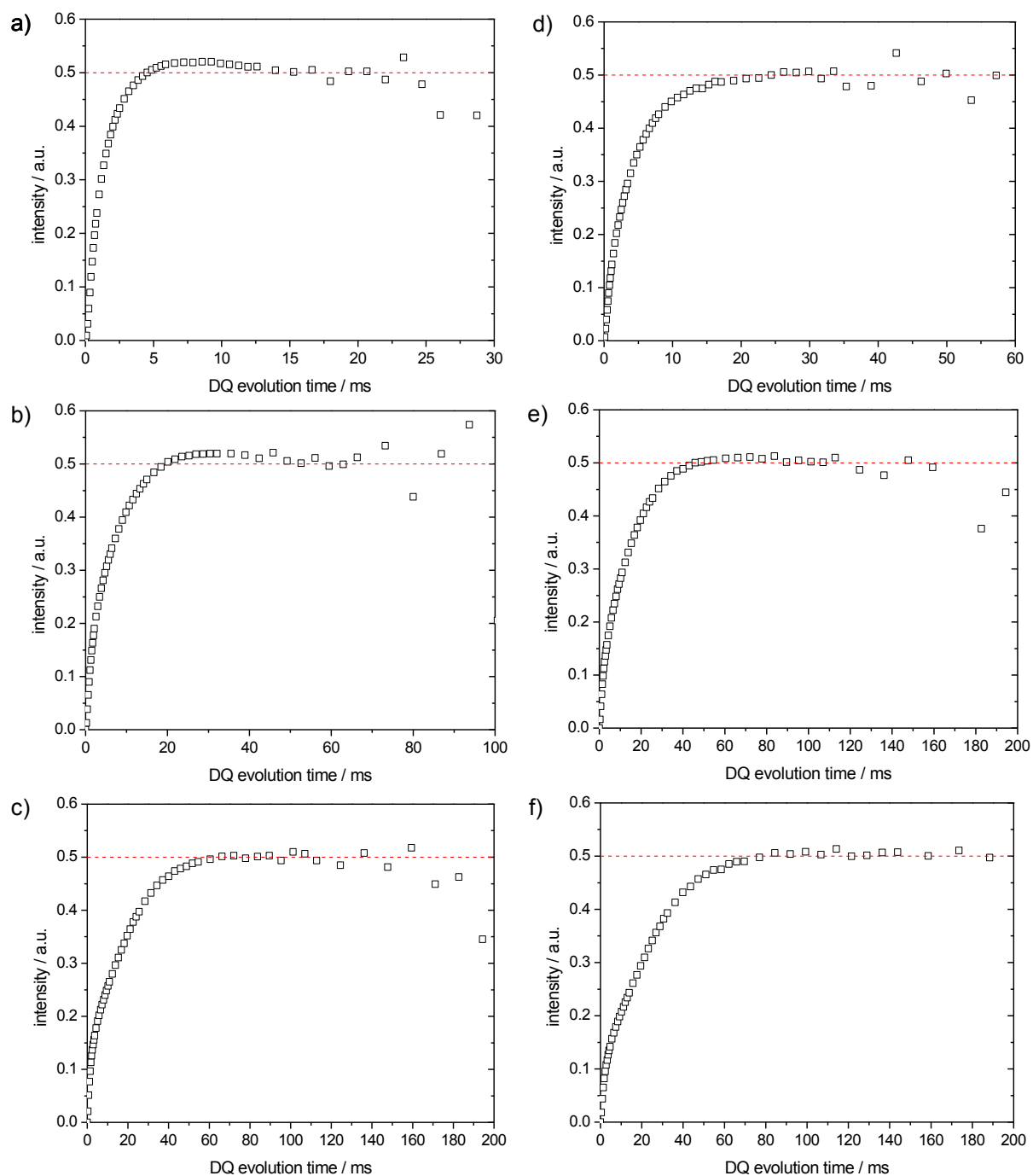


Figure 23. Normalized double quantum curves nDQ through ^1H DQ NMR for (a-c) PSA hydrogels cross-linked with the disuccinyl PEG (Suc-PEG $_n$ -Suc where $n = 9, 23, 45$) and (d-f) PSA-g-mPEG hydrogels cross-linked with the Suc-PEG $_n$ -Suc (where $n = 9, 23, 45$).

For unmodified samples of PSA networks (Figure 22 (a-c)), only the solvent *tail* could be detected. Based on the long T_2^* decay time, it can be excluded that this component results from the network. The free chain ends of the main strands could not be detected. Note that the solvent *tail* does not correspond to the total amount of water in the sample. The DQ experiments were performed with a repetition time of 2s. This delay was chosen to be sufficient for the complete relaxation of the polymer, but was significantly shorter than $5 \cdot T_1$ of the solvent. Thus, the short recycling delay acts as a T_1 filter for the solvent and the determined water content is lower than expected.

Even in modified networks of PSA-g-mPEG, where about ~45% of the monomer units contain a side chain, no second *tail* component with a short T_2^* time could be detected (Figure 22 (d-f)). This result is surprising and indicates that the network *tail*, i.e. the free chain ends and other defects, do not differ in their mobility from the network structure. In other words, the isotropic mobility of the tail is restricted by the network.

To check the *tail* subtraction procedure, the normalized DQ intensity (I_{nDQ}) was calculated (Figure 23). The nDQ intensity reaches the expected value of 0.5 for all samples, which is an indication that the correct tail fraction has been subtracted. It should be noted, however, that due to complex network structure, the DQ data may contain not just one (as is the case of natural rubber), but several network components with different T_2^* values. This makes the nDQ curves unsuitable for a quantitative evaluation due to the incorrect normalization.

For this reason, the DQ data is directly evaluated with the help of a simultaneous fitting procedure. The PEG spacers as cross-linkers, which connect the main chains, are generally randomly distributed. This means that there are no loops of well-defined length like in Tetra-PEG [250] or other PEG networks [253], which was the case in these samples. The mesh size can vary greatly, which leads to a broad distribution of dipolar couplings due to the relationship $D_{res} \propto M_c$, the average molar mass between the cross-links. Both the Gaussian and log-normal distribution were tested and the latter showed a better fit to the measured data. The simultaneous fitting function for two network components is

$$I_{\Sigma DQ}(\tau_{DQ}) = \sum_{i=1}^2 f_i \exp\left\{-\left(\tau_{DQ}/\tau_i\right)^{\beta_i}\right\} \quad (\text{eq. 13})$$

$$I_{DQ}(\tau_{DQ}) = \sum_{i=1}^2 \int_0^\infty I_{DQ}(\tau_{DQ}, D_{res}^{(i)}) p(D_{res}^{(i)}, \sigma^{(i)}) dD_{res}^{(i)} \quad (\text{eq. 14})$$

$$I_{DQ}(\tau_{DQ}) = \sum_{i=1}^2 \int_0^\infty \frac{1}{2} f_i \left[1 - \exp\left\{-\left(0.378 \cdot D_{res}^{(i)} \tau_{DQ}\right)^{1.5}\right\} \cdot \cos\left(0.583 \cdot D_{res}^{(i)} \tau_{DQ}\right)\right] \cdot \exp\left\{-\left(\frac{\tau_{DQ}}{\tau_i}\right)^{\beta_i}\right\} \cdot p(D_{res}^{(i)}, \sigma^{(i)}) dD_{res}^{(i)} \quad (\text{eq. 15})$$

Fitting parameters are the component fraction f_i , the time constant τ_i , which corresponds to the characteristic decay time T_2^* , the exponent β of the Kohlrausch–Williams–Watts (KWW) function, the residual dipolar coupling constant D_{res} and the width of the log-normal distribution σ .

Table 2 summarizes the fitting results. The most important parameters are the component fractions f_i , the residual dipolar coupling constants D_{res} and the distribution widths σ . The corresponding fitting curves are shown in Figure 24. Two network components with significantly different coupling constants were detected for all samples. The weakly coupled component dominates for all samples. With increasing length of the PEG spacers, the network becomes more mobile (T_2^* value increases and D_{res} decreases) and the proportion of more strongly coupled spins decreases. This applies generally to both PSA and PSA-g-mPEG network batches.

Table 2. Result of the simultaneous fitting to the DQ data after the tail correction. The two network components are shown.

Polymer Networks	Crosslinking Precursors	f_1 (%)	T_2^* (ms)	β	$D_{res}/2\pi$ (Hz)	σ	f_2 (%)	T_2^* (ms)	β	$D_{res}/2\pi$ (Hz)	σ
PSA Networks	Disuccinyl PEG-400	37.0	5.2	2.0	462.5	0.46	63.0	7.8	1.5	131.3	0.49
	Disuccinyl PEG-1000	31.7	10.3	1.9	217.1	0.61	68.3	26.1	1.5	34.4	0.59
	Disuccinyl PEG-2000	21.8	11.3	2.0	220.3	0.57	78.2	45.7	1.2	15.9	0.85
PSA-g-mPEG Networks	Disuccinyl PEG-400	33.5	8.3	1.5	230.1	0.85	66.5	15.0	1.2	47.0	0.69
	Disuccinyl PEG-1000	18.3	11.8	1.9	200.8	0.60	81.7	40.7	1.2	19.0	0.77
	Disuccinyl PEG-2000	19.9	12.2	1.9	159.1	0.65	80.1	60.0	1.2	11.8	0.80

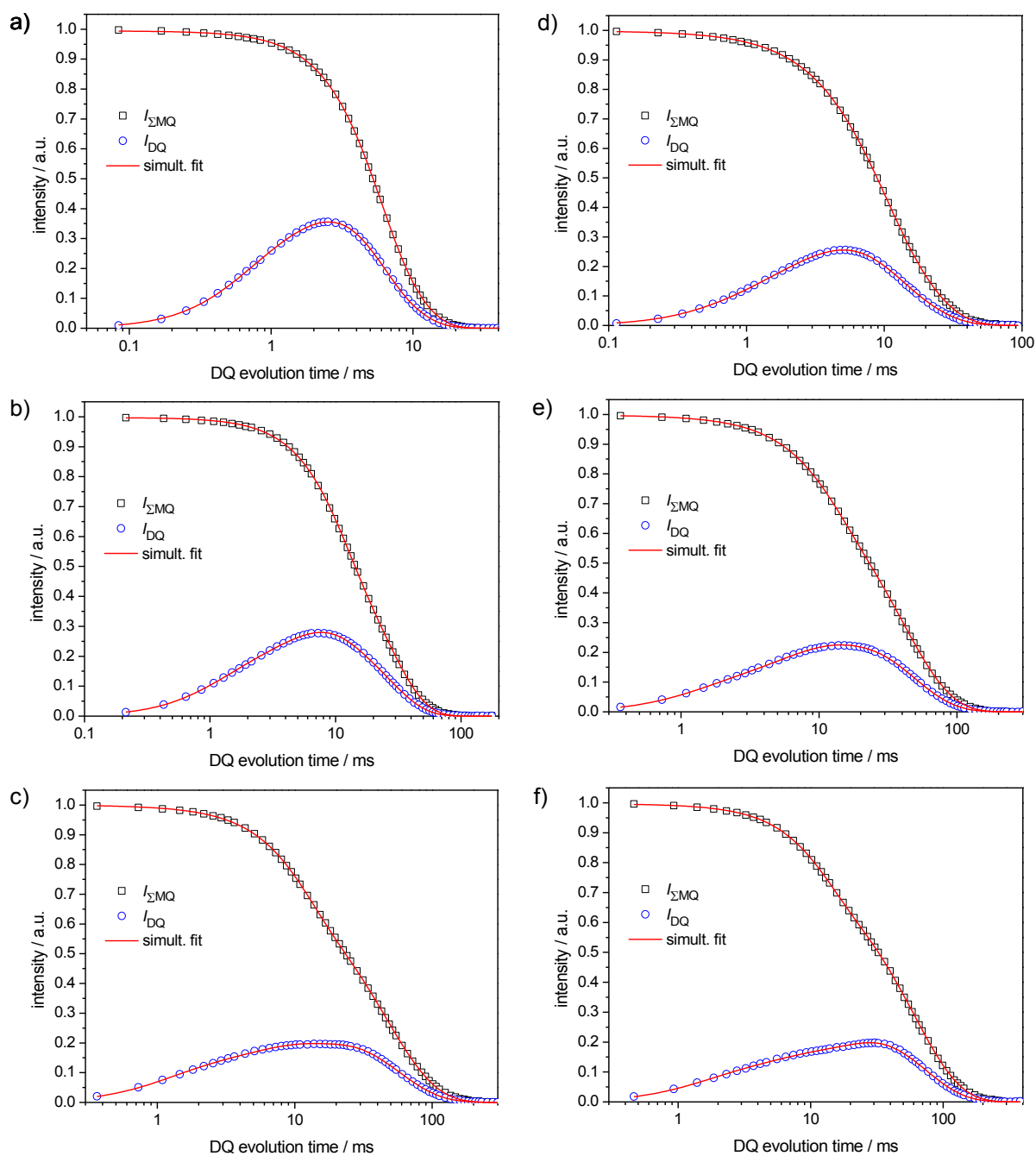


Figure 24. Simultaneous fitting to the sum intensity I_{Σ} and DQ intensity I_{DQ} through ^1H DQ NMR after tail correction for (a-c) PSA hydrogels cross-linked with the disuccinyl PEG (Suc-PEG_n-Suc (where $n = 9, 23, 45$) and (d-f) PSA-g-mPEG hydrogels cross-linked with the Suc-PEG_n-Suc (where $n = 9, 23, 45$).

The difference between PSA and PSA-g-mPEG networks lies in the strength of the dipole coupling. As can be seen from Figure 25, PSA networks are more strongly coupled. However, the proportion of such strongly coupling protons is lower in PSA-g-mPEG networks. In addition, there is a greater distribution width of the dipole couplings. The additional side chains thus lead to increasing inhomogeneity in the network. Not to be excluded is the case of phase separation with areas of high and low polymer concentration.

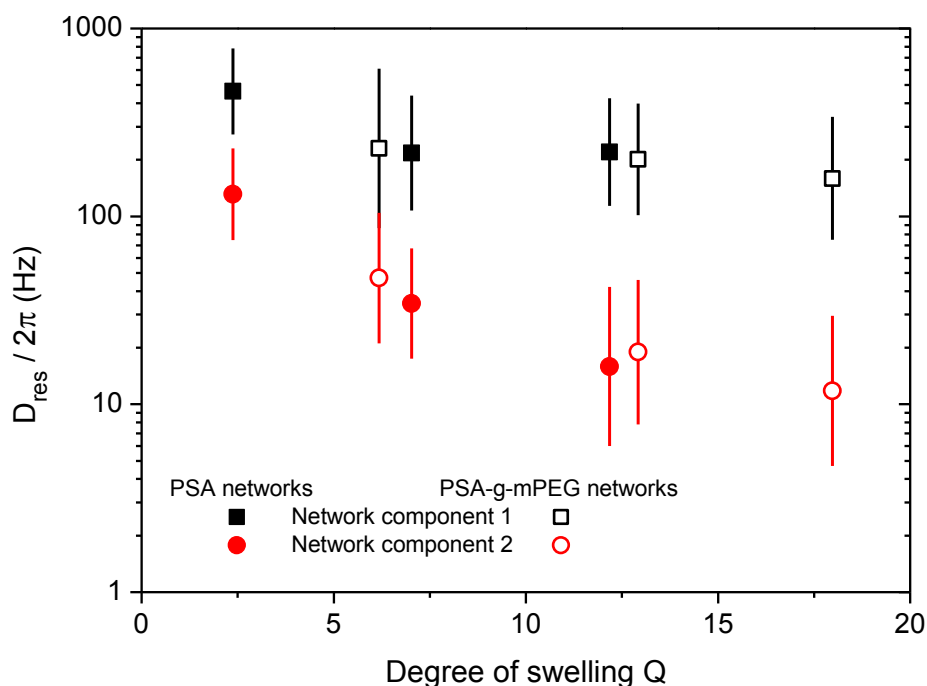


Figure 25. Relation between the dipolar coupling constant D_{res} and the degree of swelling Q of the samples. The vertical bars represent the distribution widths of σ from the Table 2.

If the side chains and free chain ends are located in the first areas, they are less mobile and show a residual dipole coupling. This could explain the "invisible" tail in PSA-g-mPEG network samples. Keeping in view data from Table 2 and Figure 25, dipolar coupling is decreasing, while T_2^* is increasing causing mobility of the network. In other words, the increase in network mobility can be attributed to an increase of the degree of swelling as shown in Figure 25.

3.8. ^1H Pulsed field gradient (PFG) NMR spectroscopy

Furthermore, the diffusion of solvent molecules in swollen networks was investigated (See Figure 27). The samples were prepared without excess D_2O , so that, diffusion outside the polymer network could be excluded. The measurement signal corresponds exclusively to the remaining HDO molecules in the polymer network.

The ^1H spectra from the diffusion measurement are shown in Figure 26 and exhibit two well resolved resonances. As the gradient strength G increases, the intensity of the left peak decreases while the right peak remains constant. The assignment of the two resonances is therefore obvious. The left peak corresponds to the mobile solvent (HDO), while the right peak is assigned to the immobile polymer network (its diffusion can be neglected on the time scale of the diffusion of water). The relationship between echo signal intensity and pulse field gradient parameters in the PFG experiment is given by

$$I_{\text{PFG}}(G) = I_{\text{PFG}}(0) \cdot \exp(-\gamma^2 G^2 D \delta^2 (\Delta - \delta/3)) \quad (\text{eq. 16})$$

where I_{PFG} is the echo signal intensity, γ is the gyromagnetic ratio of the proton, G is the field gradient strength during the gradient pulse of the length δ , D is the self-diffusion coefficient and Δ is the diffusion time [254].

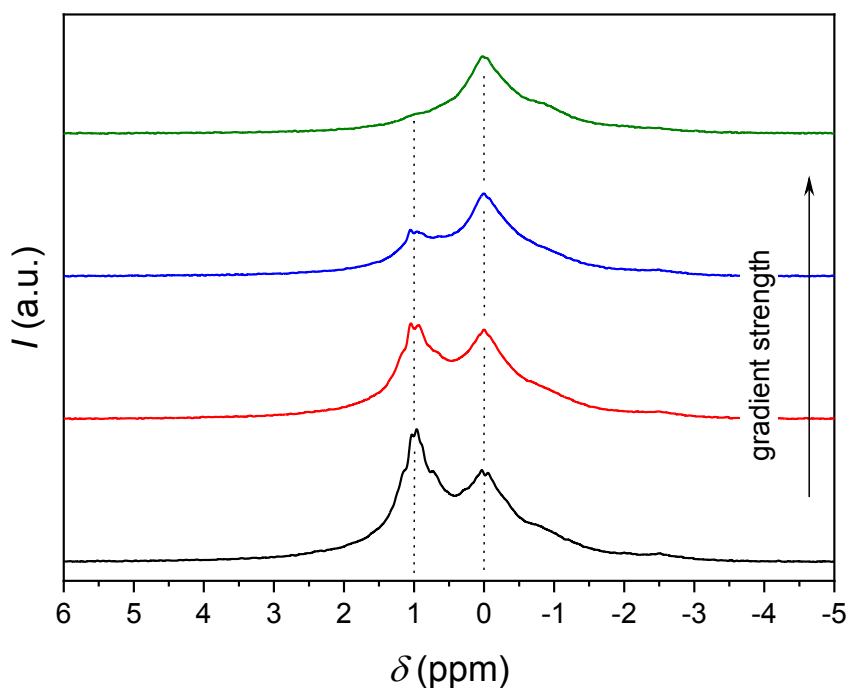


Figure 26. ^1H NMR spectra measured with PFG NMR spectroscopy of PSA-g-mPEG network (PEG-400 based crosslinker) with $Q = 6.2$ and D_2O as solvent by varying field gradient strength at $T = 30\text{ }^\circ\text{C}$. The spectrum was referenced to the center of the right peak.

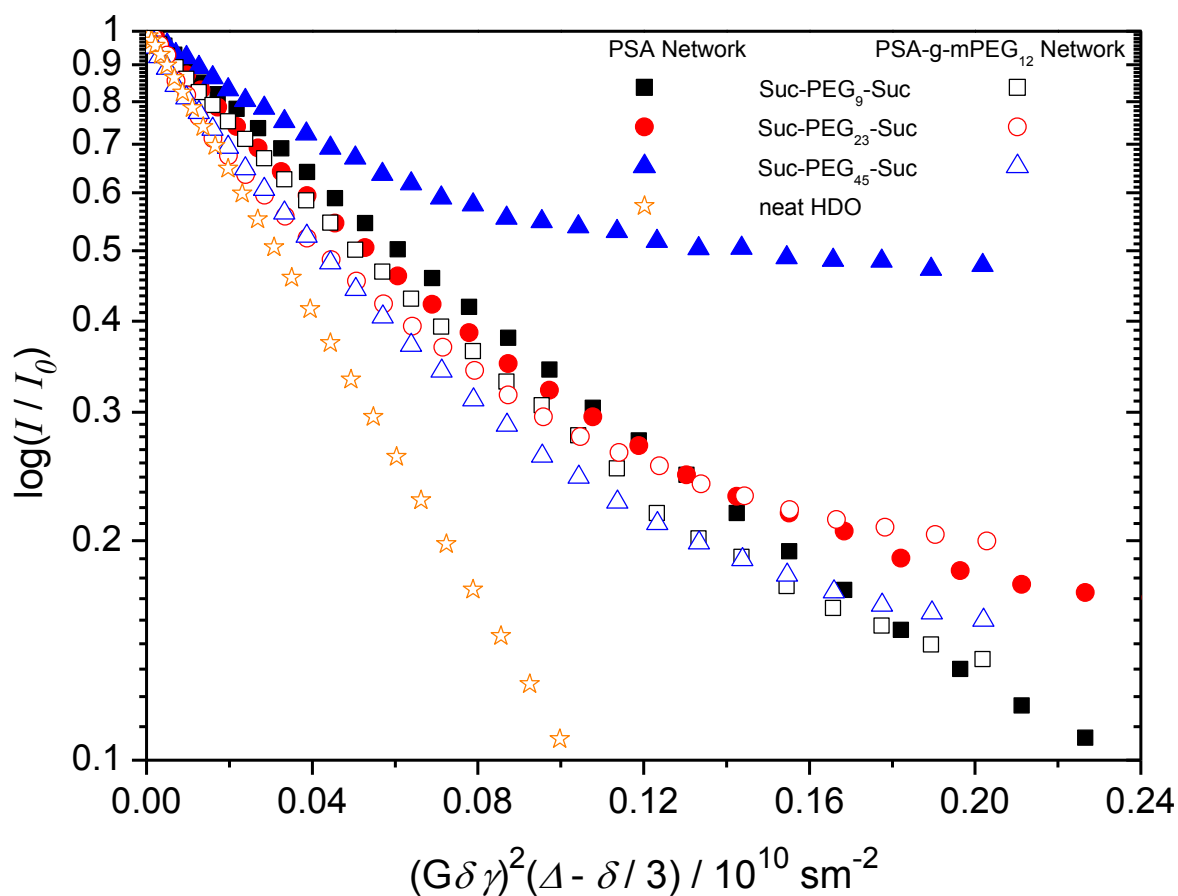


Figure 27. Normalized PFG NMR diffusion decays of HDO for different samples at $T = 30$ °C. Due to the intensity offset coming from the polymer signal, the initial slope does not reflect the translational diffusion coefficient of water (D_{HDO}) in the polymer network correctly.

The echo signal intensity was measured as a function of G . When plotting the logarithm of the echo intensity against the diffusion function $\gamma^2 G^2 \delta^2 (\Delta - \delta/3)$, the diffusion coefficient D can be determined from the slope of the curve.

In order to determine the diffusion coefficients of water, only the HDO peak was integrated. Figure 27 shows normalized PFG diffusion decays of HDO of the investigated samples. In contrast to the diffusion of HDO in pure D_2O , the decay curves of network samples show a clear nonlinear behavior. This nonlinearity can be explained in two different ways. On one hand, it could be an anisotropic diffusion movement of water, e.g. caused by hydrogen bonding with the polymer. In this case, the evaluation of the diffusion data would be more difficult. However, if the diffusion length of an HDO molecule is calculated on the time scale

of the diffusion measurement, it becomes clear that it is significantly larger than the dimensions of the smallest possible loop in the polymer network. The anisotropy of diffusion can thus be excluded. On the other hand, the non-linearity of the diffusion curves could be caused by a baseline problem in the spectrum. When looking closely at the spectra in Figure 28, it becomes clear that the HDO peak overlaps with the network peak. This results in an offset in the diffusion curve, which must be taken into account. In this case, the upper formula is revised with a constant intensity offset. It is not necessary to add a second diffusion component, because the diffusion movement of the polymer network can be neglected on the time scale of the measurement. The strength of the background signal and thus the amount of offset depends on the spectral resolution and on the T_2 relaxation time of the polymer and varies from sample to sample.

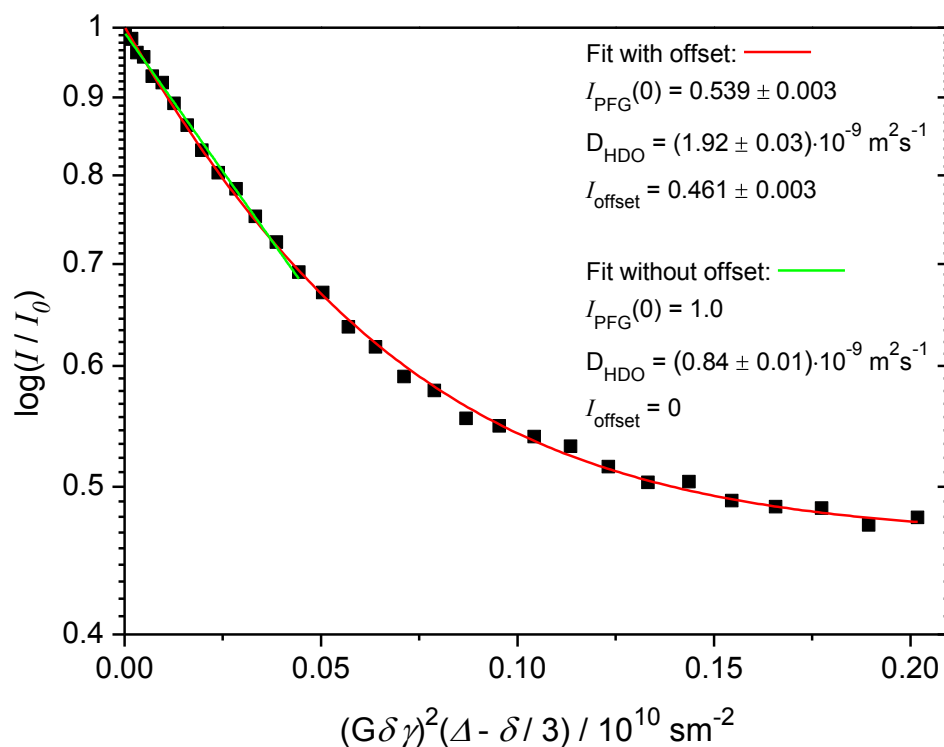


Figure 28. Fit example for the network sample cross-linked with Suc-PEG₄₅-Suc (disuccinyl PEG-2000) according to equation 2. Different fit strategies for estimation of the diffusion coefficient were tested. The red line: fit with constant offset of 46 % provides $D_{\text{HDO}} = (1.92 \pm 0.03) \cdot 10^{-9} \text{ m}^2/\text{s}$. The green line: fit of the initial decay (linear part of the decay) without offset, which provides $D_{\text{HDO}} = (0.84 \pm 0.01) \cdot 10^{-9} \text{ m}^2/\text{s}$. This value is about 50% lower and corresponds to the arithmetic average of the first value and the offset ($D_{\text{offset}} = 0$).

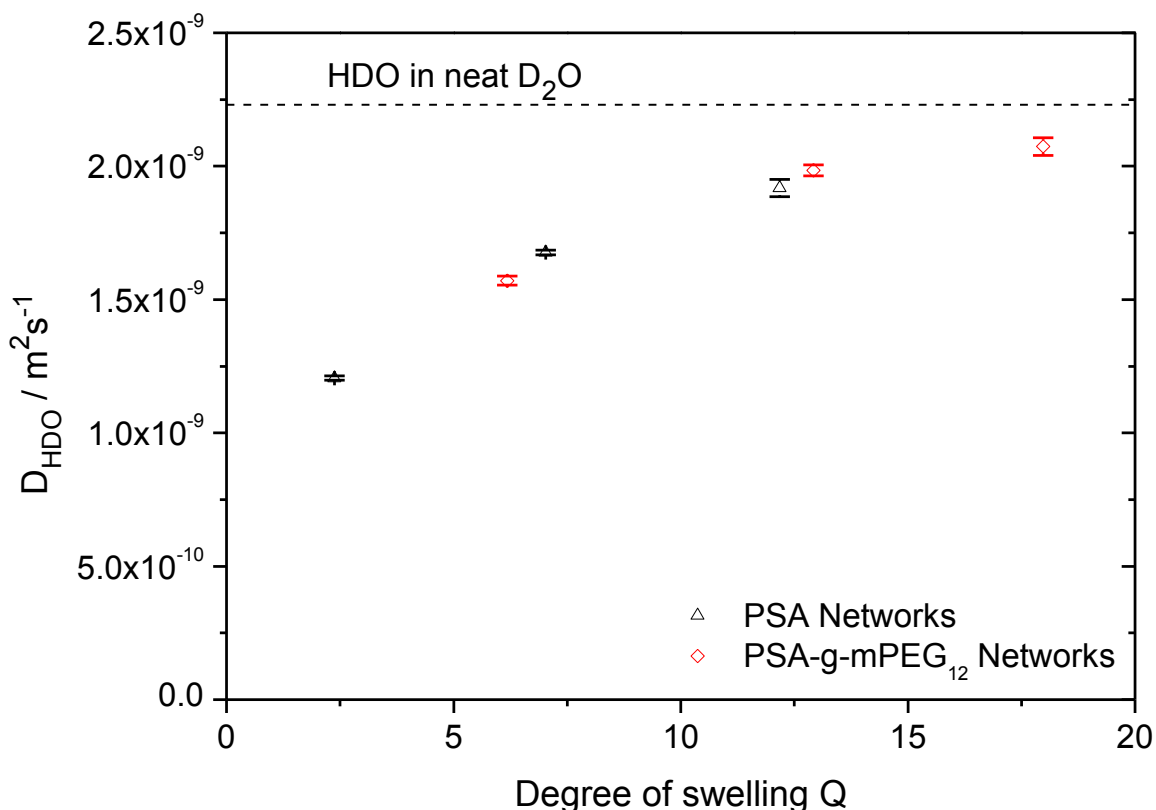


Figure 29. Dependence of the diffusion coefficient of water molecule (D_{HDO}) on the degree of swelling (Q) in PSA and PSA-g-mPEG networks at $T = 30$ °C. The dashed line represents the diffusion coefficient of HDO in neat D_2O of $D_{HDO} = 2.23 \cdot 10^{-9} m^2/s$.

The determined diffusion coefficients are shown in Figure 29 as a function of the degree of swelling Q are in good agreement with the data reported for the poly-(N,N -dimethylacrylamide) gels [255]. Especially at low swelling degrees, the network environment significantly influences the normal diffusion movement of water. With increasing length of the PEG spacers, water diffusion in the polymer network becomes faster and approaches the value of pure D_2O . In a direct comparison of the two network batches, it can be seen that the PSA-g-mPEG networks can absorb more water and therefore always show higher diffusion coefficients for the same length of the PEG spacers.

3.9. Physical structural parameters of PSA-g-mPEG hydrogels

The performance of hydrogels in a given application and their convenience as biomaterials rely heavily on their structural parameters. The most important of these parameters are $v_{2,s}$, \bar{M}_c , and ξ . $v_{2,s}$ relates to the polymer volume fraction of the hydrogels in a swollen state that illustrates the capability of the hydrogel system to absorb solvent. It is determined by calculating the volume ratio of the dry polymer gel to the swollen gel. This property is also related to the reciprocal of the swollen gel ratio and thus, can be connected to the density of dry polymer gel, density of the solvent, and ratio of the swollen gel mass as described in equation 8.

\bar{M}_c outlines the degree of crosslinking of the hydrogel structure by estimating the molar mass of the polymeric chain between two adjacent crosslinking points. It also gives an idea about the crosslinking density of the hydrogel and how will it behave after interaction with the thermodynamically compatible solvent [214].

Table 3. Degree of swelling (Q), polymer volume fraction ($v_{2,s}$), molar mass between two crosslinks (\bar{M}_c), and mesh size (ξ) of hydrogel samples.

Hydrogels	Q	$v_{2,s}$	\bar{M}_c (g/mol)	ξ (Å)
Hydrogels crosslinked with PEG-400	3.81	0.174	1941	15
Hydrogels crosslinked with PEG-1000	6.74	0.109	3869	26
Hydrogels crosslinked with PEG-2000	11.80	0.068	5772	38

Macromolecular chains achieve their optimum configuration in the solvated state when they are cross-linked and swollen in a thermodynamically compatible solvent. This can be characterized by a correlation length, which measures how far apart cross-links are on average from one another and indicates how the network affects solute diffusion. This distance is also referred to as mesh size in which length is correlated to the diffusion of solute. It can be challenging to experimentally determine this parameter and may ask for methods like light scattering [256,257] or in-depth microscopic examinations [258]. It, however, can be correlated to the theoretical estimation of molar mass between two crosslinks (\bar{M}_c) and polymer volume fraction ($v_{2,s}$). With the help of mesh size estimation, hydrogels can be

classified as non-porous, microporous, and macroporous. This classification can also be used to understand and define the phenomena of degradation, solute diffusion, and mechanical toughness of the respective hydrogels. Various factors like crosslinking degree, monomer chemistry, and stimuli including pH, temperature, etc. can affect the mesh size of the hydrogel [111,259].

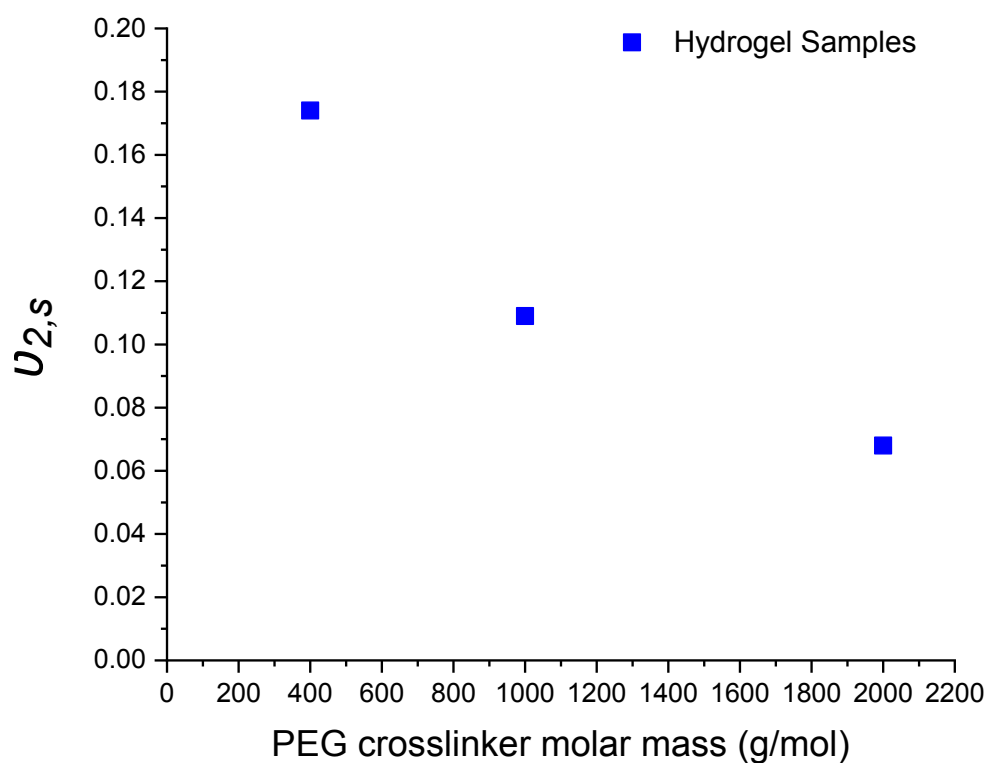


Figure 30. Polymer volume fraction of PSA-g-mPEG hydrogels vs varying the chain length of PEG crosslinking agents.

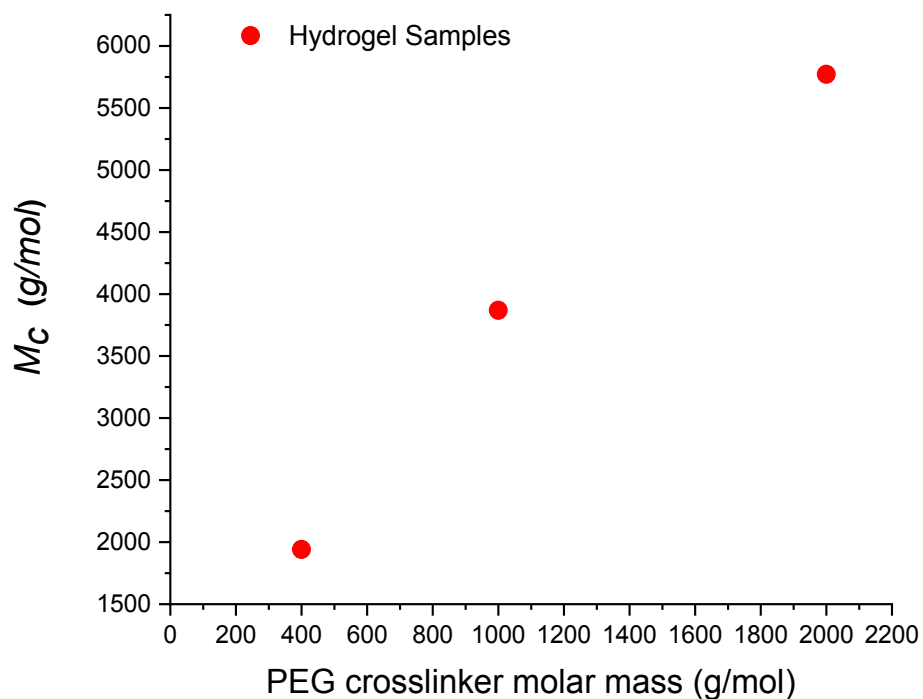


Figure 31. Molar mass between two crosslinks of PSA-g-mPEG hydrogels vs varying the chain length of PEG crosslinking agents.

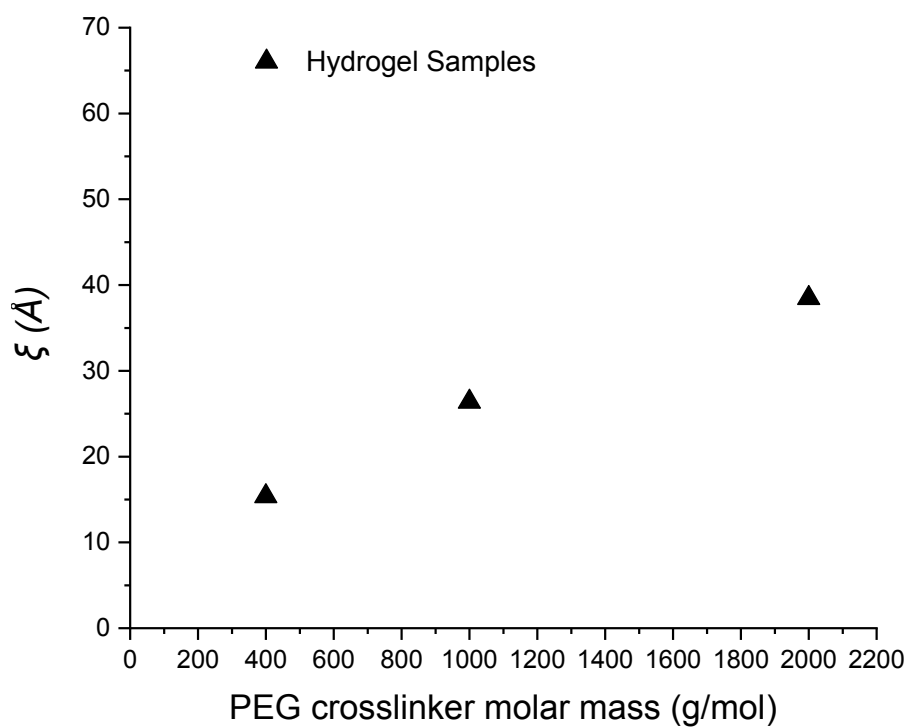


Figure 32. Mesh size of PSA-g-mPEG hydrogels vs varying the chain length of PEG crosslinking agents.

Elucidation of these interrelated hydrogel structural parameters can be made theoretically with the help of the famous equilibrium swelling theory [260] and rubber elasticity theory [261]. It is worth mentioning here that these values can only be reported as average values due to the randomness of the polymerization process. These values have been calculated and explained with the help of the equilibrium swelling theory. It can be deduced from Table 3 and Figure 30 that as the degree of swelling (Q) increases with the increase in PEG based crosslinker's chain length, the polymer volume fraction ($v_{2,s}$) decreases justifying the fact that polymer volume fraction ($v_{2,s}$) is inversely proportional to the swelling degree (Q) [257]. It was observed and reported by Waters *et al.* that using PEG macromonomers with higher molar mass results in hydrogels with lower polymer volume fraction. This is due to the fact that PEG macromonomers with higher molar mass lead to the formation of hydrogel networks with fewer cross-linking points per unit volume, resulting in weaker and less durable hydrogels [262].

Molar mass between two crosslinks (\bar{M}_c) of the hydrogels increases as the chain length of the PEG based crosslinker is increased as shown in Figure 31. This increase in the average molecular weight between two crosslinks of the hydrogels can be attributed to the chain length of the crosslinker which increases from PEG-400 to PEG-2000. A similar trend of results was also reported by Troung *et al.* when they synthesized various chain length (from 1,000 to 20,000) of PEG based hydrogels through click chemistry [206].

The swelling degree of a crosslinked polymer network demonstrates the thermodynamic expansion of the network, and the Flory-Rehner equation links this expansion to the network's particular characteristics and structure [215]. Taking advantage of these findings, Canal and Peppas discovered that the average distance between crosslinks (expressed in angstroms) known as mesh size (ξ) can be determined using \bar{M}_c [257]. It can be concluded from Figure 32 that the chain length of the crosslinkers utilized in the system is again a crucial factor in influencing the mesh size of the hydrogel system. Figure 32 shows that the hydrogel's mesh size grows as PEG-based crosslinker's chain lengths are increased. These calculated values of mesh size or correlation length can also be somehow correlated to the length of the PEG based spacers. As evident from previous studies, one unit of short chain of PEG can be correlated to the length of 1.5 Å under fully stretched helical structure [263]. Taking these calculations into account with respect to the length of the PEG spacers, they make up 14 Å, 34 Å and 67 Å for PEG-400, PEG-1000 and PEG-2000, respectively under fully stretched helical structure. It can thus be deduced that calculated length of 15 Å, 27 Å and 38 Å of

PEG-spacers can be correlated to the theoretical values of PEG-400, PEG-1000 and PEG-2000, respectively. As discussed earlier, these are the estimated values and are calculated on the assumption of Flory-Rehner derived model. Here, measured values for the PEG-400 and PEG-1000 spacer correlate well with the theoretically calculated values but correlation length value for the PEG-2000 deviates a bit from theoretical calculated value. Therefore, one can say that there is still room for improvement and establishment of more sophisticated model for the calculation of mesh size and other physical parameters of crosslinked polymeric network in case of copolymer derived network. On the other side, these varying chain lengths of PEG based spacers provide a basis for the modulation of mesh size as it varies and thus can help in the diffusion of molecules from polymer networks. It can also comprehend this evidence that the relationship between the crosslinker's chain length and mesh size can prove to be a vital factor in creating hydrogel systems with particular features to meet the unique needs and requirements.

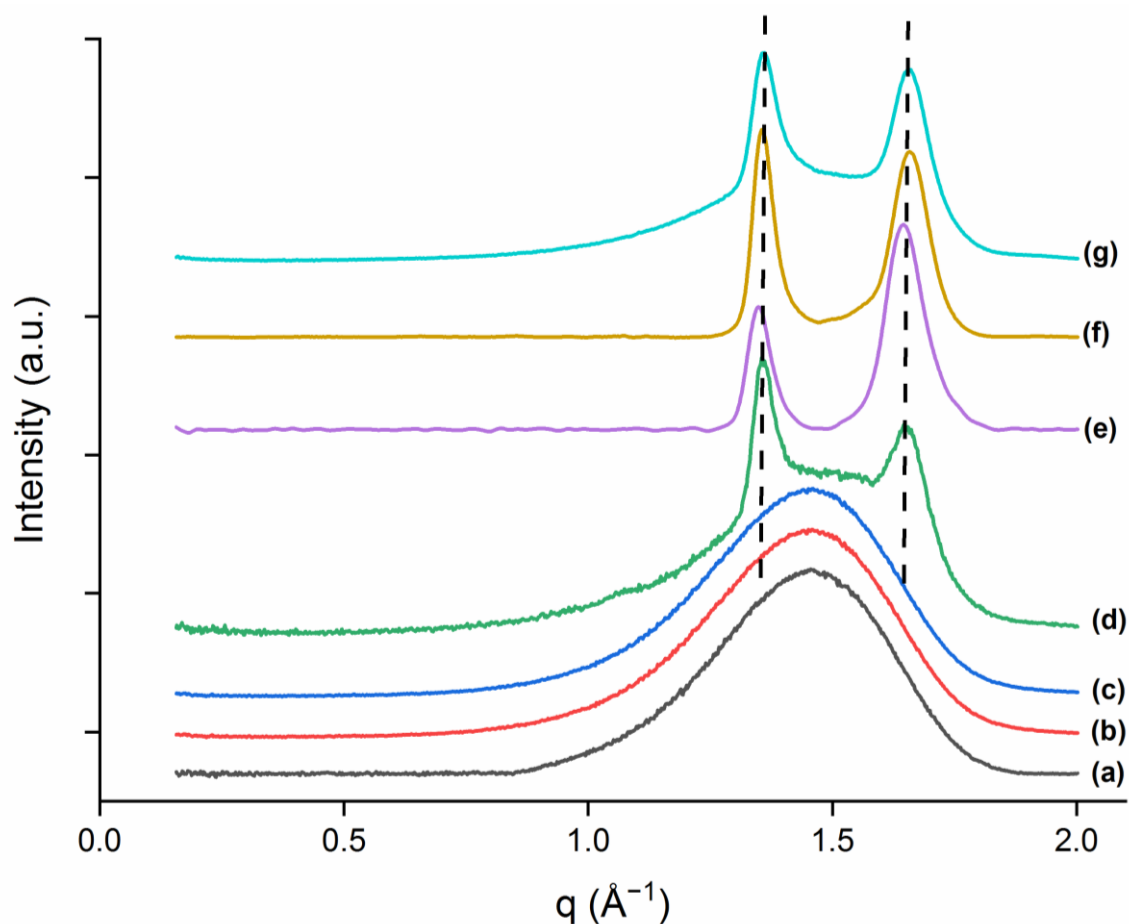


Figure 33. X-ray diffraction traces of (a) PSA-g-mPEG, (b) disuccinyl PEG-400, (c) dried PSA-g-mPEG hydrogels crosslinked with PEG-400, (d) disuccinyl PEG-1000, (e) dried PSA-g-mPEG hydrogels crosslinked with PEG-1000, (f) disuccinyl PEG-2000, (g) dried PSA-g-mPEG hydrogels crosslinked with PEG-2000.

3.10. X-ray diffraction

In order to discover about the amorphous and crystalline characteristics of the hydrogel samples as well as the reactants responsible for the material's crystallinity, X-ray diffraction measurements were performed on the samples. It can be deduced from Figure 33 and Figure 34 that neat polymer backbone (PSA-g-mPEG) and PEG-400 based crosslinker are completely amorphous in the spectra while samples with the PEG-1000 based and the PEG-2000 based crosslinkers show significant crystalline peaks. The same reflections were also observed for neat PEG-1000 and PEG-2000 and correspond to the (120) and (032) Miller planes of monoclinic PEG which are represented by the two characteristic peaks at $q = 1.36 \text{ \AA}^{-1}$ and $q = 1.66 \text{ \AA}^{-1}$, respectively. The unit cell is made up of PEG chains arranged in a 7_2 -helix structure, with seven repeating units in two turns [264]. Thus, it can be concluded from

the reactants/products data as well as previous literature that the crystalline nature of the hydrogel samples is being induced by the PEG based crosslinkers. These results are consistent with the previous findings investigated through the differential scanning calorimetry results published elsewhere [38]. It is also mentioned that exposure time for scattering patterns of d, e, and f was 30 seconds while for g was 180 seconds that's why more bright pattern of g can be seen. Furthermore, background signal of amorphous part was subtracted from scattering pattern of d, e, and f.

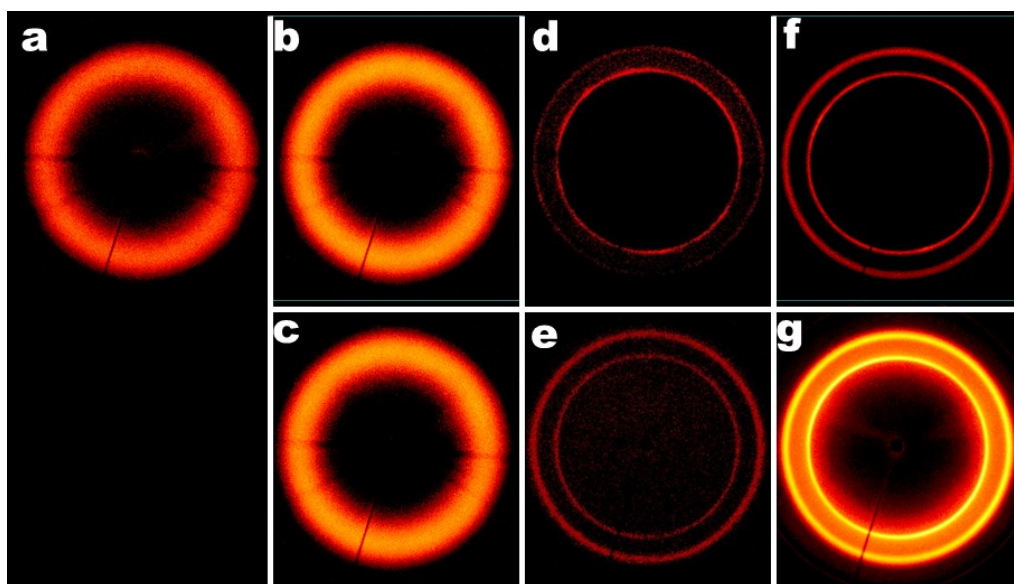


Figure 34. X-ray diffraction patterns of (a) PSA-g-mPEG, (b) Disuccinyl PEG-400, (c) PSA-g-mPEG hydrogels crosslinked with PEG-400, (d) Disuccinyl PEG-1000, (e) PSA-g-mPEG hydrogels crosslinked with PEG-1000, (f) Disuccinyl PEG-2000, (g) PSA-g-mPEG hydrogels crosslinked with PEG-2000.

3.11. Loading and release experiment of BSA-TMR and DY-781 from PSA-g-mPEG hydrogels

Loading of different molecules inside the hydrogels can be achieved by two different procedures. The first one is the post-loading which involves movement of drug/protein/dye molecules from outside (solvent solution) to inside of already formed hydrogels through diffusion being the major driving force. The second loading procedure is named as *in situ* loading which involves the mixing of drug/protein/dye molecules along with hydrogel precursors before its formation [214,265,266]. Post-loading method has been adopted here, so that, clean hydrogels without unwanted polymer traces can be used. To assess loading and

release of lower and higher molar mass molecules from hydrogels matrices, two different model molecules were used. Lower molar mass molecule used was DY-781, a fluorescent dye, having molecular weight of 781 g/mol while higher molar mass molecule used was BSA-TMR (a model protein, bovine serum albumin conjugated with a dye, i.e. tetramethylrhodamine) having molar mass of 66,000 g/mol. Loaded BSA-TMR and DY-781 were analyzed by the fluorescence spectrometer. In both DY-781 and BSA-TMR, loading was directly related to the swelling of the hydrogel samples. Hydrogels with the maximum swelling (PSA-g-mPEG crosslinked with PEG-2000 based crosslinker) attained the highest loading while hydrogel sample with the least swelling index (PSA-g-mPEG crosslinked with PEG-400 based crosslinker) achieved lowest loading (Figure 36). In Figure 37, one can easily see loading of another dye (DY-784) inside the hydrogel samples. Similarly, swelling pattern of the hydrogels can also deduced as discussed above.

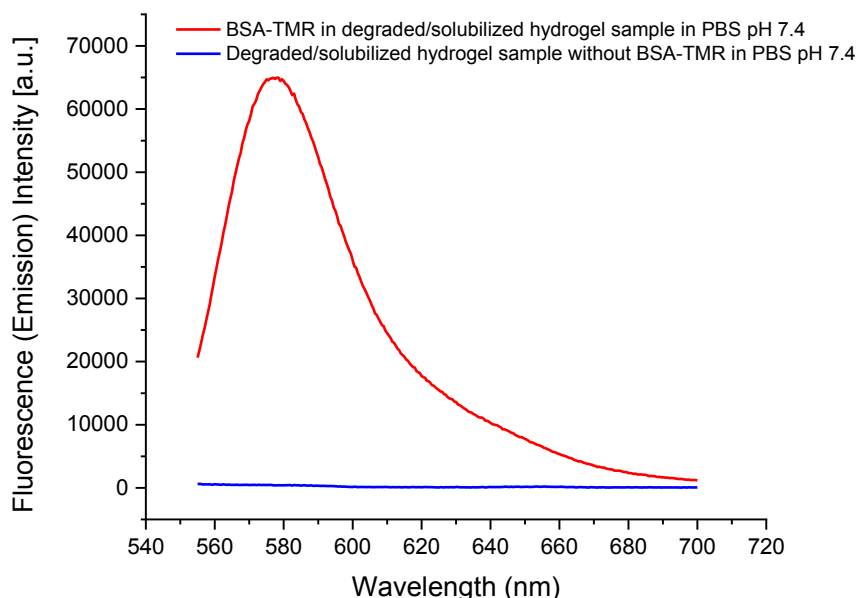


Figure 35. Fluorescence spectra of BSA-TMR along with hydrogel's degraded sample and degraded hydrogel without BSA-TMR measured via fluorescence spectrometer within wavelength range of excitation: 535 nm and emission: 576 nm, to evaluate interaction between both or any background signal.

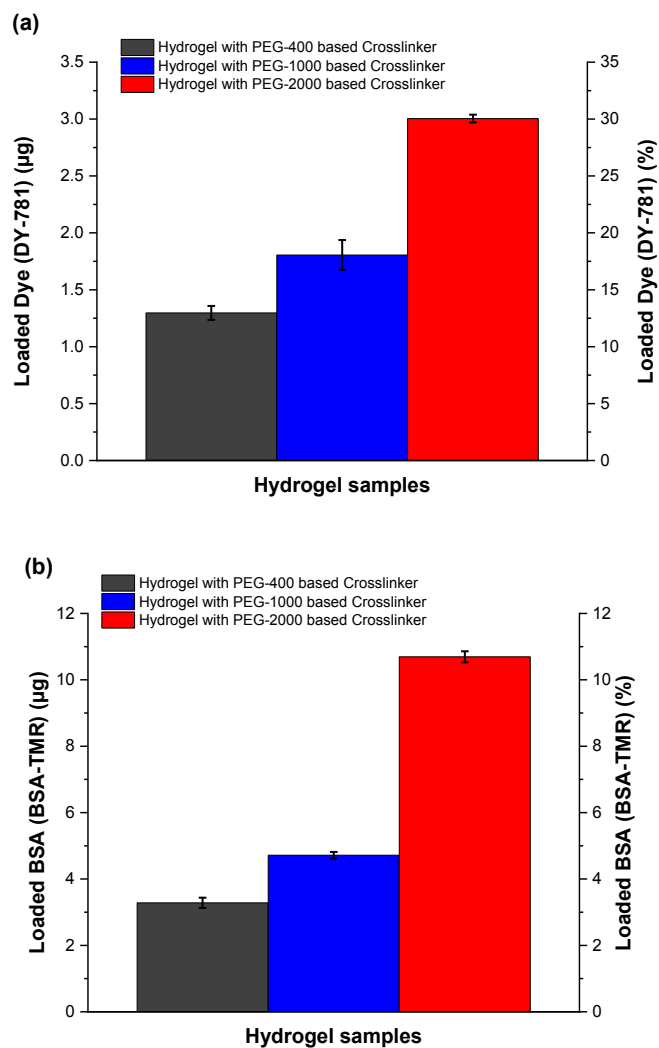


Figure 36. Post-loading efficiency of hydrogels through diffusion of molecules (a) dye loading (μg) and (%) and (b) BSA loading (μg) and (%).

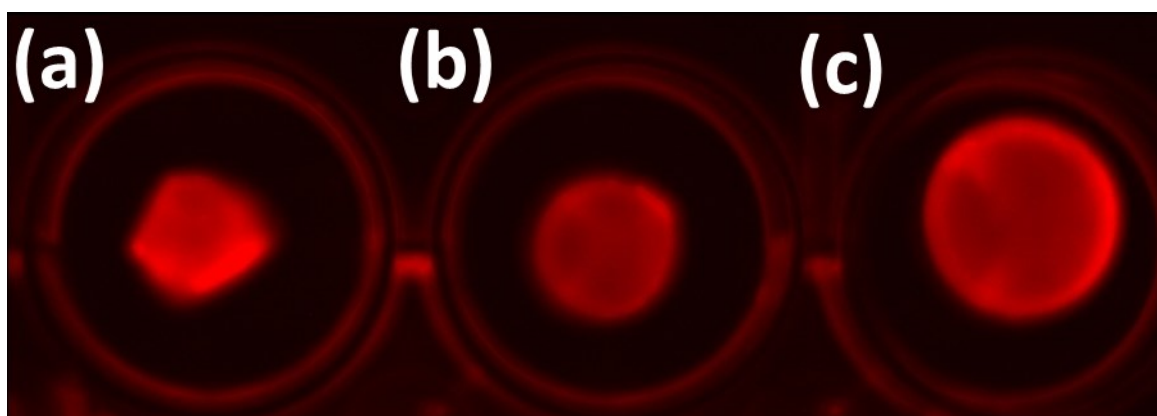


Figure 37. An illustration of, how hydrogels look like when dye is loaded inside. Post-loading fluorescence image of DY-784 into hydrogels matrices crosslinked with (a) PEG-400 based crosslinker, (b) PEG-1000 based crosslinker, and (c) PEG-2000 based crosslinker.

Thus, the loading of protein/dye molecules was directly related to the varying molar mass of the PEG crosslinker. Furthermore, theoretically estimated mesh size as shown in Figure 32 also gives an idea that diffusion of molecules through the hydrogels can be correlated to the mesh size of the chain length of the PEG crosslinker. Considering the estimated mesh size of the hydrogels and the loaded quantity of molecules as delineated in Figure 36, it is inferred that small sized molecules are being loaded to a greater extent than large sized molecules. This may be attributable to the fact that the mesh size of the hydrogels is larger than the small sized molecules, whereas in the case of BSA, the mesh size of the hydrogels somehow matches to the hydrodynamic radii of BSA, 34 Å [213].

In vitro release study of BSA-TMR and DY-781 from hydrogels was performed at 37 °C in PBS pH 7.4. Before the release study of BSA-TMR, fluorescence investigation of a blank hydrogel sample (degraded/solution form) and hydrogel sample (degraded/solution form) along with BSA-TMR was carried out to know the interaction between hydrogel and BSA-TMR. The fluorescence spectrum was recorded within the range of tetramethylrhodamine (TMR) having an excitation at 535 nm and an emission at 576 nm. The fluorescence spectrum (Figure 35) clearly shows that there was no interaction recorded between hydrogel and BSA-TMR and the spectrum only shows the TMR peak within the applied fluorescence range.

Release data of DY-781 demonstrates (Figure 38) that 40% of the DY-781 was released from all hydrogel matrices after 4 h of release study which can be attributed to the equilibrium swelling of hydrogel samples. Hydrogels swelling index (Figures 18 & 19) can be correlated to its release data as maximum swelling (equilibrium swelling) of the hydrogels occurred after 4 h. Witnessing the same pattern as of swelling, it can be seen that most amount of DY-781 was released from the hydrogel matrices in the same period of time. The majority of DY-781 was released after 24 h of study (Figure 38(d)) in which hydrogels crosslinked with PEG-400 showed 75% release, hydrogels crosslinked with PEG-1000 showed 69% whereas hydrogels crosslinked with PEG-2000 showed 67% release. 100% DY-781 release was recorded after one week of the study.

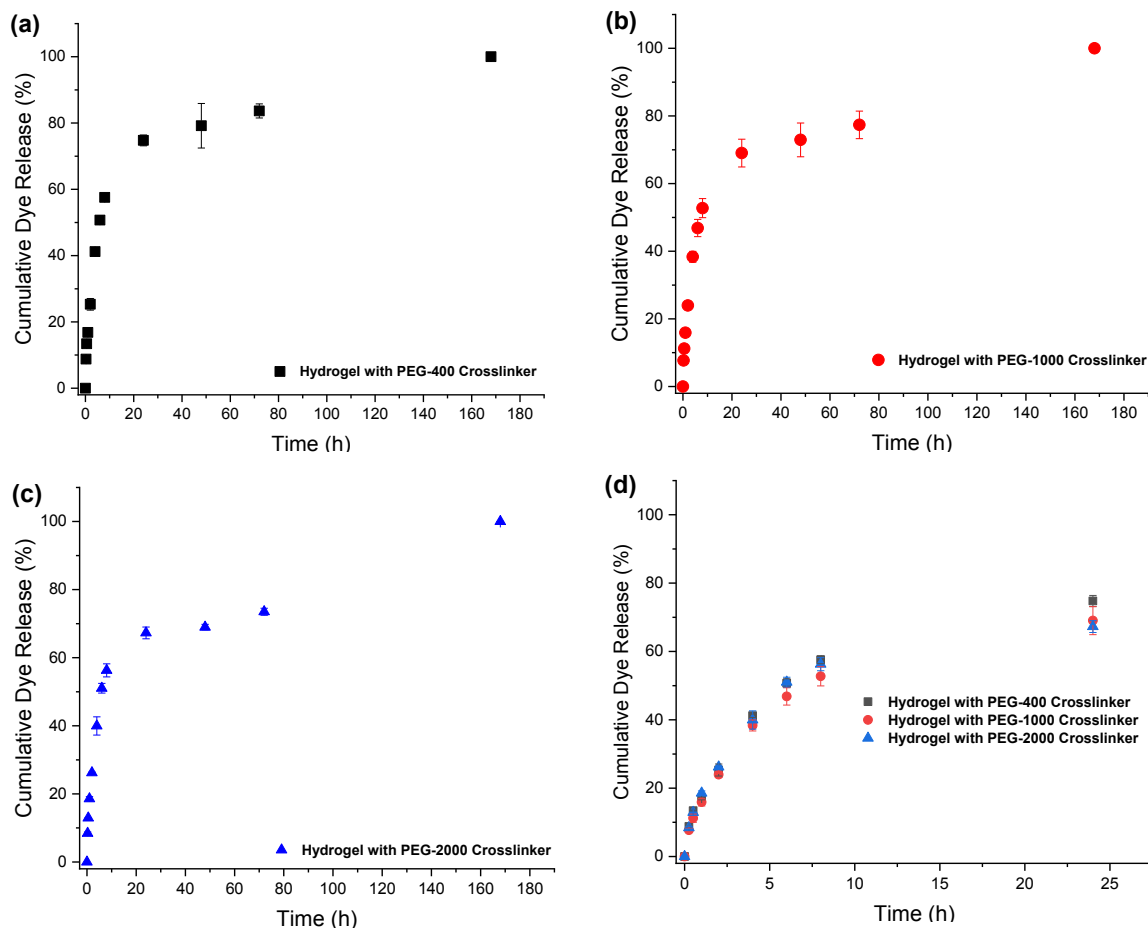


Figure 38. DY-781 cumulative release (%) in PBS with pH 7.4 + 0.2% NaN_3 at 37 °C **(a)** from hydrogels crosslinked with PEG-400 for 168 h (07 d), **(b)** from hydrogels crosslinked with PEG-1000 for 168 h (07 d), **(c)** from hydrogels crosslinked with PEG-2000 for 168 h (07 d), **(d)** from all hydrogels samples for 24 h.

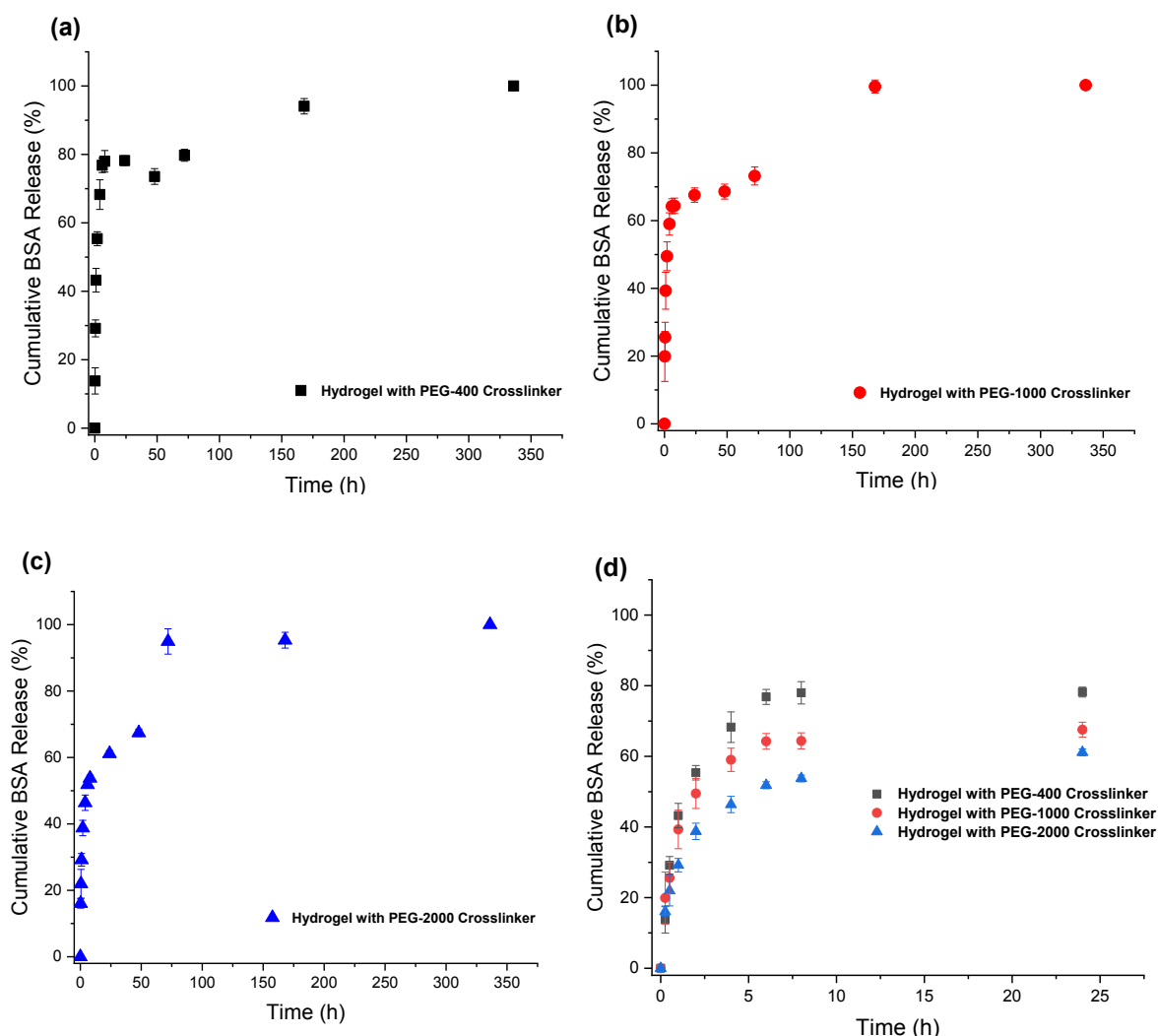


Figure 39. BSA (BSA-TMR) cumulative release (%) in PBS with pH 7.4 + 0.2% NaN_3 at 37 °C from (a) from hydrogels crosslinked with PEG-400 for 336 h (14 d), (b) from hydrogels crosslinked with PEG-1000 for 336 h (14 d), (c) from hydrogels crosslinked with PEG-2000 for 336 h (14 d), (d) initial release period from all hydrogels samples for 24 h.

Release study of BSA-TMR shows almost similar pattern of release as of DY-781 in a way that its release from hydrogel matrices continued for almost 14 d which shows 100% release at the 14th d (Figure 39). Again most percent of release can be attributed to the swelling pattern of the hydrogels. After 4 h of release study, hydrogels having PEG-400 based crosslinker released 68% BSA-TMR, PEG-1000 based crosslinked hydrogels released 59% BSA-TMR while PEG-2000 based crosslinked hydrogels released 46% BSA-TMR. After 24 h of BSA-TMR release (Figure 39 (d)), hydrogels crosslinked with PEG-400 demonstrated 78% release, hydrogels having PEG-1000 based crosslinker demonstrated 67% release whereas hydrogels crosslinked with PEG-2000 showed 61% release. Release of BSA-TMR continued for 14 d.

BSA-TMR and DY-781 release from different types of hydrogels crosslinked with the different chain lengths of PEG crosslinkers can't be compared with each other as there was a difference in the loaded amount in both cases. In addition, if BSA-TMR and DY-781 release are analyzed individually, there was a difference in the loaded amount of the protein/dye molecules for all hydrogels crosslinked with varying molar mass of PEG. It can still be deduced that molecular release from these hydrogel matrices is connected to the swelling of the hydrogels that occurs due to the interaction between water molecules and polymer chains. This interaction firstly leads to the diffusion of the water molecules inside the polymer hydrogels which initially loosens up the polymer chains and ends up in the expansion of the hydrogel systems due to the relaxation of the polymer chains [267,268] leading to the increase in the mesh size and desorption of the molecule release. The current data show that swelling plays a major part in the molecular release as most percent of the molecular release is achieved within 24 h of time. It is further assumed that this swelling-controlled release mechanism may simultaneously be followed by a chemically-controlled mechanism due to the fact that the polymer precursors consist of vinyl end groups which may interact with the amines present in the protein/dye molecules. This interaction can lead to Aza-Michael addition under mild reaction conditions without the presence of any catalyst which was reported by Razan *et. al.* also [269]. Thus, some percent of protein/dye molecular release may be attributed to the chemically-controlled release mechanism in which molecules may release after hydrolytic degradation of the hydrogels as they swell after coming in contact with the water. Such type of release mechanism can be termed as reaction diffusion-controlled mechanism in which both diffusion and chemical reaction take place [214]. For this reason, firstly the fast release of molecules was experienced through the hydrogel pores followed by slow release later on. Adding to this assumption, previously conducted proton double quantum NMR studies on this hydrogel system proves that PSA-g-mPEG hydrogel stands inhomogeneous due to the grafting of PEG side chains that can act as dangling chains. These NMR studies also tell about the two components present in the hydrogels, one is densely crosslinked regions with more crosslinking junctions while the second is loosely crosslinked regions with lesser crosslinking junctions. This may lead to the trapping of molecules in these densely crosslinked points which may take some time to diffuse outside [38]. Considering the pharmaceutical perspective, the release patterns observed with BSA-TMR and DY-781 offer promising prospects for the potential transdermal, subcutaneous and oral applications of these hydrogel matrices. These applications may involve the need for immediate drug release during the initial phase ensuring an immediate therapeutic effect followed by a delayed

release in the later stages of drug delivery maintaining a consistent therapeutic concentration over time, prolonging the efficacy of the treatment.

3.12. Cytotoxicity of PSA-g-mPEG hydrogels

Material biocompatibility is vital for its *in vivo* applications [270] and cytotoxicity can provide important insights about material biocompatibility [271]. To investigate the cytotoxicity of the hydrogels (degraded solution form), an *in vitro* resazurin assay was conducted in which the reduction of non-fluorescent blue resazurin to fluorescent red resorufin within living cellular mitochondria was measured. The comparative analysis of fluorescence intensity between treated and untreated cells enabled an assessment of cellular viability after its interaction with the hydrogels. This assay was carried out on two different cell lines; normal human dermal fibroblasts (NHDF) and mouse embryonic fibroblasts (3T3) to measure the cytotoxic traits of the hydrogels without loaded protein/dye.

Figure 40 and Figure 41 depict percent cell viabilities for the 3T3 cell line and NHDF cell line respectively, of different hydrogel samples at various concentrations after its incubation for 4 h and 96 h. It can be evaluated from the results that both types of cell lines exhibit a high percentage of cell viability for all hydrogel samples against different concentrations. It can also be indicated that cell viability of above 100% was observed across most of the hydrogel samples after 96 h. This can be interpreted in a way that the hydrogel samples point towards the enhancement of cell metabolism and proliferation. Few of the prior research studies also indicate that sorbitol has been reported as a factor that might play an important role in cell metabolism and growth in *in vitro* cell compatibility studies. Mei *et al.* conducted the same type of study by culturing 3T3 cell lines with polyesters. After 24 h of cell culture study, they analyzed that sorbitol containing polyesters can show cell proliferation, concluding that sorbitol containing compounds can prove to be promising candidates in the research and development of biomaterials [272]. In another investigation conducted on human skin fibroblasts Turner and Biermann came to the conclusion that sorbitol can proliferate similarly to glucose [273]. Keeping in view the obtained results of cytotoxicity as well as previous literature, it can still be deduced that the product may prove to be biocompatible in conducting *in vivo* experiments and the development of biomaterials.

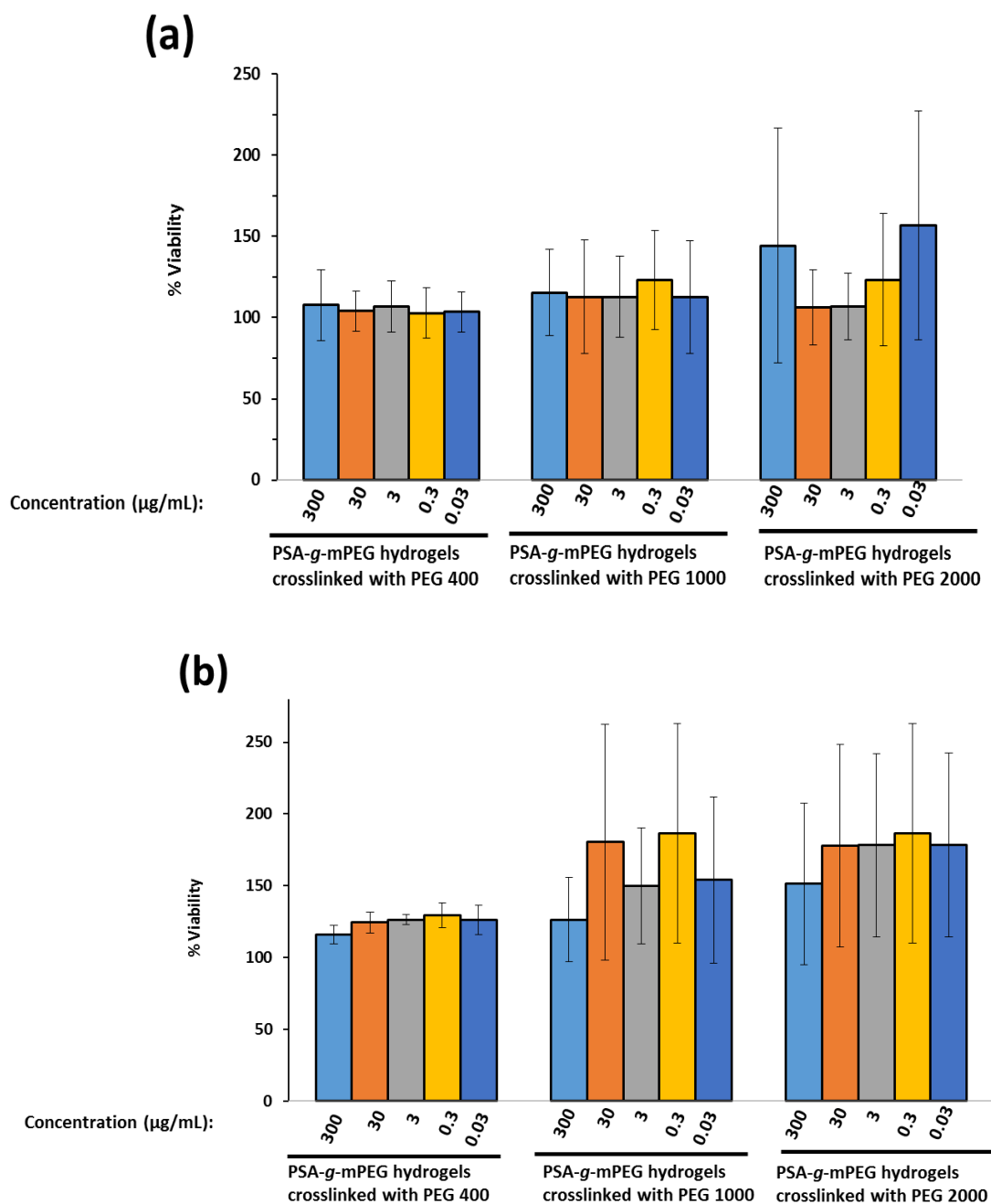


Figure 40. Viability of 3T3 cell line after being incubated with different concentrations of different types of hydrogels for **(a)** 4 h, **(b)** 96 h. The measurement was performed using a fluorescence-based resazurin reduction assay and the viability of untreated cells was taken as the reference (negative control) and set as 100%.

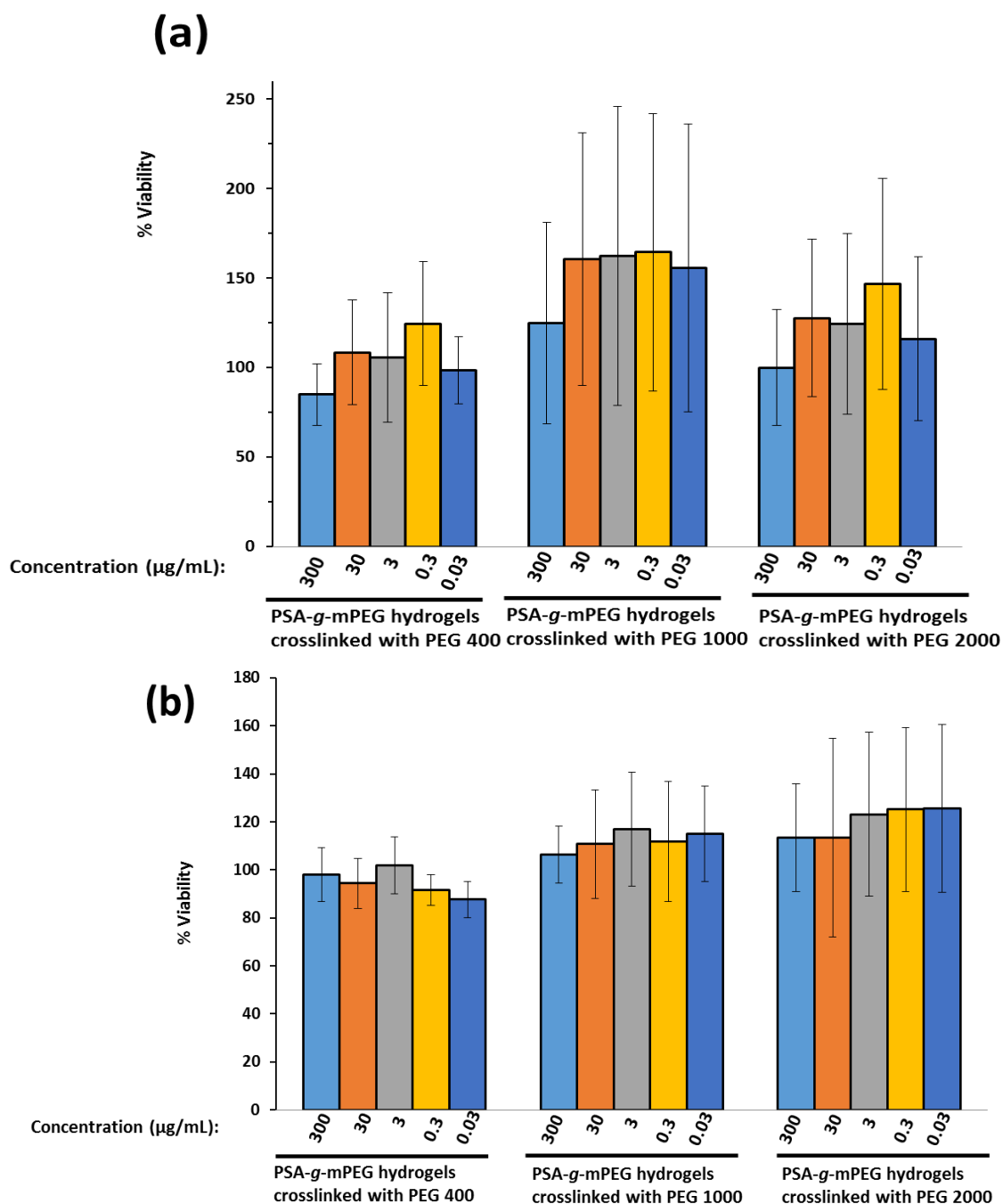


Figure 41. Viability of NHDF cell line after being incubated with different concentrations of different types of hydrogels for **(a)** 4 h, **(b)** 96 h. The measurement was performed using a fluorescence-based resazurin reduction assay and the viability of untreated cells was taken as the reference (negative control) and set as 100%.

4. Summary and Perspective

In recent years, extensive research has been conducted about various polymers to meet the diverse demands of pharmaceutical and biomedical applications. Among these synthetic polymers, aliphatic polyesters have seen notable advancements, primarily due to their ability to biodegrade and their compatibility with physiological systems. These unique attributes have positioned them as highly promising candidates for use in the biomedicine. The development of synthetic biodegradable polymers especially poly(glycolic acid), poly(lactic acid) (PLA), and poly(lactic-co-glycolic acid) (PLGA) was initiated with the specific intention of enabling biodegradation and serving various purposes in biomedicine and drug delivery. However, they have limitations like hydrophobicity and lack of free functional groups for further modifications to meet requirements of different applications. There are also concerns about their toxicity due to metal-based catalysts used in their synthesis. Additionally, these polymers exhibit complex degradation and release profiles and can create acidic microenvironments with low pH values.

Research work in this thesis discusses enzymatic polymerization as an alternative method to overcome the aforementioned limitations of the traditional polyesters followed by the fabrication of hydrogels to be used as potential carriers in pharmaceutical applications. Enzymatic polymerization utilizes eco-friendly principles and enzymes as biocatalysts to create aliphatic polyesters, avoiding the toxicity associated with metal-based catalysts. This thesis describes synthesis of poly(sorbitol adipate) through the transesterification of D-sorbitol with divinyl adipate. The sorbitol component of the linear polyester repeating unit features four pendant secondary hydroxyl groups, rendering hydrophilicity to the polyester structure. This is in contrast to poly(glycerol adipate) who is mostly utilized enzymatically synthesized polyester but is having single pendant hydroxyl functionality as well as insolubility in water. Poly(sorbitol adipate) (PSA) was successfully synthesized through lipase CAL-B catalyzed polycondensation reaction giving molar mass of 11,000 g/mol. Successful synthesis was verified by ^1H NMR and ^{13}C NMR while molar mass was calculated through gel permeation chromatography. Linearity was achieved due to the selectivity of CAL-B towards primary hydroxyl groups rather than secondary ones leaving hydroxyl groups for further modifications.

Utilizing the free hydroxyl functionalities of PSA, it was then grafted to poly(ethylene glycol) through the Steglich esterification reaction between free hydroxyl groups from PSA and

carboxyl groups from succinylated PEG to give molar mass of 22,000 g/mol. The synthesis of PSA-g-mPEG was confirmed by ^1H NMR and ^{13}C NMR. The appearance of the methyl peak at 3.23 ppm and methylene peak at 3.50 ppm of PEG in the ^1H NMR spectrum verifies the grafting of mPEG-550 chain to PSA. The grafting was also verified by GPC traces through a shift towards shorter retention time. To prepare hydrogels, next step was to synthesize bifunctional crosslinker. For that reason, disuccinyl PEG (Suc-PEG_n-Suc) with different molar masses was synthesized through carboxylation of OH-PEG-OH on both sides with succinic anhydride through esterification process. Synthesis was verified with help of ^1H NMR spectra. In last part of synthesis, hydrogels were synthesized through Steglich esterification process by using disuccinyl PEG with varying chain lengths of PEG. Esterification took place between hydroxyl groups from PSA or PSA-g-mPEG and the carboxylate groups of the succinyl part of disuccinyl PEG in order to study the effect of different chain lengths of the cross-linkers on the overall behavior of hydrogels. The hydrogel structure was verified by ^{13}C CP MAS NMR spectra.

DSC study was then performed for above mentioned polymers and hydrogels in the range between $-60\text{ }^\circ\text{C}$ and $80\text{ }^\circ\text{C}$. Measured data reveals the amorphous nature of PSA and PSA-g-mPEG since only a glass transition temperature T_g is observed in the respective heating trace. In contrast, monosuccinyl mPEG-550 shows a clear melting endotherm. Thus, the amorphous nature of PSA-g-mPEG indicates that the PSA backbone prevents the crystallization of the grafted PEG chains. Both hydrogel structures cross-linked with Suc-PEG₉-Suc (disuccinyl PEG-400) do not show any melting peak while hydrogel formed with Suc-PEG₂₃-Suc (disuccinyl PEG-1000) and Suc-PEG₄₅-Suc (disuccinyl PEG-2000), respectively, cross-linkers are semi-crystalline indicated by their melting endotherms in the DSC traces. Swelling study shows the two most important aspects of the swelling experiments: i) The degree of swelling is larger for PSA-g-mPEG samples compared to PSA based samples using identical cross-linkers and ii) The degree of swelling increases with the degree of polymerization (n) of the cross-linker molecules.

The structure and dynamics in PSA based polymer hydrogels were then investigated by ^{13}C MAS and ^1H DQ NMR measurements. Experimental data indicate that the networks have an inhomogeneous structure. For both PSA and PSA-g-mPEG networks, two network components with different dipolar coupling constants were detected. The exact amount of network defects could not be determined due to the inhomogeneity of the networks. ^1H PFG diffusion measurements on swollen networks allowed the determination of the diffusion

coefficients of HDO in the networks. As expected, the diffusion of the solvent strongly depends on the degree of swelling of the sample.

After taking into consideration the physico-chemical data of both PSA based hydrogels, PSA-g-PEG hydrogels were finalized to be used for further pharmaceutical applications. Various *in vitro* studies were conducted to evaluate its potential pharmaceutical applications. Stability data of PSA and PSA-g-PEG polymers was evaluated through GPC by processing these polymers at different temperature and humidity levels. These results suggest through GPC measurements that no change was observed in the number average molar mass (M_n) before and after modifications when polymers were kept at 4 °C. In contrast to 4 °C, a decrease in molar mass was observed when these polymers were kept at 40 °C and 75% RH. This decrease happens to be the result of the hydrolysis due to high temperature and humid conditions.

Sol-gel fraction of the hydrogels was determined to assess the amount of reactants consumed during the hydrogel formation. This property can also tell us about the efficiency of the Steglich esterification reaction when it is used to form a crosslinked polymer network. It can be revealed from the calculated data that the gel percent for the hydrogels crosslinked with PEG-400 was attained as 82%; hydrogels crosslinked with PEG-1000 attained as 77% while the hydrogels crosslinked with PEG-2000 attained as 66%. Sol% of all the mentioned hydrogels was attained as vice versa. This study suggests that when the chain length of PEG based crosslinker is increased from PEG-400 to PEG-2000, the gel percent is decreased. Dynamic and equilibrium swelling was performed to know about the swelling pattern of the PSA-g-PEG hydrogels as it was crucial in analysing release characteristics of the said polymer. Equilibrium swelling for hydrogel samples crosslinked with all types of crosslinking agents was achieved within 4 h of the study. Swelling of hydrogels was also investigated at different temperatures (22 °C, 37 °C, 50 °C and 75 °C) to know the effect of an increase in temperature over its swelling capability. Data shows that the degree of swelling for all types of hydrogels decreases as the temperature was increased from 22 °C to 75 °C. Such type of behavior has been explained as a PEG based property due to its lower critical solution temperature (LCST) which is known to be ~ 95 °C. Hence, hydrogen bonding is susceptible to breaking as the temperature rises against the hydrogels having PEG.

The performance of hydrogels in a given application and their convenience as biomaterials relies heavily on their structural parameters. So, different structural parameters consisting of

polymer volume fraction, degree of crosslinking between two adjacent crosslinking points and mesh size of the hydrogels were calculated. Results show that as the degree of swelling (Q) increases with the increase in PEG based crosslinker's chain length, the polymer volume fraction decreases. Molar mass between two crosslinks of the hydrogels increases as the chain length of the PEG based crosslinker increases. Similarly, hydrogel's mesh size grows as PEG-based crosslinker's chain lengths are increased.

In order to discover about the amorphous and crystalline characteristics of the hydrogel samples as well as the reactants responsible for the material's crystallinity, X-ray diffraction measurements were performed on the samples. It can be deduced that neat polymer backbone (PSA-g-mPEG) and PEG-400 based crosslinker are completely amorphous in the spectra while hydrogel samples with the PEG-1000 based and the PEG-2000 based crosslinkers show significant crystalline peaks.

Hydrogels were then subjected to loading and release study to evaluate them as potential drug delivery carriers. For this purpose, they were assessed against loading and release of lower and higher molar mass molecules from hydrogels matrices. Lower molar mass molecule used was DY-781, a fluorescent dye, having molar mass of 781 g/mol while higher molar mass molecule used was BSA-TMR (a model protein, bovine serum albumin conjugated with a dye, i.e. tetramethylrhodamine) having molar mass of 66,000 g/mol. Loaded BSA-TMR and DY-781 were analyzed by the fluorescence spectrometer. In both DY-781 and BSA-TMR, loading was directly related to the swelling of the hydrogel samples. Hydrogels with the maximum swelling (PSA-g-mPEG crosslinked with PEG-2000 based crosslinker) attained the highest loading while hydrogel sample with the least swelling index (PSA-g-mPEG crosslinked with PEG-400 based crosslinker) achieved lowest loading. Release study of BSA-TMR shows almost similar pattern of release as of DY-781 in a way that its release from hydrogel matrices continued for almost 14 d which shows 100% release at the 14th d. Again most percent of release can be attributed to the swelling pattern of the hydrogels. After 4 h of release study, hydrogels having PEG-400 based crosslinker released 68% BSA-TMR, PEG-1000 based crosslinked hydrogels released 59% BSA-TMR while PEG-2000 based crosslinked hydrogels released 46% BSA-TMR. After 24 h of BSA-TMR release, hydrogels crosslinked with PEG-400 demonstrated 78% release, hydrogels having PEG-1000 based crosslinker demonstrated 67% release whereas hydrogels crosslinked with PEG-2000 showed 61% release. Release of BSA-TMR continued for 14 d.

To investigate the cytotoxicity of these hydrogels, an *in vitro* resazurin assay was conducted in which the reduction of non-fluorescent blue resazurin to fluorescent red resorufin within living cellular mitochondria was measured. Percent cell viabilities for the 3T3 cell line and NHDF cell line were investigated against different hydrogel samples at various concentrations after its incubation for 4 h and 96 h. Results deduce that both types of cell lines exhibit a high percentage of cell viability for all hydrogel samples against different concentrations.

Looking at the environmentally friendly enzymatic polymerization and the multiple available pendant hydroxyl functionalities of PSA, it holds significant potential as a carrier for drug delivery across various pharmaceutical applications. From a pharmaceutical standpoint, the observed release patterns with molecules like BSA-TMR and DY-781 provide promising prospects for its use in potential wound dressing applications. Moreover, it can also be considered for potential applications which may involve the need for immediate drug release during the initial phase ensuring an immediate therapeutic effect followed by a delayed release in the later stages of drug delivery maintaining a consistent therapeutic concentration over time, prolonging the efficacy of the treatment. Furthermore, it can also be utilized in subcutaneous drug delivery systems, if immediate release from the aforementioned matrices can be regulated.

5. References

1. Saldívar- Guerra, E.; Vivaldo- Lima, E. Introduction to polymers and polymer types. *Handb. Polym. Synth. Charact. Process.* **2013**, 1–14.
2. Carbone, J.P.; Reinert, K.H. Synthetic polymers. **2015**.
3. Carothers, W.H. Studies on polymerization and ring formation. I. An introduction to the general theory of condensation polymers. *J. Am. Chem. Soc.* **1929**, *51*, 2548–2559.
4. Martinho, N.; Damgé, C.; Reis, C.P. Recent advances in drug delivery systems. *J. Biomater. Nanobiotechnol.* **2011**, *2*, 510.
5. Langer, R.; Peppas, N.A. Advances in Biomaterials, Drug Delivery, and Bionanotechnology. *AIChE J.* **2003**, *49*, 2990–3006, doi:10.1002/aic.690491202.
6. Heller, A. Integrated medical feedback systems for drug delivery. *AIChE J.* **2005**, *51*, 1054–1066.
7. Anderson, J.M.; Kim, S.W. Advances in drug delivery systems (3), book review. *J Pharm Sci* **1989**, *78*, 608–609.
8. Sung, Y.K.; Kim, S.W. Recent advances in polymeric drug delivery systems. *Biomater. Res.* **2020**, *24*, 1–12.
9. Basu, A.; Kunduru, K.R.; Doppalapudi, S.; Domb, A.J.; Khan, W. Poly (lactic acid) based hydrogels. *Adv. Drug Deliv. Rev.* **2016**, *107*, 192–205.
10. Prajapati, S.K.; Jain, A.; Jain, A.; Jain, S. Biodegradable polymers and constructs: A novel approach in drug delivery. *Eur. Polym. J.* **2019**, *120*, 109191.
11. Doppalapudi, S.; Jain, A.; Khan, W.; Domb, A.J. Biodegradable polymers—an overview. *Polym. Adv. Technol.* **2014**, *25*, 427–435.
12. Middleton, J.C.; Tipton, A.J. Synthetic biodegradable polymers as orthopedic devices. *Biomaterials* **2000**, *21*, 2335–2346.
13. Kulkarni, R.K.; Moore, E.G.; Hegyeli, A.F.; Leonard, F. Biodegradable poly (lactic acid) polymers. *J. Biomed. Mater. Res.* **1971**, *5*, 169–181.
14. Kamaly, N.; Yameen, B.; Wu, J.; Farokhzad, O.C. Degradable controlled-release polymers and polymeric nanoparticles: mechanisms of controlling drug release. *Chem. Rev.* **2016**, *116*, 2602–2663.
15. Gunatillake, P.; Mayadunne, R.; Adhikari, R. Recent developments in biodegradable synthetic polymers. *Biotechnol. Annu. Rev.* **2006**, *12*, 301–347.
16. Fu, K.; Pack, D.W.; Klibanov, A.M.; Langer, R. Visual evidence of acidic environment within degrading poly (lactic-co-glycolic acid)(PLGA) microspheres. *Pharm. Res.*

- 2000, *17*, 100–106.
17. Mäder, K.; Gallez, B.; Liu, K.J.; Swartz, H.M. Non-invasive in vivo characterization of release processes in biodegradable polymers by low-frequency electron paramagnetic resonance spectroscopy. *Biomaterials* **1996**, *17*, 457–461.
 18. Wersig, T.; Hacker, M.C.; Kressler, J.; Mäder, K. Poly (glycerol adipate)–indomethacin drug conjugates–synthesis and in vitro characterization. *Int. J. Pharm.* **2017**, *531*, 225–234.
 19. Taylor, M.S.; Daniels, A.U.; Andriano, K.P.; Heller, J. Six bioabsorbable polymers: in vitro acute toxicity of accumulated degradation products. *J. Appl. Biomater.* **1994**, *5*, 151–157.
 20. Bilal, M.H.; Hussain, H.; Prehm, M.; Baumeister, U.; Meister, A.; Hause, G.; Busse, K.; Mäder, K.; Kressler, J. Synthesis of poly(glycerol adipate)-g-oleate and its ternary phase diagram with glycerol monooleate and water. *Eur. Polym. J.* **2017**, *91*, 162–175, doi:10.1016/j.eurpolymj.2017.03.057.
 21. Vert, M. Aliphatic polyesters: Great degradable polymers that cannot do everything. *Biomacromolecules* **2005**, *6*, 538–546, doi:10.1021/bm0494702.
 22. Seyednejad, H.; Ghassemi, A.H.; Van Nostrum, C.F.; Vermonden, T.; Hennink, W.E. Functional aliphatic polyesters for biomedical and pharmaceutical applications. *J. Control. Release* **2011**, *152*, 168–176, doi:10.1016/j.jconrel.2010.12.016.
 23. Albertsson, A.C.; Varma, I.K. Recent developments in ring opening polymerization of lactones for biomedical applications. *Biomacromolecules* **2003**, *4*, 1466–1486, doi:10.1021/bm034247a.
 24. Jiang, Y.; Loos, K. Enzymatic synthesis of biobased polyesters and polyamides. *Polymers (Basel)*. **2016**, *8*, 243, doi:10.3390/polym8070243.
 25. Fich, E.A.; Segerson, N.A.; Rose, J.K.C. The Plant Polyester Cutin: Biosynthesis, Structure, and Biological Roles. *Annu. Rev. Plant Biol.* **2016**, *67*, 207–233, doi:10.1146/annurev-arplant-043015-111929.
 26. Hefetz, A.; Fales, H.M.; Batra, S.W.T. Natural polyesters: Dufour's gland macrocyclic lactones form brood cell laminesters in *Colletes* bees. *Science (80-.)*. **1979**, *204*, 415–417, doi:10.1126/science.204.4391.415.
 27. Zellin, G.; Hedner, E.; Linde, A. Bone regeneration by a combination of osteopromotive membranes with different BMP preparations: A review. *Connect. Tissue Res.* **1996**, *35*, 279–284, doi:10.3109/03008209609029202.
 28. Saito, N.; Murakami, N.; Takahashi, J.; Horiuchi, H.; Ota, H.; Kato, H.; Okada, T.;

- Nozaki, K.; Takaoka, K. Synthetic biodegradable polymers as drug delivery systems for bone morphogenetic proteins. *Adv. Drug Deliv. Rev.* **2005**, *57*, 1037–1048, doi:10.1016/j.addr.2004.12.016.
29. Budak, K.; Sogut, O.; Aydemir Sezer, U. A review on synthesis and biomedical applications of polyglycolic acid. *J. Polym. Res.* **2020**, *27*, 1–19, doi:10.1007/s10965-020-02187-1.
30. Tong, R. New chemistry in functional aliphatic polyesters. *Ind. Eng. Chem. Res.* **2017**, *56*, 4207–4219.
31. Jérôme, C.; Lecomte, P. Recent advances in the synthesis of aliphatic polyesters by ring-opening polymerization. *Adv. Drug Deliv. Rev.* **2008**, *60*, 1056–1076, doi:http://dx.doi.org/10.1016/j.addr.2008.02.008.
32. Naolou, T.; Busse, K.; Kressler, J. Synthesis of well-defined graft copolymers by combination of enzymatic polycondensation and “Click” chemistry. *Biomacromolecules* **2010**, *11*, 3660–3667, doi:10.1021/bm1011085.
33. Naolou, T. Green Route to Prepare Renewable Polyesters from Monomers: Enzymatic Polymerization. *Introd. to Renew. Biomater.* **2017**, 219–237, doi:10.1002/9781118698600.ch7.
34. Métraï, G.; Wentland, J.; Thomann, Y.; Tiller, J.C. Biodegradable poly(ester hydrazide)s via enzymatic polymerization. *Macromol. Rapid Commun.* **2005**, *26*, 1330–1335, doi:10.1002/marc.200500341.
35. Gross, R.A.; Ganesh, M.; Lu, W. Enzyme-catalysis breathes new life into polyester condensation polymerizations. *Trends Biotechnol.* **2010**, *28*, 435–443, doi:10.1016/j.tibtech.2010.05.004.
36. Kobayashi, S.; Uyama, H.; Kimura, S. Enzymatic polymerization. *Chem. Rev.* **2001**, *101*, 3793–3818, doi:10.1021/cr990121l.
37. Douka, A.; Vouyiouka, S.; Papaspyridi, L.M.; Papaspyrides, C.D. A review on enzymatic polymerization to produce polycondensation polymers: The case of aliphatic polyesters, polyamides and polyesteramides. *Prog. Polym. Sci.* **2018**, *79*, 1–25, doi:10.1016/j.progpolymsci.2017.10.001.
38. Rashid, H.; Golitsyn, Y.; Bilal, M.H.; Mäder, K.; Reichert, D.; Kressler, J. Polymer networks synthesized from poly(Sorbitol adipate) and functionalized poly(ethylene glycol). *Gels* **2021**, *7*, 1–20, doi:10.3390/GELS7010022.
39. Fischer, E. Einfluss der Configuration auf die Wirkung der Enzyme. II. *Berichte der Dtsch. Chem. Gesellschaft* **1894**, *27*, 3479–3483, doi:10.1002/cber.189402703169.

40. Pauling, L. Molecular architecture and biological reactions. *Chem. Eng. News* **1946**, *24*, 1375–1377, doi:10.1021/cen-v024n010.p1375.
41. Kollman, P.A.; Kuhn, B.; Donini, O.; Perakyla, M.; Stanton, R.; Bakowies, D. Elucidating the nature of enzyme catalysis utilizing a new twist on an old methodology: Quantum mechanical-free energy calculations on chemical reactions in enzymes and in aqueous solution. *Acc. Chem. Res.* **2001**, *34*, 72–79, doi:10.1021/ar000032r.
42. Kobayashi, S. 5.10—Enzymatic Polymerization. *Polym. Sci. A Compr. Ref. Matyjaszewski, K., Möller, M., Eds* **2012**, 217–237.
43. Stavila, E.; Loos, K. Synthesis of polyamides and their copolymers via enzymatic polymerization. *J. Renew. Mater.* **2015**, *3*, 268–280.
44. Jiang, Y.; Loos, K. Enzymatic synthesis of biobased polyesters and polyamides. *Polymers (Basel)*. **2016**, *8*, doi:10.3390/polym8070243.
45. Lundberg, H.; Tinnis, F.; Selander, N.; Adolfsson, H. Catalytic amide formation from non-activated carboxylic acids and amines. *Chem. Soc. Rev.* **2014**, *43*, 2714–2742.
46. Gotor-Fernández, V.; Vicente, G. Use of lipases in organic synthesis. In *Industrial enzymes: Structure, function and applications*; Springer, 2007; pp. 301–315.
47. Pellis, A.; Corici, L.; Sinigoi, L.; D’Amelio, N.; Fattor, D.; Ferrario, V.; Ebert, C.; Gardossi, L. Towards feasible and scalable solvent-free enzymatic polycondensations: Integrating robust biocatalysts with thin film reactions. *Green Chem.* **2015**, *17*, 1756–1766.
48. Engel, S.; Höck, H.; Bocola, M.; Keul, H.; Schwaneberg, U.; Möller, M. CaLB catalyzed conversion of ϵ -caprolactone in aqueous medium. Part 1: immobilization of CaLB to microgels. *Polymers (Basel)*. **2016**, *8*, 372.
49. Błaszczuk, J.; Kiełbasiński, P. Quarter of a Century after: A Glimpse at the Conformation and Mechanism of *Candida antarctica* Lipase B. *Crystals* **2020**, *10*, 404.
50. Cen, Y.; Singh, W.; Arkin, M.; Moody, T.S.; Huang, M.; Zhou, J.; Wu, Q.; Reetz, M.T. Artificial cysteine-lipases with high activity and altered catalytic mechanism created by laboratory evolution. *Nat. Commun.* **2019**, *10*, 3198.
51. da Silva, R.T.P.; de Barros, H.R.; Fernandes, R.F.; Toro-Mendoza, J.; Colluzza, I.; Temperini, M.L.A.; de Torresi, S.I.C. Physicochemical insights into the LSPR-driven Enzymatic Activity of Lipase Adsorbed on Gold Nanoparticles. *Nanobiocatalysts Nanozymes Nanobioconjugates Heterog. Catal. Electrocatal.* **2022**, 100.
52. Khairul Anuar, N.F.S.; Huyop, F.; Ur-Rehman, G.; Abdullah, F.; Normi, Y.M.;

- Sabullah, M.K.; Abdul Wahab, R. An overview into polyethylene terephthalate (PET) hydrolases and efforts in tailoring enzymes for improved plastic degradation. *Int. J. Mol. Sci.* **2022**, *23*, 12644.
53. Ma'ruf, I.F.; Widhiastuty, M.P.; Moeis, M.R. Effect of mutation at oxyanion hole residu (H110F) on activity of Lk4 lipase. *Biotechnol. Reports* **2021**, *29*, e00590.
54. Hevilla, V.; Sonseca, A.; Echeverría, C.; Muñoz-Bonilla, A.; Fernández-García, M. Enzymatic Synthesis of Polyesters and Their Bioapplications: Recent Advances and Perspectives. *Macromol. Biosci.* **2021**, *21*, 2100156, doi:10.1002/mabi.202100156.
55. Zhang, Y.-R.; Spinella, S.; Xie, W.; Cai, J.; Yang, Y.; Wang, Y.-Z.; Gross, R.A. Polymeric triglyceride analogs prepared by enzyme-catalyzed condensation polymerization. *Eur. Polym. J.* **2013**, *49*, 793–803, doi:http://dx.doi.org/10.1016/j.eurpolymj.2012.11.011.
56. Yang, Y.; Lu, W.; Cai, J.; Hou, Y.; Ouyang, S.; Xie, W.; Gross, R.A. Poly (oleic diacid-co-glycerol): Comparison of polymer structure resulting from chemical and lipase catalysis. *Macromolecules* **2011**, *44*, 1977–1985.
57. Tanaka, A.; Kohri, M.; Takiguchi, T.; Kato, M.; Matsumura, S. Enzymatic synthesis of reversibly crosslinkable polyesters with pendant mercapto groups. *Polym. Degrad. Stab.* **2012**, *97*, 1415–1422, doi:http://dx.doi.org/10.1016/j.polymdegradstab.2012.05.016.
58. Okumura, S.; Iwai, M.; Tominaga, Y. Synthesis of ester oligomer by *Aspergillus niger* lipase. *Agric. Biol. Chem.* **1984**, *48*, 2805–2808.
59. Uyama, H.; Yaguchi, S.; Kobayashi, S. Lipase-catalyzed polycondensation of dicarboxylic acid–divinyl esters and glycols to aliphatic polyesters. *J. Polym. Sci. Part A Polym. Chem.* **1999**, *37*, 2737–2745.
60. Varma, I.K.; Albertsson, A.-C.; Rajkhowa, R.; Srivastava, R.K. Enzyme catalyzed synthesis of polyesters. *Prog. Polym. Sci.* **2005**, *30*, 949–981.
61. Brazwell, E.M.; Filos, D.Y.; Morrow, C.J. Biocatalytic synthesis of polymers. III. Formation of a high molecular weight polyester through limitation of hydrolysis by enzyme-bound water and through equilibrium control. *J. Polym. Sci. Part A Polym. Chem.* **1995**, *33*, 89–95.
62. Silva, M.R. da; Montenegro, T.G.C.; Mattos, M.C. de; Oliveira, M. da C.F. de; de Lemos, T.L.G.; Gonzalo, G. de; Lavandera, I.; Gotor-Fernández, V.; Gotor, V. Regioselective preparation of thiamphenicol esters through lipase-catalyzed processes. *J. Braz. Chem. Soc.* **2014**, *25*, 987–994.

63. Uyama, H.; Kobayashi, S. Lipase-catalyzed polymerization of divinyl adipate with glycols to polyesters. *Chem. Lett.* **1994**, *23*, 1687–1690.
64. Uyama, H.; Inada, K.; Kobayashi, S. Regioselective polymerization of divinyl sebacate and triols using lipase catalyst. *Macromol. Rapid Commun.* **1999**, *20*, 171–174, doi:10.1002/(sici)1521-3927(19990401)20:4<171::aid-marc171>3.3.co;2-u.
65. Bhattacharya, A.; Rawlins, J.W.; Ray, P. *Polymer Grafting and Crosslinking*; John Wiley & Sons, 2008; ISBN 9780470404652.
66. Feng, C.; Li, Y.; Yang, D.; Hu, J.; Zhang, X.; Huang, X. Well-defined graft copolymers: From controlled synthesis to multipurpose applications. *Chem. Soc. Rev.* **2011**, *40*, 1282–1295, doi:10.1039/b921358a.
67. Kallinteri, P.; Higgins, S.; Hutcheon, G.A.; St. Pourçain, C.B.; Garnett, M.C. Novel functionalized biodegradable polymers for nanoparticle drug delivery systems. *Biomacromolecules* **2005**, *6*, 1885–1894, doi:10.1021/bm049200j.
68. Alaneed, R.; Hauenschild, T.; Mäder, K.; Pietzsch, M.; Kressler, J. Conjugation of amine-functionalized polyesters with dimethylcasein using microbial transglutaminase. *J. Pharm. Sci.* **2020**, *109*, 981–991.
69. Naolou, T.; Weiss, V.M.; Conrad, D.; Busse, K.; Mäder, K.; Kressler, J. Fatty acid modified poly (glycerol adipate)-Polymeric analogues of glycerides. In *Tailored polymer architectures for pharmaceutical and biomedical applications*; ACS Publications, 2013; pp. 39–52 ISBN 1947-5918.
70. Taresco, V.; Suksiriworapong, J.; Creasey, R.; Burley, J.C.; Mantovani, G.; Alexander, C.; Treacher, K.; Booth, J.; Garnett, M.C. Properties of acyl modified poly(glycerol-adipate) comb-like polymers and their self-assembly into nanoparticles. *J. Polym. Sci. Part A Polym. Chem.* **2016**, *54*, 3267–3278, doi:10.1002/pola.28215.
71. Tawfeek, H.; Khidr, S.; Samy, E.; Ahmed, S.; Murphy, M.; Mohammed, A.; Shabir, A.; Hutcheon, G.; Saleem, I. Poly (glycerol adipate-co- ω -pentadecalactone) spray-dried microparticles as sustained release carriers for pulmonary delivery. *Pharm. Res.* **2011**, *28*, 2086–2097.
72. Orafi, H.; Kallinteri, P.; Garnett, M.; Huggins, S.; Hutcheon, G.; Pourcain, C. Novel poly(glycerol-adipate) polymers used for nanoparticle making: A study of surface free energy. *Iran. J. Pharm. Res.* **2008**, *7*, 11–19.
73. Pfefferkorn, D.; Pulst, M.; Naolou, T.; Busse, K.; Balko, J.; Kressler, J. Crystallization and melting of poly(glycerol adipate)-based graft copolymers with single and double crystallizable side chains. *J. Polym. Sci. Part B Polym. Phys.* **2013**, *51*, 1581–1591,

- doi:10.1002/polb.23373.
74. Naolou, T.; Busse, K.; Lechner, B.D.; Kressler, J. The behavior of poly(ϵ -caprolactone) and poly(ethylene oxide)-b-poly(ϵ -caprolactone) grafted to a poly(glycerol adipate) backbone at the air/water interface. *Colloid Polym. Sci.* **2014**, *292*, 1199–1208, doi:10.1007/s00396-014-3168-1.
75. Jbeily, M.; Naolou, T.; Bilal, M.; Amado, E.; Kressler, J. Enzymatically synthesized polyesters with pendent OH groups as macroinitiators for the preparation of well-defined graft copolymers by atom transfer radical polymerization. *Polym. Int.* **2014**, *63*, 894–901, doi:10.1002/pi.4676.
76. Weiss, V.M.; Naolou, T.; Amado, E.; Busse, K.; Mäder, K.; Kressler, J. Formation of structured polygonal nanoparticles by phase-separated comb-like polymers. *Macromol. Rapid Commun.* **2012**, *33*, 35–40, doi:10.1002/marc.201100565.
77. Weiss, V.M.; Naolou, T.; Hause, G.; Kuntsche, J.; Kressler, J.; Mäder, K. Poly(glycerol adipate)-fatty acid esters as versatile nanocarriers: From nanocubes over ellipsoids to nanospheres. *J. Control. Release* **2012**, *158*, 156–164, doi:10.1016/j.jconrel.2011.09.077.
78. Meng, W.; Parker, T.L.; Kallinteri, P.; Walker, D.A.; Higgins, S.; Hutcheon, G.A.; Garnett, M.C. Uptake and metabolism of novel biodegradable poly (glycerol-adipate) nanoparticles in DAOY monolayer. *J. Control. Release* **2006**, *116*, 314–321, doi:10.1016/j.jconrel.2006.09.014.
79. Abo-zeid, Y.; Mantovani, G.; Irving, W.L.; Garnett, M.C. Synthesis of nucleoside-boronic esters hydrophobic pro-drugs: A possible route to improve hydrophilic nucleoside drug loading into polymer nanoparticles. *J. Drug Deliv. Sci. Technol.* **2018**, *46*, 354–364, doi:10.1016/j.jddst.2018.05.027.
80. Tchoryk, A.; Taresco, V.; Argent, R.H.; Ashford, M.; Gellert, P.R.; Stolnik, S.; Grabowska, A.; Garnett, M.C. Penetration and uptake of nanoparticles in 3D tumor spheroids. *Bioconjug. Chem.* **2019**, *30*, 1371–1384, doi:10.1021/acs.bioconjchem.9b00136.
81. Thompson, C.J.; Hansford, D.; Munday, D.L.; Higgins, S.; Rostron, C.; Hutcheon, G.A. Synthesis and evaluation of novel polyester-ibuprofen conjugates for modified drug release. *Drug Dev. Ind. Pharm.* **2008**, *34*, 877–884, doi:10.1080/03639040801929075.
82. Thompson, C.J.; Hansford, D.; Higgins, S.; Hutcheon, G.A.; Rostron, C.; Munday, D.L. Enzymatic synthesis and evaluation of new novel ω -pentadecalactone polymers

- for the production of biodegradable microspheres. *J. Microencapsul.* **2006**, *23*, 213–226, doi:10.1080/02652040500444123.
83. Wersig, T.; Krombholz, R.; Janich, C.; Meister, A.; Kressler, J.; Mäder, K. Indomethacin functionalised poly(glycerol adipate) nanospheres as promising candidates for modified drug release. *Eur. J. Pharm. Sci.* **2018**, *123*, 350–361, doi:10.1016/j.ejps.2018.07.053.
84. Wersig, T. Poly(glycerol adipate) - indomethacin conjugates for modified drug release. PhD Dissertation, Martin-Luther-University Halle-Wittenberg, Halle (Saale), 19.07.2019.
85. Suksiriworapong, J.; Taresco, V.; Ivanov, D.P.; Styliari, I.D.; Sakchaisri, K.; Junyaprasert, V.B.; Garnett, M.C. Synthesis and properties of a biodegradable polymer-drug conjugate: Methotrexate-poly(glycerol adipate). *Colloids Surfaces B Biointerfaces* **2018**, *167*, 115–125, doi:10.1016/j.colsurfb.2018.03.048.
86. Chu, B.C.F.; Whiteley, J.M. High molecular weight derivatives of methotrexate as chemotherapeutic agents. *Mol. Pharmacol.* **1977**, *13*, 80–88.
87. Pawar, H.A.; Kamat, S.R.; Choudhary, P.D. An overview of natural polysaccharides as biological macromolecules: their chemical modifications and pharmaceutical applications. *Biol Med* **2015**, *6*, 2.
88. Di Lorenzo, F.; Seiffert, S. Nanostructural heterogeneity in polymer networks and gels. *Polym. Chem.* **2015**, *6*, 5515–5528.
89. Nielsen, L.E. Cross-linking—effect on physical properties of polymers. *J. Macromol. Sci. Part C* **1969**, *3*, 69–103.
90. Maitra, J.; Shukla, V.K. Cross-linking in hydrogels—a review. *Am. J. Polym. Sci* **2014**, *4*, 25–31.
91. Gu, Y.; Zhao, J.; Johnson, J.A. Polymer Networks: From Plastics and Gels to Porous Frameworks. *Angew. Chemie - Int. Ed.* **2020**, *59*, 5022–5049, doi:10.1002/anie.201902900.
92. Buwalda, S.J.; Boere, K.W.M.; Dijkstra, P.J.; Feijen, J.; Vermonden, T.; Hennink, W.E. Hydrogels in a historical perspective: From simple networks to smart materials. *J. Control. release* **2014**, *190*, 254–273.
93. Li, J.; Mooney, D.J. Designing hydrogels for controlled drug delivery. *Nat. Rev. Mater.* **2016**, *1*, 1–17.
94. Schexnailder, P.; Schmidt, G. Nanocomposite polymer hydrogels. *Colloid Polym. Sci.* **2009**, *287*, 1–11.

95. Hoffman, A.S. Hydrogels for biomedical applications. *Adv. Drug Deliv. Rev.* **2012**, *64*, 18–23, doi:10.1016/j.addr.2012.09.010.
96. Xiang, H.P.; Qian, H.J.; Lu, Z.Y.; Rong, M.Z.; Zhang, M.Q. Crack healing and reclaiming of vulcanized rubber by triggering the rearrangement of inherent sulfur crosslinked networks. *Green Chem.* **2015**, *17*, 4315–4325, doi:10.1039/c5gc00754b.
97. Xu, C.; Cui, R.; Fu, L.; Lin, B. Recyclable and heat-healable epoxidized natural rubber/bentonite composites. *Compos. Sci. Technol.* **2018**, *167*, 421–430, doi:10.1016/j.compscitech.2018.08.027.
98. Peppas, N.A.; Mikos, A.G. Preparation methods and structure of hydrogels. In *Hydrogels in medicine and pharmacy*; CRC press, 2019; pp. 1–26.
99. Hennink, W.E.; van Nostrum, C.F. Novel crosslinking methods to design hydrogels. *Adv. Drug Deliv. Rev.* **2012**, *64*, 223–236, doi:10.1016/j.addr.2012.09.009.
100. Gottlieb, M. Swelling of polymer networks. *Biol. Synth. Polym. Networks* **1988**, 403–414.
101. Hennink, W.E.; De Jong, S.J.; Bos, G.W.; Veldhuis, T.F.J.; Van Nostrum, C.F. Biodegradable dextran hydrogels crosslinked by stereocomplex formation for the controlled release of pharmaceutical proteins. *Int. J. Pharm.* **2004**, *277*, 99–104.
102. Lin, Y.-H.; Liang, H.-F.; Chung, C.-K.; Chen, M.-C.; Sung, H.-W. Physically crosslinked alginate/N, O-carboxymethyl chitosan hydrogels with calcium for oral delivery of protein drugs. *Biomaterials* **2005**, *26*, 2105–2113.
103. Flory, P.J.; Rehner, J. Statistical mechanics of cross-linked polymer networks II. Swelling. *J. Chem. Phys.* **1943**, *11*, 521–526, doi:10.1063/1.1723792.
104. Ganji, F.; Vasheghani, F.S.; Vasheghani, F.E. Theoretical description of hydrogel swelling: a review. **2010**.
105. Borges, F.T.P.; Papavasiliou, G.; Teymour, F. Characterizing the Molecular Architecture of Hydrogels and Crosslinked Polymer Networks beyond Flory-Rehner-I. Theory. *Biomacromolecules* **2020**, *21*, 5104–5118, doi:10.1021/acs.biomac.0c01256.
106. Şen, M.; Güven, O. Prediction of swelling behaviour of hydrogels containing diprotic acid moieties. *Polymer (Guildf)*. **1998**, *39*, 1165–1172, doi:10.1016/S0032-3861(97)00391-1.
107. Peppas, N.A.; Bures, P.; Leobandung, W.; Ichikawa, H. Hydrogels in pharmaceutical formulations. *Eur. J. Pharm. Biopharm.* **2000**, *50*, 27–46, doi:10.1016/S0939-6411(00)00090-4.
108. De, K.S.; Aluru, N.R.; Johnson, B.; Crone, W.C.; Beebe, D.J.; Moore, J. Equilibrium

- swelling and kinetics of pH-responsive hydrogels: Models, experiments, and simulations. *J. Microelectromechanical Syst.* **2002**, *11*, 544–555, doi:10.1109/JMEMS.2002.803281.
109. Chai, Q.; Jiao, Y.; Yu, X. Hydrogels for biomedical applications: Their characteristics and the mechanisms behind them. *Gels* **2017**, *3*, 6, doi:10.3390/gels3010006.
110. Flory, P.J. *Principles of polymer chemistry*; Cornell university press, 1953; ISBN 0801401348.
111. Peppas, N.A.; Hilt, J.Z.; Khademhosseini, A.; Langer, R. Hydrogels in biology and medicine: From molecular principles to bionanotechnology. *Adv. Mater.* **2006**, *18*, 1345–1360, doi:10.1002/adma.200501612.
112. Treloar, L.R.G.; Montgomery, D.J. The Physics of Rubber Elasticity. *Phys. Today* 1959, *12*, 32–34.
113. Peppas, N.A.; Merrill, E.W. Crosslinked poly(vinyl alcohol) hydrogels as swollen elastic networks. *J. Appl. Polym. Sci.* **1977**, *21*, 1763–1770, doi:10.1002/app.1977.070210704.
114. Karoyo, A.H.; Wilson, L.D. A review on the design and hydration properties of natural polymer-based hydrogels. *Materials (Basel)*. **2021**, *14*, 1–36, doi:10.3390/ma14051095.
115. Smetana Jr, K. Cell biology of hydrogels. *Biomaterials* **1993**, *14*, 1046–1050.
116. Ratner, B.D.; Hoffman, A.S.; Schoen, F.J.; Lemons, J.E. *Biomaterials science: an introduction to materials in medicine*; Elsevier, 2004; ISBN 008047036X.
117. Lowman, A.M.; Peppas, N.A. Analysis of the complexation/decomplexation phenomena in graft copolymer networks. *Macromolecules* **1997**, *30*, 4959–4965.
118. Ratner, B.D.; Hoffman, A.S. Synthetic hydrogels for biomedical applications. In; ACS Publications, 1976 ISBN 1947-5918.
119. Bustamante-Torres, M.; Romero-Fierro, D.; Arcentales-Vera, B.; Palomino, K.; Magaña, H.; Bucio, E. Hydrogels classification according to the physical or chemical interactions and as stimuli-sensitive materials. *Gels* **2021**, *7*, 182, doi:10.3390/gels7040182.
120. Hoare, T.R.; Kohane, D.S. Hydrogels in drug delivery: Progress and challenges. *Polymer (Guildf)*. **2008**, *49*, 1993–2007, doi:10.1016/j.polymer.2008.01.027.
121. Caló, E.; Khutoryanskiy, V. V. Biomedical applications of hydrogels: A review of patents and commercial products. *Eur. Polym. J.* **2015**, *65*, 252–267, doi:10.1016/j.eurpolymj.2014.11.024.

122. Gacesa, P. Alginates. *Carbohydr. Polym.* **1988**, *8*, 161–182.
123. Goosen, M.F.A.; O’Shea, G.M.; Gharapetian, H.M.; Chou, S.; Sun, A.M. Optimization of microencapsulation parameters: Semipermeable microcapsules as a bioartificial pancreas. *Biotechnol. Bioeng.* **1985**, *27*, 146–150, doi:10.1002/bit.260270207.
124. Gombotz, W.R.; Wee, S.F. Protein release from alginate matrices. *Adv. Drug Deliv. Rev.* **2012**, *64*, 194–205, doi:10.1016/j.addr.2012.09.007.
125. Polk, A.; Amsden, B.; De Yao, K.; Peng, T.; Goosen, M.F.A. Controlled release of albumin from chitosan—alginate microcapsules. *J. Pharm. Sci.* **1994**, *83*, 178–185, doi:10.1002/jps.2600830213.
126. Liu, L.S.; Liu, S.Q.; Ng, S.Y.; Froix, M.; Ohno, T.; Heller, J. Controlled release of interleukin-2 for tumour immunotherapy using alginate/chitosan porous microspheres. *J. Control. Release* **1997**, *43*, 65–74, doi:10.1016/S0168-3659(96)01471-X.
127. Li, Y.; Zhu, L.; Fan, Y.; Li, Y.; Cheng, L.; Liu, W.; Li, X.; Fan, X. Formation and controlled drug release using a three-component supramolecular hydrogel for anti-schistosoma japonicum cercariae. *Nanomaterials* **2016**, *6*, 46, doi:10.3390/nano6030046.
128. Munim, S.A.; Raza, Z.A. Poly(lactic acid) based hydrogels: formation, characteristics and biomedical applications. *J. Porous Mater.* **2019**, *26*, 881–901, doi:10.1007/s10934-018-0687-z.
129. Eagland, D.; Crowther, N.J.; Butler, C.J. Complexation between polyoxyethylene and polymethacrylic acid—the importance of the molar mass of polyoxyethylene. *Eur. Polym. J.* **1994**, *30*, 767–773, doi:10.1016/0014-3057(94)90003-5.
130. Bell, C.L.; Peppas, N.A. Modulation of drug permeation through interpolymer complexed hydrogels for drug delivery applications. *J. Control. Release* **1996**, *39*, 201–207, doi:10.1016/0168-3659(95)00154-9.
131. Mathur, A.M.; Hammonds, K.F.; Klier, J.; Scranton, A.B. Equilibrium swelling of poly(methacrylic acid-g-ethylene glycol) hydrogels. Effect of swelling medium and synthesis conditions. *J. Control. Release* **1998**, *54*, 177–184, doi:10.1016/S0168-3659(97)00186-7.
132. Haglund, B.O.; Joshi, R.; Himmelstein, K.J. An in situ gelling system for parenteral delivery. *J. Control. release* **1996**, *41*, 229–235.
133. García, L.; Aguilar, M.R.; Román, J.S. Biodegradable hydrogels for controlled drug release. *Biomed. Appl. Hydrogels Handb.* **2010**, 147–155.
134. Frutos, G.; Prior-Cabanillas, A.; París, R.; Quijada-Garrido, I. A novel controlled drug

- delivery system based on pH-responsive hydrogels included in soft gelatin capsules. *Acta Biomater.* **2010**, *6*, 4650–4656, doi:10.1016/j.actbio.2010.07.018.
135. Guiseppi-Elie, A. Electroconductive hydrogels: synthesis, characterization and biomedical applications. *Biomaterials* **2010**, *31*, 2701–2716.
136. Chen, L.; Ci, T.; Yu, L.; Ding, J. Effects of molecular weight and its distribution of PEG block on micellization and thermogellability of PLGA–PEG–PLGA copolymer aqueous solutions. *Macromolecules* **2015**, *48*, 3662–3671.
137. Chen, L.; Ci, T.; Li, T.; Yu, L.; Ding, J. Effects of molecular weight distribution of amphiphilic block copolymers on their solubility, micellization, and temperature-induced sol–gel transition in water. *Macromolecules* **2014**, *47*, 5895–5903.
138. Akiyoshi, K.; Deguchi, S.; Tajima, H.; Nishikawa, T.; Sunamoto, J. Microscopic structure and thermoresponsiveness of a hydrogel nanoparticle by self-assembly of a hydrophobized polysaccharide. *Macromolecules* **1997**, *30*, 857–861.
139. Akiyoshi, K.; Deguchi, S.; Moriguchi, N.; Yamaguchi, S.; Sunamoto, J. Self-aggregates of hydrophobized polysaccharides in water. Formation and characteristics of nanoparticles. *Macromolecules* **1993**, *26*, 3062–3068.
140. Akiyoshi, K.; Kobayashi, S.; Shichibe, S.; Mix, D.; Baudys, M.; Kim, S.W.; Sunamoto, J. Self-assembled hydrogel nanoparticle of cholesterol-bearing pullulan as a carrier of protein drugs: complexation and stabilization of insulin. *J. Control. Release* **1998**, *54*, 313–320.
141. Akiyoshi, K.; Taniguchi, I.; Fukui, H.; Sunamoto, J. Hydrogel nanoparticles formed by self-assembly of hydrophobized polysaccharide. Stabilization of adriamycin by complexation. *Eur. J. Pharm. Biopharm.* **1996**, *42*, 286–290.
142. Uchegbu, I.F.; Schätzlein, A.G.; Tetley, L.; Gray, A.I.; Sludden, J.; Siddique, S.; Mosha, E. Polymeric chitosan-based vesicles for drug delivery. *J. Pharm. Pharmacol.* **1998**, *50*, 453–458.
143. Sludden, J.; Uchegbu, I.F.; Schätzlein, A.G. The encapsulation of bleomycin within chitosan based polymeric vesicles does not alter its biodistribution. *J. Pharm. Pharmacol.* **2000**, *52*, 377–382.
144. Slager, J.; Domb, A.J. Biopolymer stereocomplexes. *Adv. Drug Deliv. Rev.* **2003**, *55*, 549–583.
145. Tsuji, H. Poly (lactide) stereocomplexes: formation, structure, properties, degradation, and applications. *Macromol. Biosci.* **2005**, *5*, 569–597.
146. Geschwind, J.; Rathi, S.; Tonhauser, C.; Schömer, M.; Hsu, S.L.; Coughlin, E.B.; Frey,

- H. Stereocomplex formation in polylactide multiarm stars and comb copolymers with linear and hyperbranched multifunctional PEG. *Macromol. Chem. Phys.* **2013**, *214*, 1434–1444.
147. Mao, H.; Pan, P.; Shan, G.; Bao, Y. In situ formation and gelation mechanism of thermoresponsive stereocomplexed hydrogels upon mixing diblock and triblock poly (lactic acid)/poly (ethylene glycol) copolymers. *J. Phys. Chem. B* **2015**, *119*, 6471–6480.
148. Lee, K.Z.; Jeon, J.; Jiang, B.; Subramani, S.V.; Li, J.; Zhang, F. Protein-Based Hydrogels and Their Biomedical Applications. *Molecules* **2023**, *28*, 4988.
149. McGrath, K.P.; Fournier, M.J.; Mason, T.L.; Tirrell, D.A. Genetically directed syntheses of new polymeric materials. Expression of artificial genes encoding proteins with repeating-(AlaGly) 3ProGluGly-elements. *J. Am. Chem. Soc.* **1992**, *114*, 727–733.
150. Cappello, J.; Crissman, J.; Dorman, M.; Mikolajczak, M.; Textor, G.; Marquet, M.; Ferrari, F. Genetic engineering of structural protein polymers. *Biotechnol. Prog.* **1990**, *6*, 198–202.
151. Cappello, J.; Crissman, J.W.; Crissman, M.; Ferrari, F.A.; Textor, G.; Wallis, O.; Whitley, J.R.; Zhou, X.; Burman, D.; Aukerman, L. In-situ self-assembling protein polymer gel systems for administration, delivery, and release of drugs. *J. Control. Release* **1998**, *53*, 105–117.
152. Petka, W.A.; Harden, J.L.; McGrath, K.P.; Wirtz, D.; Tirrell, D.A. Reversible hydrogels from self-assembling artificial proteins. *Science (80-.)*. **1998**, *281*, 389–392.
153. Sawada, T.; Serizawa, T. Antigen-antibody interaction-based self-healing capability of hybrid hydrogels composed of genetically engineered filamentous viruses and gold nanoparticles. *Protein Pept. Lett.* **2018**, *25*, 64–67.
154. Sawada, T.; Yanagimachi, M.; Serizawa, T. Controlled release of antibody proteins from liquid crystalline hydrogels composed of genetically engineered filamentous viruses. *Mater. Chem. Front.* **2017**, *1*, 146–151.
155. Lu, Z.; Kopečková, P.; Kopeček, J. Antigen responsive hydrogels based on polymerizable antibody Fab' fragment. *Macromol. Biosci.* **2003**, *3*, 296–300.
156. Ong, J.; Zhao, J.; Justin, A.W.; Markaki, A.E. Albumin- based hydrogels for regenerative engineering and cell transplantation. *Biotechnol. Bioeng.* **2019**, *116*, 3457–3468.
157. Arabi, S.H.; Aghelnejad, B.; Schwieger, C.; Meister, A.; Kerth, A.; Hinderberger, D. Serum albumin hydrogels in broad pH and temperature ranges: Characterization of

- their self-assembled structures and nanoscopic and macroscopic properties. *Biomater. Sci.* **2018**, *6*, 478–492.
158. Sanaeifar, N.; Mäder, K.; Hinderberger, D. Macro-and Nanoscale Effect of Ethanol on Bovine Serum Albumin Gelation and Naproxen Release. *Int. J. Mol. Sci.* **2022**, *23*, 7352.
159. Wichterle, O.; Lim, D. Hydrophilic gels for biological use. *Nature* **1960**, *185*, 117–118.
160. Langer, R.S.; Peppas, N.A. Present and future applications of biomaterials in controlled drug delivery systems. *Biomaterials* **1981**, *2*, 201–214.
161. Thorén, L. The dextrans--clinical data. *Dev. Biol. Stand.* **1980**, *48*, 157–167.
162. Mehvar, R. Dextran for targeted and sustained delivery of therapeutic and imaging agents. *J. Control. release* **2000**, *69*, 1–25.
163. Sawhney, A.S.; Pathak, C.P.; Hubbell, J.A. Bioerodible hydrogels based on photopolymerized poly (ethylene glycol)-co-poly (. alpha.-hydroxy acid) diacrylate macromers. *Macromolecules* **1993**, *26*, 581–587.
164. Zhang, Y.; Won, C.; Chu, C. Synthesis and characterization of biodegradable network hydrogels having both hydrophobic and hydrophilic components with controlled swelling behavior. *J. Polym. Sci. Part A Polym. Chem.* **1999**, *37*, 4554–4569.
165. Zhang, Y.; Chu, C. Biodegradable dextran- polylactide hydrogel network and its controlled release of albumin. *J. Biomed. Mater. Res. An Off. J. Soc. Biomater. Japanese Soc. Biomater.* **2001**, *54*, 1–11.
166. Jones, A.; Vaughan, D. Hydrogel dressings in the management of a variety of wound types: A review. *J. Orthop. Nurs.* **2005**, *9*, S1–S11.
167. Chen, T.; Embree, H.D.; Brown, E.M.; Taylor, M.M.; Payne, G.F. Enzyme-catalyzed gel formation of gelatin and chitosan: potential for in situ applications. *Biomaterials* **2003**, *24*, 2831–2841.
168. Westhaus, E.; Messersmith, P.B. Triggered release of calcium from lipid vesicles: a bioinspired strategy for rapid gelation of polysaccharide and protein hydrogels. *Biomaterials* **2001**, *22*, 453–462.
169. Munoz-Munoz, F.; Ruiz, J.-C.; Alvarez-Lorenzo, C.; Concheiro, A.; Bucio, E. Temperature-and pH-sensitive interpenetrating polymer networks grafted on PP: cross-linking irradiation dose as a critical variable for the performance as vancomycin-eluting systems. *Radiat. Phys. Chem.* **2012**, *81*, 531–540.
170. Meléndez-Ortiz, H.I.; Alvarez-Lorenzo, C.; Concheiro, A.; Jiménez-Páez, V.M.; Bucio, E. Modification of medical grade PVC with N-vinylimidazole to obtain

- bactericidal surface. *Radiat. Phys. Chem.* **2016**, *119*, 37–43.
171. Romero-Fierro, D.A.; Camacho-Cruz, L.A.; Bustamante-Torres, M.R.; Hidalgo-Bonilla, S.P.; Bucio, E. Modification of cotton gauzes with poly (acrylic acid) and poly (methacrylic acid) using gamma radiation for drug loading studies. *Radiat. Phys. Chem.* **2022**, *190*, 109787.
172. Bustamante-Torres, M.; Pino-Ramos, V.H.; Romero-Fierro, D.; Hidalgo-Bonilla, S.P.; Magaña, H.; Bucio, E. Synthesis and antimicrobial properties of highly cross-linked pH-sensitive hydrogels through gamma radiation. *Polymers (Basel)*. **2021**, *13*, 2223.
173. Gulrez, S.K.H.; Al-Assaf, S.; Phillips, G.O. Hydrogels: methods of preparation, characterisation and applications. *Prog. Mol. Environ. Bioeng. Anal. Model. to Technol. Appl.* **2011**, 117150.
174. Omidian, H.; Park, K. Introduction to hydrogels. *Biomed. Appl. hydrogels Handb.* **2010**, 1–16.
175. Jin, R.; Dijkstra, P.J. Hydrogels for tissue engineering applications. *Biomed. Appl. hydrogels Handb.* **2010**, 203–225.
176. Kuijpers, A.J.; Van Wachem, P.B.; Van Luyn, M.J.A.; Engbers, G.H.M.; Krijgsveld, J.; Zaat, S.A.J.; Dankert, J.; Feijen, J. In vivo and in vitro release of lysozyme from cross-linked gelatin hydrogels: a model system for the delivery of antibacterial proteins from prosthetic heart valves. *J. Control. release* **2000**, *67*, 323–336.
177. Ichi, T.; Watanabe, J.; Ooya, T.; Yui, N. Controllable erosion time and profile in poly (ethylene glycol) hydrogels by supramolecular structure of hydrolyzable polyrotaxane. *Biomacromolecules* **2001**, *2*, 204–210.
178. Tang, R.-C.; Yang, I.-H.; Lin, F.-H. Current Role and Potential of Polymeric Biomaterials in Clinical Obesity Treatment. *Biomacromolecules* **2023**.
179. Saxena, S.; Jayakannan, M. Development of L-amino-acid-based hydroxyl functionalized biodegradable amphiphilic polyesters and their drug delivery capabilities to cancer cells. *Biomacromolecules* **2019**, *21*, 171–187.
180. Mane, S.R.; Sathyan, A.; Shunmugam, R. Biomedical applications of pH-responsive amphiphilic polymer nanoassemblies. *ACS Appl. Nano Mater.* **2020**, *3*, 2104–2117.
181. Gonçalves, M.; Kairys, V.; Rodrigues, J.; Tomás, H. Polyester Dendrimers Based on Bis-MPA for Doxorubicin Delivery. *Biomacromolecules* **2021**, *23*, 20–33.
182. Espinoza, S.M.; Patil, H.I.; San Martin Martinez, E.; Casañas Pimentel, R.; Ige, P.P. Poly- ϵ -caprolactone (PCL), a promising polymer for pharmaceutical and biomedical applications: Focus on nanomedicine in cancer. *Int. J. Polym. Mater. Polym. Biomater.*

- 2020**, *69*, 85–126.
183. Puppi, D.; Chiellini, F. Biodegradable polymers for biomedical additive manufacturing. *Appl. Mater. today* **2020**, *20*, 100700.
184. Maadani, A.M.; Salahinejad, E. Performance comparison of PLA-and PLGA-coated porous bioceramic scaffolds: Mechanical, biodegradability, bioactivity, delivery and biocompatibility assessments. *J. Control. Release* **2022**, *351*, 1–7.
185. Ivanova, T.A.; Golubeva, E.N. Aliphatic polyesters for biomedical purposes: design and kinetic regularities of degradation in vitro. *Russ. J. Phys. Chem. B* **2022**, *16*, 426–444.
186. Okhovatian, S.; Shakeri, A.; Davenport Huyer, L.; Radisic, M. Elastomeric Polyesters in Cardiovascular Tissue Engineering and Organs-on-a-Chip. *Biomacromolecules* **2023**.
187. Blasi, P. Poly (lactic acid)/poly (lactic-co-glycolic acid)-based microparticles: An overview. *J. Pharm. Investig.* **2019**, *49*, 337–346.
188. Bajwa, N.; Singh, P.A.; Jyoti, K.; Baldi, A.; Chandra, R.; Madan, J. Scale-up, Preclinical and Clinical Status of Poly (Lactide-Co-Glycolide) and its Copolymers based Drug Delivery Systems. *Nanomater. Evol. Adv. Towar. Ther. Drug Deliv. (Part II)* **2021**, *13*, 246.
189. Stepanova, M.; Korzhikova-Vlakh, E. Modification of cellulose micro-and nanomaterials to improve properties of aliphatic polyesters/cellulose composites: A review. *Polymers (Basel)*. **2022**, *14*, 1477.
190. Shan, P.; Lian, X.; Lu, W.; Yin, X.; Lu, Y.; Zhang, M.; Wen, X.; Xin, G.; Li, Z.; Li, Z. Direct Synthesis of Aliphatic Polyesters with Pendant Hydroxyl Groups from Bio-Renewable Monomers: A Reactive Precursor for Functionalized Biomaterials. *Biomacromolecules* **2023**.
191. Thakor, P.; Bhavana, V.; Sharma, R.; Srivastava, S.; Singh, S.B.; Mehra, N.K. Polymer–drug conjugates: Recent advances and future perspectives. *Drug Discov. Today* **2020**, *25*, 1718–1726.
192. Messina, M.S.; Messina, K.M.M.; Bhattacharya, A.; Montgomery, H.R.; Maynard, H.D. Preparation of biomolecule-polymer conjugates by grafting-from using ATRP, RAFT, or ROMP. *Prog. Polym. Sci.* **2020**, *100*, 101186.
193. Kim, J.S.; Sirois, A.R.; Vazquez Cegla, A.J.; Jumai'an, E.; Murata, N.; Buck, M.E.; Moore, S.J. Protein–Polymer Conjugates Synthesized Using Water-Soluble Azlactone-Functionalized Polymers Enable Receptor-Specific Cellular Uptake toward Targeted

- Drug Delivery. *Bioconjug. Chem.* **2019**, *30*, 1220–1231.
194. Ansari, I.; Singh, P.; Mittal, A.; Mahato, R.I.; Chitkara, D. 2, 2-Bis (hydroxymethyl) propionic acid based cyclic carbonate monomers and their (co) polymers as advanced materials for biomedical applications. *Biomaterials* **2021**, *275*, 120953.
195. Holback, H.; Yeo, Y.; Park, K. *Hydrogel swelling behavior and its biomedical applications*; Woodhead Publishing Limited, 2011;
196. Karmegam, V.; Soltantabar, P.; Calubaquib, E.J.L.; Kularatne, R.N.; Stefan, M.C. Biodegradable Aliphatic Polyesters for Drug Delivery. *Mater. Matters* **2017**, *12*, 37–41.
197. Zhang, H.; Zhang, Q.; Cai, Q.; Luo, Q.; Li, X.; Li, X.; Zhang, K.; Zhu, W. In-reactor engineering of bioactive aliphatic polyesters via magnesium-catalyzed polycondensation for guided tissue regeneration. *Chem. Eng. J.* **2021**, *424*, 130432.
198. Mohammadi-Samani, S.; Taghipour, B. PLGA micro and nanoparticles in delivery of peptides and proteins; problems and approaches. *Pharm. Dev. Technol.* **2015**, *20*, 385–393.
199. Gonzalez-Miro, M.; Chen, S.; Gonzaga, Z.J.; Evert, B.; Wibowo, D.; Rehm, B.H.A. Polyester as antigen carrier toward particulate vaccines. *Biomacromolecules* **2019**, *20*, 3213–3232.
200. Naolou, T.; Meister, A.; Schöps, R.; Pietzsch, M.; Kressler, J. Synthesis and characterization of graft copolymers able to form polymersomes and worm-like aggregates. *Soft Matter* **2013**, *9*, 10364–10372, doi:10.1039/c3sm51716k.
201. Steiner, J.; Alaneed, R.; Kressler, J.; Mäder, K. Fatty acid-modified poly (glycerol adipate) microparticles for controlled drug delivery. *J. Drug Deliv. Sci. Technol.* **2021**, *61*, 102206.
202. Bilal, M.H.; Prehm, M.; Njau, A.E.; Samiullah, M.H.; Meister, A.; Kressler, J. Enzymatic synthesis and characterization of hydrophilic sugar based polyesters and their modification with stearic acid. *Polymers (Basel)*. **2016**, *8*, 80.
203. Colombo, P. Swelling-controlled release in hydrogel matrices for oral route. *Adv. Drug Deliv. Rev.* **1993**, *11*, 37–57.
204. Siegel, R.A.; Gu, Y.; Lei, M.; Baldi, A.; Nuxoll, E.E.; Ziaie, B. Hard and soft micro- and nanofabrication: An integrated approach to hydrogel-based biosensing and drug delivery. *J. Control. release* **2010**, *141*, 303–313.
205. Peppas, N.A. Hydrogels and drug delivery. *Curr. Opin. Colloid Interface Sci.* **1997**, *2*, 531–537.

-
206. Truong, V.; Blakey, I.; Whittaker, A.K. Hydrophilic and amphiphilic polyethylene glycol-based hydrogels with tunable degradability prepared by “click” chemistry. *Biomacromolecules* **2012**, *13*, 4012–4021, doi:10.1021/bm3012924.
207. Peppas, N.A.; Huang, Y.; Torres-Lugo, M.; Ward, J.H.; Zhang, J. Physicochemical foundations and structural design of hydrogels in medicine and biology. *Annu. Rev. Biomed. Eng.* **2000**, *2*, 9–29, doi:10.1146/annurev.bioeng.2.1.9.
208. Bilal, M.H.; Alaneed, R.; Steiner, J.; Mäder, K.; Pietzsch, M.; Kressler, J. Multiple grafting to enzymatically synthesized polyesters. *Methods Enzymol.* **2019**, *627*, 57–97, doi:10.1016/bs.mie.2019.04.031.
209. Lu, C.; Zhong, W. Synthesis of propargyl-terminated heterobifunctional poly(ethylene glycol). *Polymers (Basel)*. **2010**, *2*, 407–417, doi:10.3390/polym2040407.
210. Neises, B.; Steglich, W. Simple method for the esterification of carboxylic acids. *Angew. Chemie Int. Ed. English* **1978**, *17*, 522–524.
211. Ullah, K.; Sohail, M.; Murtaza, G.; Khan, S.A. Natural and synthetic materials based CMCh/PVA hydrogels for oxaliplatin delivery: Fabrication, characterization, In-Vitro and In-Vivo safety profiling. *Int. J. Biol. Macromol.* **2019**, *122*, 538–548, doi:10.1016/j.ijbiomac.2018.10.203.
212. Ullah, K.; Ali Khan, S.; Murtaza, G.; Sohail, M.; Azizullah; Manan, A.; Afzal, A. Gelatin-based hydrogels as potential biomaterials for colonic delivery of oxaliplatin. *Int. J. Pharm.* **2019**, *556*, 236–245, doi:10.1016/j.ijpharm.2018.12.020.
213. Lu, S.; Anseth, K.S. Release behavior of high molecular weight solutes from poly(ethylene glycol)-based degradable networks. *Macromolecules* **2000**, *33*, 2509–2515.
214. Lin, C.-C.; Metters, A.T. Hydrogels in controlled release formulations: network design and mathematical modeling. *Adv. Drug Deliv. Rev.* **2006**, *58*, 1379–1408.
215. Borges, F.T.P.; Papavasiliou, G.; Teymour, F. Characterizing the molecular architecture of hydrogels and crosslinked polymer networks beyond Flory–Rehner—I. Theory. *Biomacromolecules* **2020**, *21*, 5104–5118.
216. Nakajima, A.; Tanaami, K. Dissolution and Chain Dimensions of Nylon 6 in Metal Halide—Alcohol Systems. *Polymer Journal* **1974**, *5*, 248–254.
217. Uyama, H.; Kobayashi, S. Enzymatic synthesis of polyesters via polycondensation. In *Advances in Polymer Science*; Springer, 2006; Vol. 194, pp. 133–158.
218. Nitta, S.; Iwamoto, H. Lipase-catalyzed synthesis of epigallocatechin gallate-based polymer for long-term release of epigallocatechin gallate with antioxidant property. *J. Appl. Polym. Sci.* **2019**, *136*, 47693, doi:10.1002/app.47693.

-
219. Adharis, A.; Loos, K. Synthesis of glycomonomers via biocatalytic methods. In *Methods in Enzymology*; Elsevier, 2019; Vol. 627, pp. 215–247 ISBN 9780128170953.
220. Uyama, H.; Wada, S.; Fukui, T.; Kobayashi, S. Lipase-catalyzed synthesis of polyesters from anhydride derivatives involving dehydration. *Biochem. Eng. J.* **2003**, *16*, 145–152, doi:10.1016/S1369-703X(03)00028-7.
221. Uyama, H. Enzymatic Polymerization. *Futur. Dir. Biocatal.* **2007**, *101*, 205–251, doi:10.1016/B978-044453059-2/50010-8.
222. Hu, J.; Gao, W.; Kulshrestha, A.; Gross, R.A. “ Sweet Polyesters”: Lipase-Catalyzed Condensation-Polymerizations of Alditols. In; ACS Publications, 2008 ISBN 1947-5918.
223. D’souza, A.A.; Shegokar, R. Polyethylene glycol (PEG): a versatile polymer for pharmaceutical applications. *Expert Opin. Drug Deliv.* **2016**, *13*, 1257–1275.
224. Kolate, A.; Baradia, D.; Patil, S.; Vhora, I.; Kore, G.; Misra, A. PEG—a versatile conjugating ligand for drugs and drug delivery systems. *J. Control. release* **2014**, *192*, 67–81.
225. Hsieh, Y.-C.; Wang, H.-E.; Lin, W.-W.; Roffler, S.R.; Cheng, T.-C.; Su, Y.-C.; Li, J.-J.; Chen, C.-C.; Huang, C.-H.; Chen, B.-M. Pre-existing anti-polyethylene glycol antibody reduces the therapeutic efficacy and pharmacokinetics of PEGylated liposomes. *Theranostics* **2018**, *8*, 3164.
226. Mittag, J.J.; Trutschel, M.-L.; Kruschwitz, H.; Mäder, K.; Buske, J.; Garidel, P. Characterization of radicals in polysorbate 80 using electron paramagnetic resonance (EPR) spectroscopy and spin trapping. *Int. J. Pharm. X* **2022**, *4*, 100123.
227. Swainson, S.M.E.; Taresco, V.; Pearce, A.K.; Clapp, L.H.; Ager, B.; McAllister, M.; Bosquillon, C.; Garnett, M.C. Exploring the enzymatic degradation of poly (glycerol adipate). *Eur. J. Pharm. Biopharm.* **2019**, *142*, 377–386.
228. Pasupuleti, S.; Madras, G. Synthesis and degradation of sorbitol-based polymers. *J. Appl. Polym. Sci.* **2011**, *121*, doi:10.1002/app.33840.
229. Lv, A.; Cui, Y.; Du, F.-S.; Li, Z.-C. Thermally degradable polyesters with tunable degradation temperatures via postpolymerization modification and intramolecular cyclization. *Macromolecules* **2016**, *49*, 8449–8458.
230. Griffith, L.G. Polymeric biomaterials. *Acta Mater.* **2000**, *48*, 263–277.
231. Merkli, A.; Tabatabay, C.; Gurny, R.; Heller, J. Biodegradable polymers for the controlled release of ocular drugs. *Prog. Polym. Sci.* **1998**, *23*, 563–580.
232. Steiner, J. Fatty acid-modified poly (glycerol adipate) as a versatile matrix for

- parenteral depot formulations. PhD Dissertation, Martin-Luther-University Halle-Wittenberg, Halle (Saale), 07.07.2022.
233. Baird, J.A.; Olayo-Valles, R.; Rinaldi, C.; Taylor, L.S. Effect of molecular weight, temperature, and additives on the moisture sorption properties of polyethylene glycol. *J. Pharm. Sci.* **2010**, *99*, 154–168.
234. Wunderlich, B. Theory of cold crystallization of high polymers. *J. Chem. Phys.* **1958**, *29*, 1395–1404, doi:10.1063/1.1744729.
235. Pielichowski, K.; Flejtuch, K. Differential scanning calorimetry studies on poly(ethylene glycol) with different molecular weights for thermal energy storage materials. *Polym. Adv. Technol.* **2002**, *13*, 690–696, doi:10.1002/pat.276.
236. Wang, J.; Andriamitantsoa, R.S.; Atinafu, D.G.; Gao, H.; Dong, W.; Wang, G. A one-step in-situ assembly strategy to construct PEG@MOG-100-Fe shape-stabilized composite phase change material with enhanced storage capacity for thermal energy storage. *Chem. Phys. Lett.* **2018**, *695*, 99–106, doi:10.1016/j.cplett.2017.12.004.
237. Chen, S.; Liu, M.; Jin, S.; Wang, B. Preparation of ionic-crosslinked chitosan-based gel beads and effect of reaction conditions on drug release behaviors. *Int. J. Pharm.* **2008**, *349*, 180–187, doi:10.1016/j.ijpharm.2007.08.029.
238. Le Ouay, B.; Uemura, T. Polymer in MOF Nanospace: from Controlled Chain Assembly to New Functional Materials. *Isr. J. Chem.* **2018**, *58*, 995–1009, doi:10.1002/ijch.201800074.
239. Buenger, D.; Topuz, F.; Groll, J. Hydrogels in sensing applications. *Prog. Polym. Sci.* **2012**, *37*, 1678–1719, doi:10.1016/j.progpolymsci.2012.09.001.
240. Lowman, A.M.; Peppas, N.A.; Morishita, M.; Nagai, T. Novel Bioadhesive Complexation Networks for Oral Protein Drug Delivery. In *ACS Symposium Series*; ACS Publications, 1998; Vol. 709, pp. 156–164 ISBN 1947-5918.
241. Kaşgöz, H.; Aydın, İ.; Kaşgöz, A. The effect of PEG (400) DA crosslinking agent on swelling behaviour of acrylamide-maleic acid hydrogels. *Polym. Bull.* **2005**, *54*, 387–397.
242. Atta, S.; Khaliq, S.; Islam, A.; Javeria, I.; Jamil, T.; Athar, M.M.; Shafiq, M.I.; Ghaffar, A. Injectable biopolymer based hydrogels for drug delivery applications. *Int. J. Biol. Macromol.* **2015**, *80*, 240–245.
243. Gnanou, Y.; Hild, G.; Bastide, J.; Rempp, P. Hydrophilic polyurethane networks exhibiting anisotropic swelling behaviour. *J. Polym. Mater.* **1987**, *4*, 123–130.
244. Graham, N.B.; Zulfikar, M. Interaction of poly(ethylene oxide) with solvents: 3.

- Synthesis and swelling in water of crosslinked poly(ethylene glycol) urethane networks. *Polymer (Guildf)*. **1989**, *30*, 2130–2135, doi:10.1016/0032-3861(89)90305-4.
245. Iza, M.; Stoianovici, G.; Viora, L.; Grossiord, J.L.; Couarraze, G. Hydrogels of poly(ethylene glycol): Mechanical characterization and release of a model drug. *J. Control. Release* **1998**, *52*, 41–51, doi:10.1016/S0168-3659(97)00191-0.
246. Hocine, S.; Li, M.H. Thermoresponsive self-assembled polymer colloids in water. *Soft Matter* **2013**, *9*, 5839–5861, doi:10.1039/c3sm50428j.
247. de Vringer, T.; Joosten, J.G.H.; Junginger, H.E. A study of the hydration of polyoxyethylene at low temperatures by differential scanning calorimetry. *Colloid Polym. Sci.* **1986**, *264*, 623–630, doi:10.1007/BF01412602.
248. Antonsen, K.P.; Hoffman, A.S. Water Structure of PEG Solutions by Differential Scanning Calorimetry Measurements. In *Poly(Ethylene Glycol) Chemistry*; Springer, 1992; pp. 15–28.
249. Graham, N.B.; Chen, C.F. Interaction of poly (ethylene oxide) with solvent—5. The densities of water/poly (ethylene glycol) mixtures. *Eur. Polym. J.* **1993**, *29*, 149–151.
250. Lange, F.; Schwenke, K.; Kurakazu, M.; Akagi, Y.; Chung, U. Il; Lang, M.; Sommer, J.U.; Sakai, T.; Saalwächter, K. Connectivity and structural defects in model hydrogels: A combined proton NMR and Monte Carlo simulation study. *Macromolecules* **2011**, *44*, 9666–9674, doi:10.1021/ma201847v.
251. Baum, J.; Pines, A. NMR Studies of Clustering in Solids. *J. Am. Chem. Soc.* **1986**, *108*, 7447–7454, doi:10.1021/ja00284a001.
252. Saalwächter, K. Proton multiple-quantum NMR for the study of chain dynamics and structural constraints in polymeric soft materials. *Prog. Nucl. Magn. Reson. Spectrosc.* **2007**, *51*, 1–35, doi:10.1016/j.pnmrs.2007.01.001.
253. Golitsyn, Y.; Pulst, M.; Samiullah, M.H.; Busse, K.; Kressler, J.; Reichert, D. Crystallization in PEG networks: The importance of network topology and chain tilt in crystals. *Polymer (Guildf)*. **2019**, *165*, 72–82, doi:10.1016/j.polymer.2019.01.018.
254. Stejskal, E.O.; Tanner, J.E. Spin diffusion measurements: Spin echoes in the presence of a time-dependent field gradient. *J. Chem. Phys.* **1965**, *42*, 288–292, doi:10.1063/1.1695690.
255. Matsukawa, S.; Ando, I. Study of self-diffusion of molecules in polymer gel by pulsed-gradient spin-echo ¹H NMR. *Macromolecules* **1996**, *29*, 7136–7140, doi:10.1021/ma960426r.

256. Munch, J.P.; Candau, S.; Herz, J.; Hild, G. Inelastic Light Scattering By Gel Modes in Semi-Dilute Polymer Solutions and Permanent Networks At Equilibrium Swollen State. *J Phys* **1977**, *38*, 971–976, doi:10.1051/jphys:01977003808097100.
257. Canal, T.; Peppas, N.A. Correlation between mesh size and equilibrium degree of swelling of polymeric networks. *J. Biomed. Mater. Res.* **1989**, *23*, 1183–1193.
258. Liao, H.; Munoz-Pinto, D.; Qu, X.; Hou, Y.; Grunlan, M.A.; Hahn, M.S. Influence of hydrogel mechanical properties and mesh size on vocal fold fibroblast extracellular matrix production and phenotype. *Acta Biomater.* **2008**, *4*, 1161–1171, doi:10.1016/j.actbio.2008.04.013.
259. am Ende, M.T.; Mikos, A.G. Diffusion-controlled delivery of proteins from hydrogels and other hydrophilic systems. *Protein Deliv. Phys. Syst.* **2002**, 139–165.
260. Brannon-Peppas, L.; Peppas, N.A. Equilibrium swelling behavior of pH-sensitive hydrogels. *Chem. Eng. Sci.* **1991**, *46*, 715–722.
261. Martens, P.; Anseth, K.S. Characterization of hydrogels formed from acrylate modified poly (vinyl alcohol) macromers. *Polymer (Guildf)*. **2000**, *41*, 7715–7722.
262. Waters, D.J.; Engberg, K.; Parke-Houben, R.; Hartmann, L.; Ta, C.N.; Toney, M.F.; Frank, C.W. Morphology of photopolymerized end-linked poly (ethylene glycol) hydrogels by small-angle X-ray scattering. *Macromolecules* **2010**, *43*, 6861–6870.
263. Tasaki, K. Poly (oxyethylene)– water interactions: a molecular dynamics study. *J. Am. Chem. Soc.* **1996**, *118*, 8459–8469.
264. Takahashi, Y.; Sumita, I.; Tadokoro, H. Structural studies of polyethers. IX. Planar zigzag modification of poly(ethylene oxide). *J. Polym. Sci. Part A-2 Polym. Phys.* **1973**, *11*, 2113–2122, doi:10.1002/pol.1973.180111103.
265. Kim, S.W.; Bae, Y.H.; Okano, T. Hydrogels: swelling, drug loading, and release. *Pharm. Res.* **1992**, *9*, 283–290.
266. Andrade, J. Hydrogels in medicine and pharmacy: NA Peppas (Editor), CRC Press, Boca Raton, FL, 1987: Vol. I, Fundamentals, 192 pages, \$94.00 1989.
267. Ferreira, L.; Vidal, M.M.; Gil, M.H. Evaluation of poly(2-hydroxyethyl methacrylate) gels as drug delivery systems at different pH values. *Int. J. Pharm.* **2000**, *194*, 169–180, doi:10.1016/S0378-5173(99)00375-0.
268. Gutowska, A.; Bae, Y.H.; Feijen, J.; Kim, S.W. Heparin release from thermosensitive hydrogels. *J. Control. Release* **1992**, *22*, 95–104, doi:10.1016/0168-3659(92)90194-V.
269. Alaneed, R.; Golitsyn, Y.; Hauenschild, T.; Pietzsch, M.; Reichert, D.; Kressler, J. Network formation by aza- Michael addition of primary amines to vinyl end groups of

- enzymatically synthesized poly (glycerol adipate). *Polym. Int.* **2021**, *70*, 135–144.
270. Anderson, J.M. Future challenges in the in vitro and in vivo evaluation of biomaterial biocompatibility. *Regen. Biomater.* **2016**, *3*, 73–77.
271. Wiegand, C.; Hipler, U.-C. Evaluation of biocompatibility and cytotoxicity using keratinocyte and fibroblast cultures. *Skin Pharmacol. Physiol.* **2009**, *22*, 74–82.
272. Mei, Y.; Kumar, A.; Gao, W.; Gross, R.; Kennedy, S.B.; Washburn, N.R.; Amis, E.J.; Elliott, J.T. Biocompatibility of sorbitol-containing polyesters. Part I: Synthesis, surface analysis and cell response in vitro. *Biomaterials* **2004**, *25*, 4195–4201, doi:10.1016/j.biomaterials.2003.10.087.
273. Turner, J.L.; Bierman, E.L. Effects of glucose and sorbitol on proliferation of cultured human skin fibroblasts and arterial smooth-muscle cells. *Diabetes* **1978**, *27*, 583–588, doi:10.2337/diab.27.5.583.

Supplementary Data

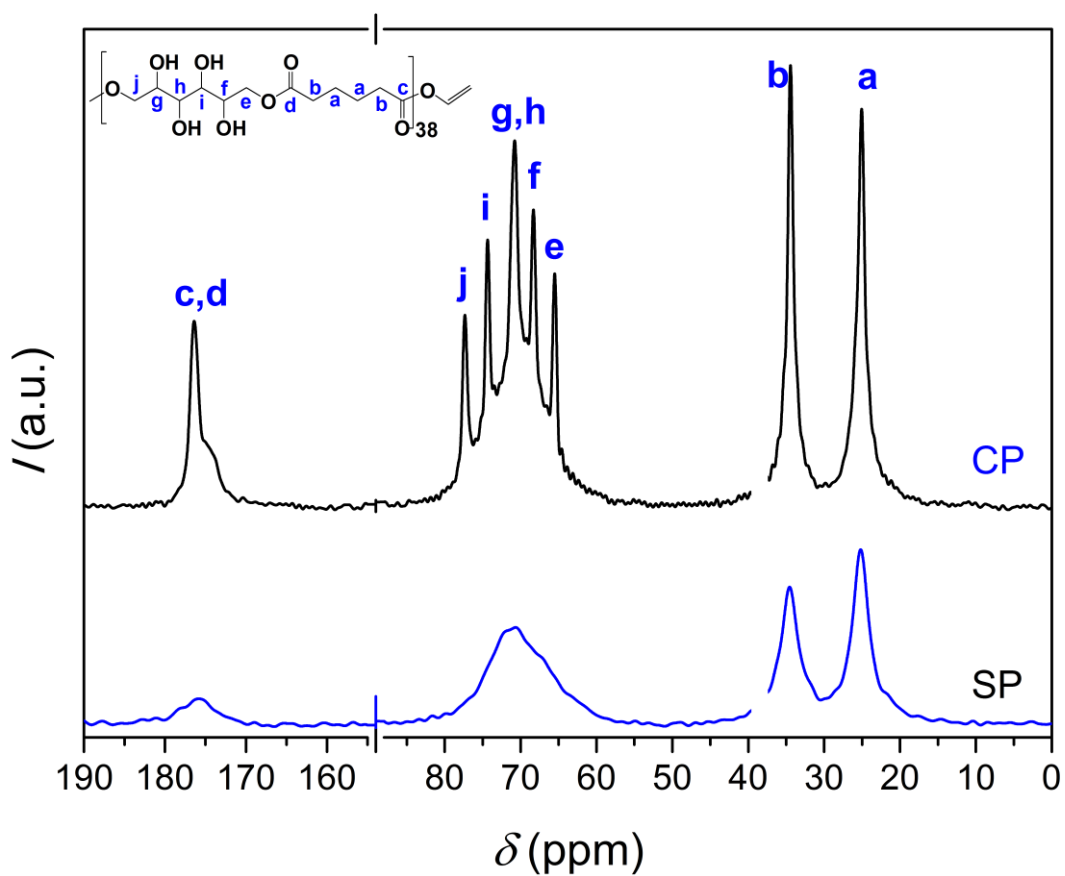


Figure S1. ^{13}C CP (top) and SP (bottom) MAS spectra of poly(sorbitol adipate). PSA is a highly viscous substance with low mobility. The SP experiment, therefore, does not provide spectral resolution. The CP experiment shows a well resolved spectrum.

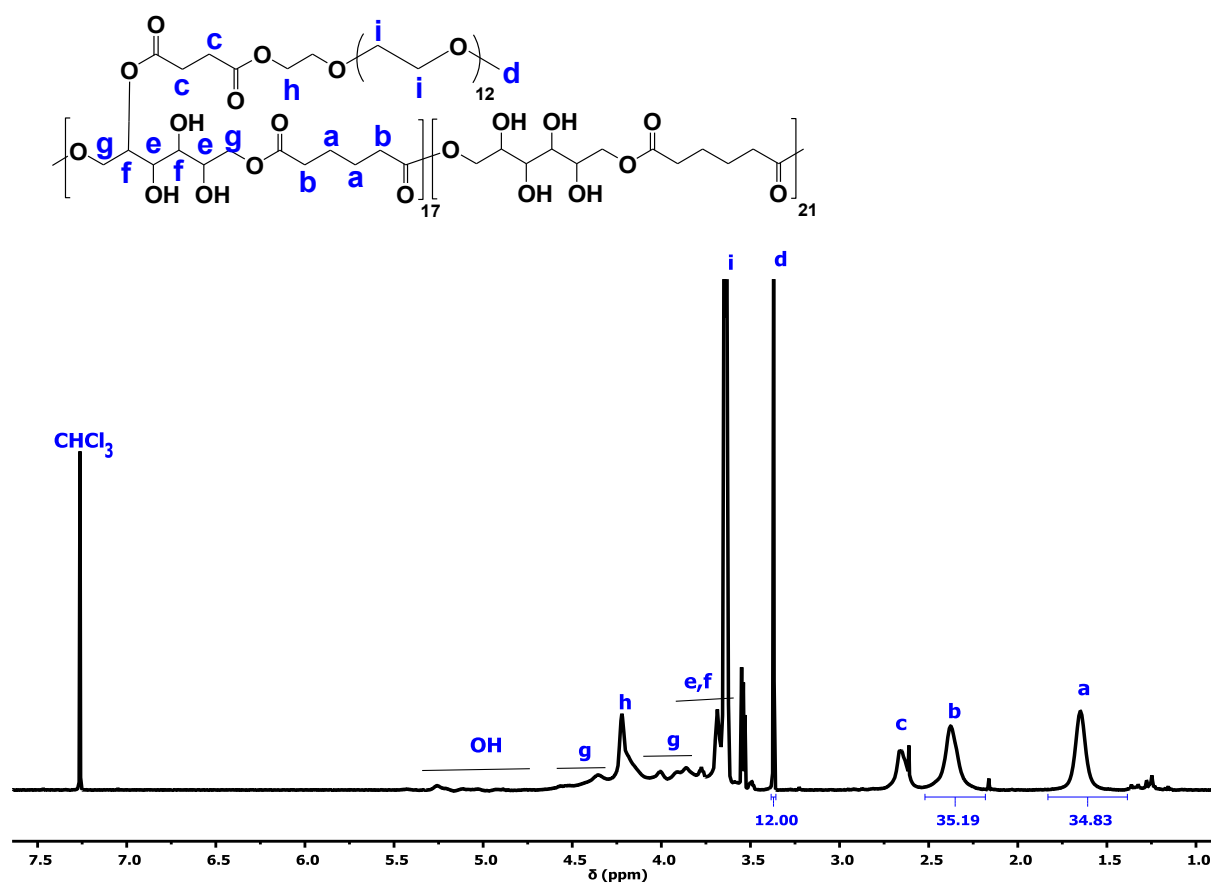


Figure S2. ¹H NMR spectrum of PSA-g-mPEG measured at 27 °C using CDCl₃ as solvent.

Acknowledgment

I extend my heartfelt gratitude to all those who have been instrumental in supporting me throughout my doctoral journey. I am indebted to Prof. Dr. Jörg Kressler for providing me the opportunity to undertake my research under his mentorship, delving into the intricacies of this interdisciplinary subject. His consistent scientific guidance, open-door policy and encouragement have been invaluable throughout my research journey. I will forever appreciate Prof. Kressler's incredible support. I am equally grateful to Prof. Dr. Karsten Mäder for the enriching collaboration, his support, and insightful discussions. They were instrumental in shaping my Ph.D. work towards end stage at Martin-Luther-University Halle-Wittenberg.

I would like to express my profound gratitude to the Higher Education Commission of Pakistan for their crucial role as the funding agency for my Ph.D. project. Their financial support was instrumental in enabling the successful execution of my research endeavors. This backing not only provided me with the necessary resources and tools but also served as a testament to the commission's commitment to advancing academic pursuits and fostering research excellence.

I extend my sincere thanks to Dr. Marie-Luise Trutschel for her incredible support in Pharmacy Department and engaging with myself in enriching scientific discussions and fostering an interdisciplinary project. My appreciation also goes to Dr. Karsten Busse for his valuable insights into polymer and polymer network related discussions. I also extend word of thanks to Dr. Yury Golitsyn for his collaborative support related to Solid State NMR. My appreciation also goes to Dr. Henrike Lucas for her support in cytotoxicity studies. I thank you Dr. Jonas Steiner for his support in stability studies. I also extend my heartfelt thanks to Dr. Humayun Bilal for mentoring me in polymer synthesis. I learned a lot from his invaluable discussions, comments and suggestions.

Last but not the least, my appreciation also goes to all members of Prof. Jörg Kressler's group for the conducive work environment, as well as for their insightful comments and suggestions. Special thanks to Dr. Razan Alaneed, Mr. Rana Hore.

This milestone would not have been possible without all of the above mentioned. Thank you all.

Curriculum Vitae*Personal data*

Family name	Rashid
First name	Haroon
Place of birth	Tank, Pakistan
Nationality	Pakistani

Education

2017 – 2024	Ph.D. Student Martin Luther University, Halle-Wittenberg Institute of Pharmacy Supervisors: Prof. Dr. Karsten Maeder Prof. Dr. Joerg Kressler
2012-2014	Master of Philosophy in Pharmaceutics Islamia University, Bahawalpur, Pakistan
2005-2010	Pharm. D. (Doctor of Pharmacy) Gomal University, Dera Ismail Khan, Pakistan
2002-2004	Higher Secondary School Cadet College, Kohat, Pakistan

Halle (Saale) den 08.04.2024

Haroon Rashid

Publications

Rashid, H., Golitsyn, Y., Bilal, M. H., Maeder, K., Reichert, D., and Kressler, J. (2021). Polymer networks synthesized from poly (sorbitol adipate) and functionalized poly (ethylene glycol). *Gels*, 7(1), 22.

Rashid, H., Lucas, H., Karsten, B., Kressler, J., Maeder, K., and Trutschel, M.-L., (2023). Development of poly(sorbitol adipate)-g-poly(ethylene glycol) mono methyl ether based hydrogel matrices for model drug release. *Gels*. 10(1):17.

Abstracts and Posters

Rashid, H., and Kreßler, J. “Fabrication of polyester based gels for pharmaceutical application”, 22nd annual meeting, Controlled Release Society Local Chapter 2018, Halle (Saale), Germany

Rashid, H., and Kreßler, J. “Development of modified functional polyester network for pharmaceutical applications”, 23rd annual meeting, Controlled Release Society Local Chapter 2019, Leipzig, Germany

Rashid, H., and Kreßler, J. “Fabrication of polyester based gels for pharmaceutical application“, 1st Doktoranden- und PostDoc-Konferenz, ProMatLeben Polymere, Berlin, Germany

Selbstständigkeitserklärung

Hiermit erkläre ich, dass ich dieses Werk ohne fremde Hilfe und selbstständig verfasst habe. Ich versichere, dass ich ausschließlich die angegebenen Quellen und Hilfsmittel genutzt und auf jegliche externe Hilfsmittel verzichtet habe. Alle Fälle, in denen ich Inhalte aus anderen Werken direkt zitiert oder reproduziert habe, werden ausdrücklich anerkannt und gekennzeichnet.

Darüber hinaus erkläre ich, dass ich nicht versucht habe, meine Doktorandenkandidatur auf andere Weise voranzutreiben, und dass diese Dissertation in ihrer derzeitigen Form weder in ihrem gegenwärtigen Zustand noch in einer alternativen Fassung bei einer anderen akademischen Einrichtung eingereicht wurde.

Halle (Saale), den 08.04.2024

Haroon Rashid